Reliability of Aging in Microstructures for Sn-Ag-Cu Solder Joints with Different Surface Finishes during Thermal Cycling

by

Chaobo Shen

A dissertation submitted to the Graduate Faculty of
Auburn University
in partial fulfillment of the
requirements for the Degree of
Doctor of Philosophy

Auburn, Alabama
May 7, 2016

Keywords: Electronics Packaging Reliability, SAC, ENIG,
Thermal Cycling, IMC

Copyright 2016 by Chaobo Shen

Approved by

John Evans, Chair, Thomas Walter Professor, Industrial and Systems Engineering Department
Richard Sesek, Tim Cook Professor, Industrial and Systems Engineering Department
Michael Bozack, Professor, Physics Department
Andres Carrano, Associate Professor, Industrial and Systems Engineering Department

Abstract

A direct and deleterious effect on packaging reliability has been observed during elevated temperature isothermal aging for fine-pitch ball grid array (BGA) packages with Sn-1.0Ag-0.5Cu (SAC105) and Sn-3.0Ag-0.5Cu (SAC305) solder ball interconnects. Package sizes ranging from 19 mm with 0.8 mm pitch BGAs to 5 mm with 0.4 mm pitch BGAs with three different board finishes (ImAg, ENIG, ENEPIG) were evaluated.

The aging temperatures were 125°C, applied for a period of 6 months and 12 months. Subsequently, the specimens were thermally cycled from -40°C to 125°C with 15 min dwell times at the high temperature. The Weibull characteristic lifetime is dramatically reduced during isothermal aging at 125°C for SAC105/305 on a variety of finishes. In particular, SAC105 undergoes a considerable lifetime reduction during aging and illustrates the risk in using SAC105 solder balls in applications where thermal fatigue failure is a concern. IMC analysis showed the IMC is thicker at corner side solder balls compared to center balls in most cases. For the 0.8mm pitch 15mm package size BGA, the investigating of degradation charts shows that the characteristic lifetimes for both SAC105 and SAC305 decrease as: ENIG > ENEPIG > ImAg. However, the order is ENIG ≈ ENEPIG> ImAg for 0.4mm pitch 10mm package size BGA. In all cases, ENIG performs better than Immersion Ag for applications involving long-term isothermal aging. SAC305, with a higher relative fraction of Ag_3Sn IMC within the solder, performs better than SAC105. SEM and polarized light microscope analysis show most cracks happened at package side, propagated from corner to center or even to solder bulk, which eventually cause

fatigue failures. Three factors are discussed: IMC, Grain Structure and Ag_3Sn particle. The continuous growth of Cu-Sn intermetallic compounds (IMC) and grains increase the risk of failure, while Ag_3Sn particle seems helpful to block the crack propagation.

Acknowledgments

The author would like to thank his advisor Dr. John L. Evans for his support, guidance, and mentorship throughout this research. Sincere gratitude and appreciation are also extended to my committee members, Dr. Richard Sesek, Dr. M. J. Bozack, and Dr. Andres Carrano for their valuable insights and precious time in the course of this research. The author particularly thanks Dr. Michael Bozack for his editorial guidance during the publication of several journal papers and this thesis, with many useful discussions during the lead-free soldering project. Thanks are also extended to all my lab-mates, coworkers, and friends: Dr. Jiawei Zhang, Dr. Zhou Hai, Cong Zhao, and Thomas Sanders, and thank you Dr. Michael Miller and John Marcell for your encouragement and friendship. Finally, the author is in debt to his parents who have supported him endlessly although they are so far away.

Table of Contents

Abstract ii

Acknowledgments iv

List of Tables viii

List of Illustrations x

Chapter 1 1

General Introduction 1

1.1 Development in Packaging Technology 1

1.2 SMT components 1

1.2.1 QFP (Quad Flat Package) 2

1.2.2 QFN (Quad Flat No-leads) 4

1.2.3 PGA (Pin Grid Array) 5

1.2.4 BGA (Ball Grid Array) 6

1.2.5 LGA (Land Grid Array) 8

1.3 PCB Substrate 9

1.4 Solder Mask 9

1.5 Lead-free PCB Surface Finish 10

1.5.1 HASL 10

1.5.2 OSP 11

1.5.3 ENIG 12

1.5.4 ENEPIG 13

1.5.5 ImAg 14

1.5.6 ImSn 15

1.6 Solder Paste 15

1.7 Solder Alloys 16

1.7.1 Sn-Ag-Cu Solder Alloy 18
1.8 SMT Assembly 19
1.8.1 Assembly Process 21
1.9 Reflow-Soldering 23
1.10 Accelerated Life Testing 24
1.11 Outline of the Dissertation 25
Chapter 2 27
Literature Review 27
2.1 Introduction 27
2.2 Effect of IMC 28
2.2.1 General Information 28
2.2.2 Effect of Ag_3Sn IMC 29
2.2.3 Effect of Cu-Sn IMC 31
2.2.4 Effect of IMC Thickness Growth 32
2.2.5 Effect of IMC with different Surface Finish 34
2.2.6 Effect of Sn Recrystallization 34
2.3 Drop Test Effect for ENIG, ENEPIG finishes 36
2.4 Vibration Test for ENEPIG/ImAg Finishes 38
2.5 Thermal Aging and Cycling 40
Chapter 3 42
Test Introduction 42
3.1 Introduction 42
3.2 Test Vehicle Design and Assembly 43
3.2.1 Test Vehicle 43
3.2.2 Surface Finish 44
3.2.3 Solder Paste and Stencils 46
3.2.4 SMT Assembly Processes 47
3.2.5 Inspection Test Vehicle 50
3.3 Thermal Test 50
3.3.1 Test Matrix and Test Conditions 50
3.3.2 Data Acquisition System 52
3.4 Failure Analysis 52

Chapter 4 55
Reliability Data Analysis 55
4.1 Data Analysis of Aging Effect 55
4.2 Data Analysis of Package Size Effect 61
4.3 Data Analysis of Pb-Free Effect 63
4.4 Data Analysis of Surface Finish Effect 72
Chapter 5 77
Failure Analysis 77
5.1 IMC Analysis 77
5.1.1 IMC Properties 77
5.1.2 IMC Thickness Analysis 84
5.1.3 IMC Thickness Growth Effect 88
5.2 Failure Mode 90
5.3 Crack Propagation 94
Chapter 6 97
6.1 Conclusion 97
6.2 Limitation and Uncertainty 99
6.3 Publications 99
Chapter 7 102
Future Work 102
References 106

List of Tables

Table 1. Quad Flat Package Types 3

Table 2. Different Types of BGA [4] 7

Table 3. Details of Three Solder Alloys 18

Table 4. Elastic modulus measured by ultrasonic stress wave propagation 19

Table 5. Example of Reflow Solder Profile 24

Table 6. Test Vehicle Surface Finish 39

Table 7. Weibull Parameters (a) SnPb Solder (b) SAC 305 Solder 40

Table 8. Component Matrix 44

Table 9. Lead-free Solder Paste Parameters 46

Table 10. Test Plan 51

Table 11. Characteristic Life for BGA for Different Aging Times (aging at 125 ℃; M = months) 60

Table 12. Degradation Rate of Each Aging Group (M = months) 61

Table 13. Degradation Rate Differences with Aging Time (M = months) 61

Table 14. Characteristic Life Time for Immersion Ag, SAC305 BGA with Different Package Sizes 62

Table 15. Characteristic Life Time for SnPb, SAC105 and SAC305 BGA with 10mm package size and ENIG, ENEPIG Plating after Aging at 125oC 66

Table 16. Characteristic life comparison (η) for SnPb, SAC105 and SAC305 BGA with 15mm package size and ENIG, ENEPIG Plating 71

Table 17. Degradation Rate Comparison for 10mm BGA Package after Aging 76

Table 18. 0.8mm pitch SAC305 Board Side IMC Thickness Growth during 125oC Aging 84

Table 19. 0.8mm Pitch SAC105/SAC305 Board Side IMC Thickness Growth with ENIG Finish 85

Table 20. Component Matrix 104

List of Illustrations

Figure 1. Traditional DIP Components ... 2

Figure 2. Quad Flat Package ... 3

Figure 3. QFN Package ... 4

Figure 4. Cross Section of a Flat No-leads Package ... 5

Figure 5. Pin Grid Array Package ... 6

Figure 6. BGA and CSP Package ... 7

Figure 7. Cross Section of LGA Package ... 8

Figure 8. NSMD (Left) and SMD (Right) ... 9

Figure 9. Surface Finish Thickness [11] ... 10

Figure 10. Advantages and Disadvantages of HASL ... 11

Figure 11. Advantages and Disadvantages of OSP ... 12

Figure 12. Advantages and Disadvantages of ENIG ... 13

Figure 13. Advantages and Disadvantages of ENEPIG ... 14

Figure 14. Advantages and Disadvantages of ImAg ... 14

Figure 15. Advantages and Disadvantages of ImSn ... 15

Figure 16. Solder Paste Sample ... 16

Figure 17. Melting Point of Solder Alloy ... 17

Figure 18. Sn-Ag-Cu Tenary Phase Diagram ... 19

Figure 19. SMT Assembly Process Flow [17] ... 21

Figure 20. General Reflow Solder Profile ... 24

Figure 21. Binary phase diagram (a) Sn–Ag and (b) Sn–Cu 29

Figure 22. The initial microstructure of Sn–xAg–Cu bulk solders. 30

Figure 23. Intermetallic growth with isothermal aging.. 33

Figure 24. IMC Layer of ENIG (a) and ENEPIG (b) 34

Figure 25. Sn grain boundaries under cross polarized light, zone (1) and (2). 35

Figure 26. Recrystallization 35

Figure 27. Drop Test Setup 37

Figure 28. Weibull Life Time Analysis 38

Figure 29. (a) Drop impact test and (b) Temperature cycling test. 41

Figure 30. Test vehicle. 43

Figure 31. ENIG (Left) and ENEPIG (Right) 44

Figure 32. RBS Analysis for ENIG and ENEPIG 45

Figure 33. Printing Machine 46

Figure 34. The Continental Electronics prototype manufacturing lab.......................... 48

Figure 35. Reflow Oven 49

Figure 36. Reflow Profile (X-axis: Time-Second; Y-axis: Temperature-Celsius)......... 49

Figure 37. Skewed Pad on the Left and Solder Bridging on the right 50

Figure 38. Thermal Cycling Profile... 51

Figure 39. Schematic Design of the Monitoring System... 52

Figure 40. (a): SEM schematic showing the ion attack to release surface ions; (b): SEM schematic for beam signal 53

Figure 41. Weibull Plot for up to 24 Month Aging at 125 ℃ for Immersion Ag, SAC305 BGA with Various Package Size: (a) 19mm, (b) 15mm, (c) 10mm and (d) 5mm. 57

Figure 42. Weibull Plot for up to 24 Month Aging at 125 ℃ for Immersion Ag, SAC105 BGA with Various Package Size: (a) 19mm, (b) 15mm, (c) 10mm and (d) 5mm. 59

Figure 43. Characteristic Life Time for BGA for Different Aging Times..................... 60

Figure 44. Degradation Chart for Immersion Ag, SAC305 BGA after Aging at 125oC with Varying Package Sizes. 62

Figure 45. Weibull Plot for 10mm BGA Package on ENIG Plating after Aging at 125oC (a) SnPb (b) SAC105 (c) SAC305 64

Figure 46. Weibull Plot for 10mm BGA Package on ENEPIG Plating after Aging at 125oC (a) SnPb (b) SAC105 (c) SAC305 66

Figure 47. Characteristic Life Time for SnPb, SAC105 and SAC305 BGA with 10mm package size and ENIG, ENEPIG Plating after Aging at 125oC 67

Figure 48. Weibull Plot for 15mm BGA Package on ENIG Plating after Aging at 125oC (a) SnPb (b) SAC105 (c) SAC305 69

Figure 49. Weibull Plot for 15mm BGA Package on ENEPIG Plating (a) SnPb (b) SAC105 (c) SAC305 70

Figure 50. Characteristic life comparison (η) for SnPb, SAC105 and SAC305 BGA with 15mm package size and ENIG, ENEPIG Plating 71

Figure 51. Characteristic life comparison (η) for 10mm BGA finished with ENIG, ENEPIG & ImAg subject to 125oC/12 months aging. 72

Figure 52. Characteristic life comparison (η) for 15mm BGA finished with ENIG, ENEPIG & ImAg subject to 125oC/12 months aging. 72

Figure 53. Characteristic life comparison (η) for 10mm BGA soldered with SAC105 & SAC305 subject to 125oC/12 months aging. 74

Figure 54. Characteristic life comparison (η) for 15mm BGA soldered with SAC105 & SAC305 subject to 125oC/12 months aging. 75

Figure 55. Degradation Rate Comparison for 10mm BGA Package after Aging 76

Figure 56. SAC305 solder joint on ENIG, no aging, BSE imaging. 78

Figure 57. Plate-Like Ag3Sn on 15mm SAC305 solder joint with ENIG, 6 month aging, BSE imaging 78

Figure 58. IMC Layer of 10mm SAC105 solder joint finished with ENIG at Package Side (a) and Board Side (b). 80

Figure 59. Package side IMC EDX for SAC305 (0.8 mm pitch) solder joint on ENEPIG, 6 months aging. 81

Figure 60. Board side IMC EDX for SAC305 (0.8 mm pitch) solder joint on ENEPIG, 6 months aging. 82

Figure 61. Board side IMC EDX for SAC305 (0.8 mm pitch) solder joint on ENIG, 6 months aging. 83

Figure 62. 0.8mm pitch SAC305 Board Side IMC Thickness Growth during 125oC Aging 84

Figure 63. 0.8mm Pitch SAC105/SAC305 Board Side IMC Thickness Growth with ENIG Finish 85

Figure 64. IMC thickness analyses for 15mm BGAs with ENIG finish. (a) Board Side (b) Package Side 86

Figure 65. IMC thickness growth with ENIG finish on package (top) and board (bottom) side for 15mm solder balls. 87

Figure 66. IMC Thickness Growths with the Effect of Aging for 10mm SAC 105 solder joints finished with ENIG (a) Board Side, (b) Package Side 89

Figure 67. SEM Images of 10mm Package SAC105 Solder Interconnections after 1 Year Aging at 125oC: (a) Crack at Package Side and Goes Along with IMC Boundary, ENEPIG Finished, (b) Crack Goes into The Solder Ball, ENIG Finished, (c) Crack Generates from The Inside of Solder Ball, ENIG Finished... 91

Figure 68. Cross-polarized Image of Figure 5.10(c). 92

Figure 69. SEM images of 15mm package SAC305 solder interconnections after 1 year thermal aging at 125oC: (a) Crack at package side, ENIG finished, (b) Crack at both sides, ImAg finished, (c) Crack at board side, ENEPIG finished. 93

Figure 70. SEM Images of 10mm Package SAC105 Solder Interconnections after 6 Months aging at 125oC: (a) Crack Goes Along with IMC Boundary and Blocked by Ag3Sn Particle, ENEPIG Finished, (b) Crack Propagation is subject to IMC Layer Boundary, Grain Boundary and Ag3Sn Particles. ENIG Finished. 95

Figure 71. Test Board Design 103

Figure 72. Componet Matrix 104

Chapter 1

General Introduction

1.1 Development in Packaging Technology

Over the past years, a lot of consumer electronics have been significantly reduced in size, thickness and weight. Products such as cell phones, laptops, Pads, televisions, etc., have been reduced by as much as 3/4 of their original introduction size and weight. The inclusion of fine pitch, surface mount components is the most significant contributing factor to this reduction. Because the heavier, larger, and thicker leaded Through-Hole (TH) package led to too much power and space. And it contributed significantly to the total weight of the product. The trend of packaging is towards smaller, lighter and less expensive.

1.2 SMT components

The Surface Mount (SM) package was developed to provide increased component density and performance over the Dual-Inline-Package (DIP). The Surface Mount package also provides good reliability performance. We illustrate several types of SMT components in the following. Figure 1 shows the DIP component.

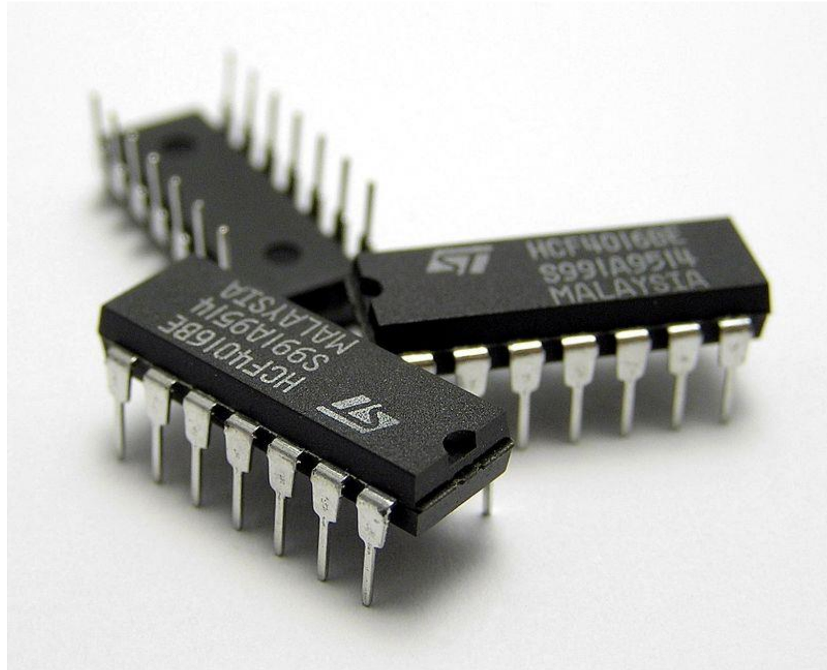

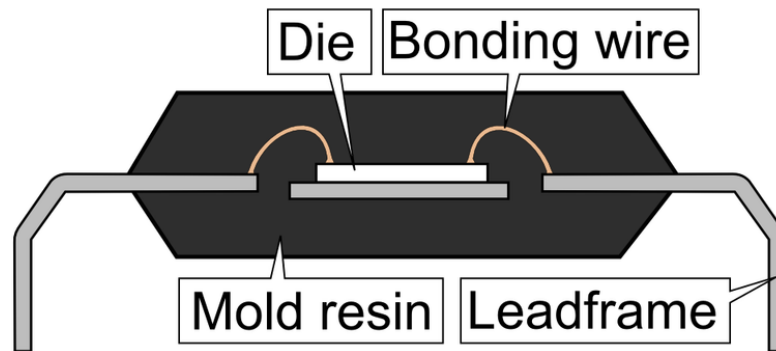

Figure 1. Traditional DIP Components

1.2.1 QFP (Quad Flat Package)

The Quad Flat Package (QFP) is a four-sided package with lead extending from the component body on all sides, largely used to ASIC and processor devices. Normally, Quad Flat Package components are packaged in trays to protect the component lead which can be easily damaged. Figure 2 shows the DIP component.

This kind of package is ideal for processors, gate arrays (FPGA/PLD) and computer motherboard chips. It is also particularly good for light-weight portable electronic products which requiring broad performance, such as laptops, pads, smart phones, data transmission, office automation, CD/DVD drives and communication boards.

Figure 2. Quad Flat Package

QFP types are listed in table 1[1]:

Table 1. Quad Flat Package Types

Plastic	
MQFP	Metric QFP (most popular)
FQFP	Fine pitch QFP
BQFP	Bumpered QFP
LQFP	Low-profile QFP
TQFP	Thin-profile QFP
SQFP	Shrink QFP (same as MQFP)
Ceramic	
CQFP	Ceramic QFP

1.2.2 QFN (Quad Flat No-leads)

The Quad Flat No-leads (QFN) package, pictured in (Figure 3), is a flat plastic package that has perimeter leads underneath the device and larger pads in the center area. The appeal of it is the compact size and slim body. The Quad Flat No-leads package is a small contained package with a near chip-scale sized footprint. Its thin body makes it ideal for applications where product thickness is a consideration. The QFN package provides excellent thermal and electrical performance and utilizes perimeter pads to ease circuit board trace routing. These traits make the QFN to be the choice for many situations where electrical performance, weight, and size are important factors.

Figure 3. QFN Package

The figure 4 shows the cross section of a Flat No lead package with a lead frame and wire bonding. There are two types of body designs, punch singulation and saw singulation.[3] Saw singulation cuts a large set of packages in parts. In punch singulation, a single package is molded into shape.

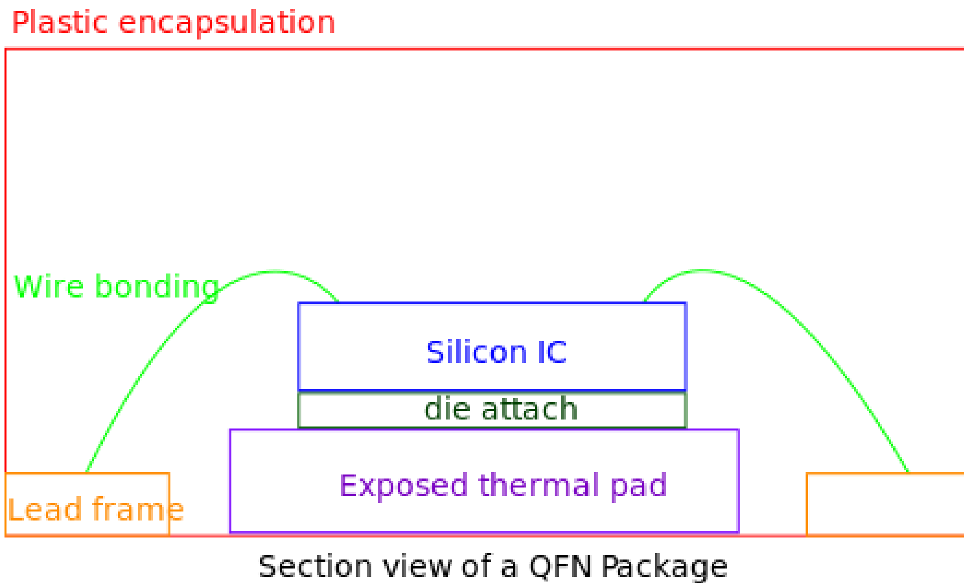

Figure 4. Cross Section of a Flat No-leads Package

The cross section picture shows a saw-singulated body with an attached thermal head pad. The lead frame is made of copper alloy. And for attaching the silicon die to the thermal pad, a thermally conductive adhesive is used. The silicon die is wired to the lead frame by 1-2 mil diameter gold lines. The pads of a saw-singulated package can either be totally placed under the package, or they could fold around the edge of the package. [2]

1.2.3 PGA (Pin Grid Array)

Pin Grid Array (PGA) is a type of integrated circuit packaging technology. The package shape is square or rectangular. Its pins are placed in a regular array on the underneath of the package (Figure 5) that are commonly spaced 2.54 mm (0.1") apart, and may or may not cover the entire underside of the package.

Pin Grid Array package is often mounted on printed circuit boards (PCB) using the through-hole method or inserted into a socket. It provides space for more pins per integrated circuit than older packages such as DIP package.

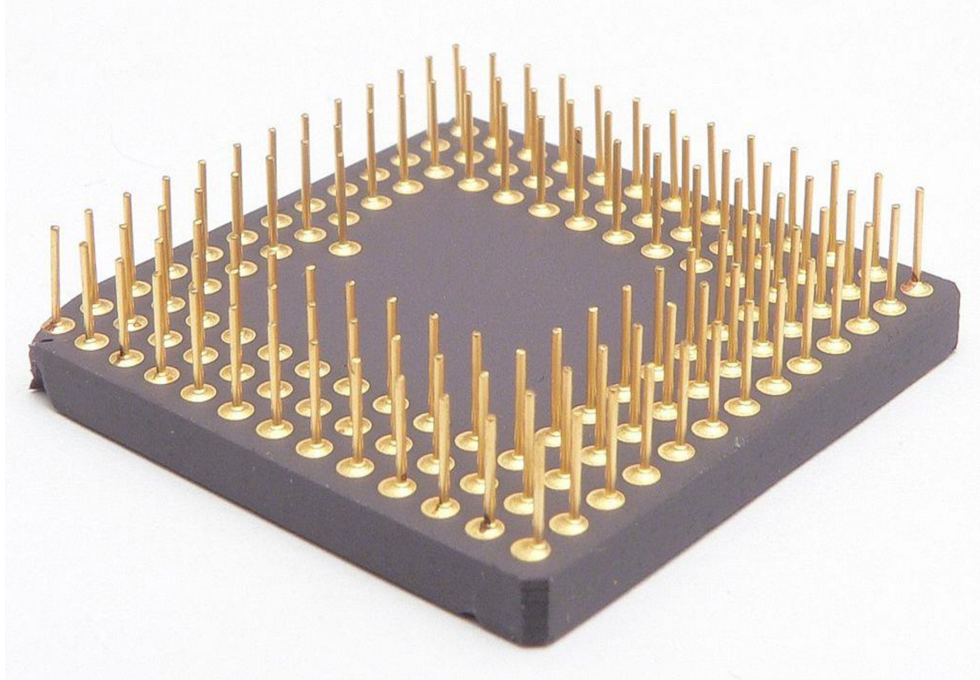

Figure 5. Pin Grid Array Package

1.2.4 BGA (Ball Grid Array)

BGA package is a very popular surface mount package that provides a grid of solder balls as its connectors. This package is available in plastic and ceramic varieties. BGA allows lower voltages to be used because of its compact size, high lead count and low inductance. BGA chips are much easier to align to the PCB, because the solder balls are farther apart than leaded packages. [3]

Since the solder balls are underneath the chip, BGA has led the way to chip scale packaging (CSP) that the package size is less than 1.2 times of the semiconductor die itself. (Figure 6)

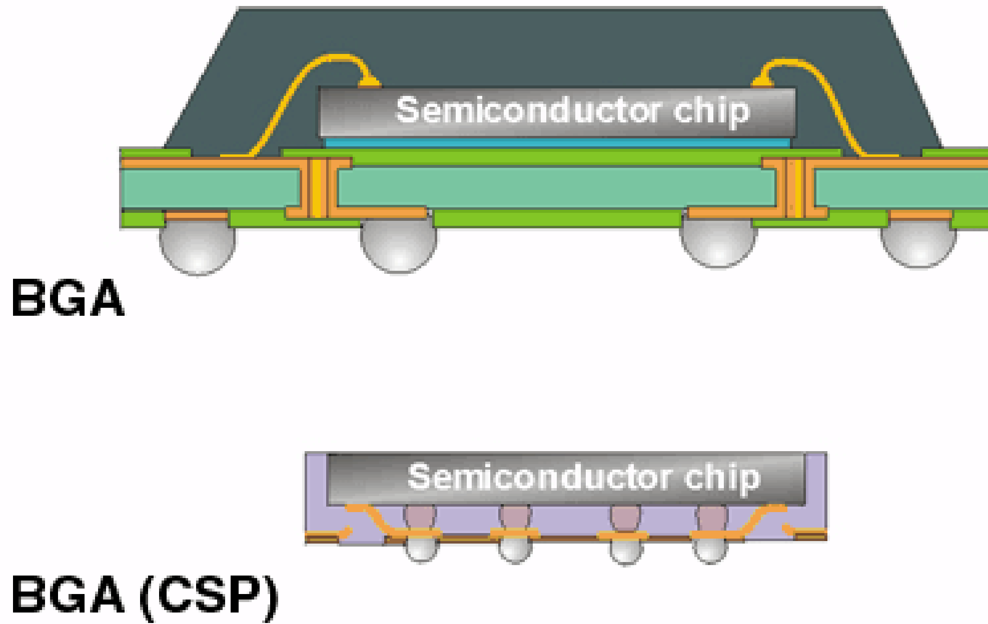

Figure 6. BGA and CSP Package

A number of BGA variants have been developed to meet the variety of requirements for different types of assembly and equipment. (Table 2)

Table 2. Different Types of BGA [4]

Abbreviation	Full Name	Description
MAPBGA	Moulded Array Process Ball Grid Array	This BGA package is aimed at low-performance to mid-performance devices that require packaging with low inductance, ease of surface mounting.
PBGA	Plastic Ball Grid Array	This BGA package is intended for mid- to high-performance devices that require low inductance, ease of surface mounting, relatively low cost, while also retaining high levels of reliability.
TEPBGA	Thermally Enhanced Plastic Ball Grid Array	This package provides for much higher heat dissipation levels. It uses thick copper planes in the substrate to draw heat from the die to the customer board.
TBGA	Tape Ball Grid Array	This BGA package is a mid- to high-end solution for applications needing high thermal performance without an external heatsink.
PoP	Package on Package	This package may be used in applications where space is at a real premium. It allows for stacking a memory package on top of a base device.
MicroBGA		As the name indicates this type of BGA package is smaller than the standard BGA package. There are three pitches that are prevalent in the industry: 0.65, 0.75 and 0.8mm.

1.2.5 LGA (Land Grid Array)

The land grid array (LGA) is a packaging technology with a square grid of contacts on the underneath of a package. The contacts are to be connected to a grid of contacts on the PCB. Not all rows and columns of the grid need to be used. The contacts can either be made by using an LGA socket, or by using solder paste. [5]

LGA packaging is related to ball grid array (BGA) and pin grid array (PGA) packaging. For LGA and PGA, LGA package is designed to fit either in a socket, or be soldered by surface mount technology. However, PGA package cannot be soldered down using surface mount technology. When comparing LGA with BGA, LAG package in non-socketed configurations has no balls, and uses flat contacts which are soldered directly to the PCB. However, BGA package has solder balls as their contacts between the IC and the PCB. [6]

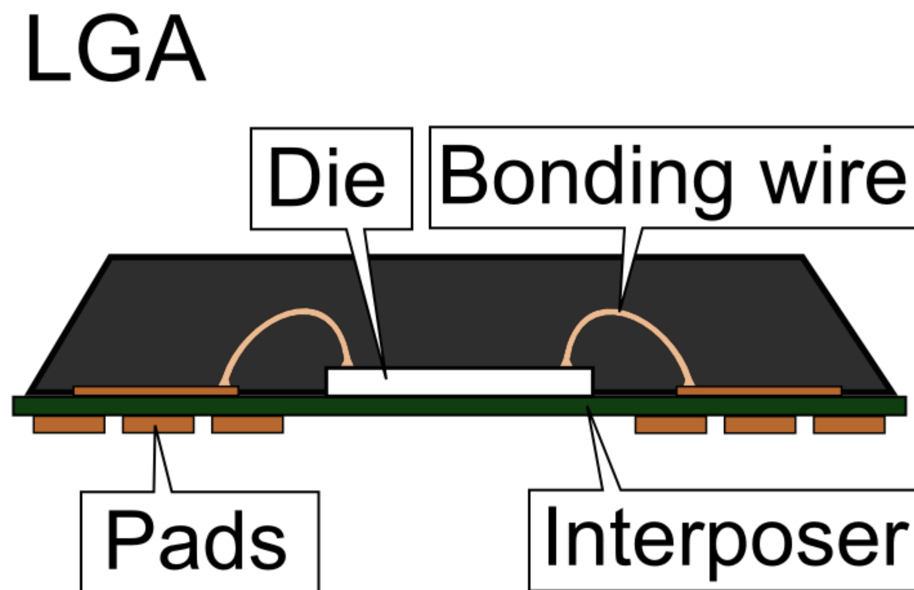

Figure 7. Cross Section of LGA Package

1.3 PCB Substrate

Substrate is the dielectric material between two conducting layers on a PCB. Unlike the conductor, though the vast majority of PCBs manufactured today use a glass reinforced substrate known as FR4, there is a much wider range of choices available for use as substrate. [7] FR-4, at glass transition temperatures higher than 125 °C, which can withstand a process temperature up to 230 ° C is inexpensive, flame resistant, resists the absorption of water and generally functions very good for many applications. It could provide the base standard for PCB substrates, delivering a widely effective balance between cost, electrical properties, durability, manufacturability and performance. [8]

1.4 Solder Mask

Solder Mask is a thin layer of polymer that is applied to the copper traces of a PCB for protection against oxidation and to prevent solder bridges from forming between closely spaced solder pads. [9]

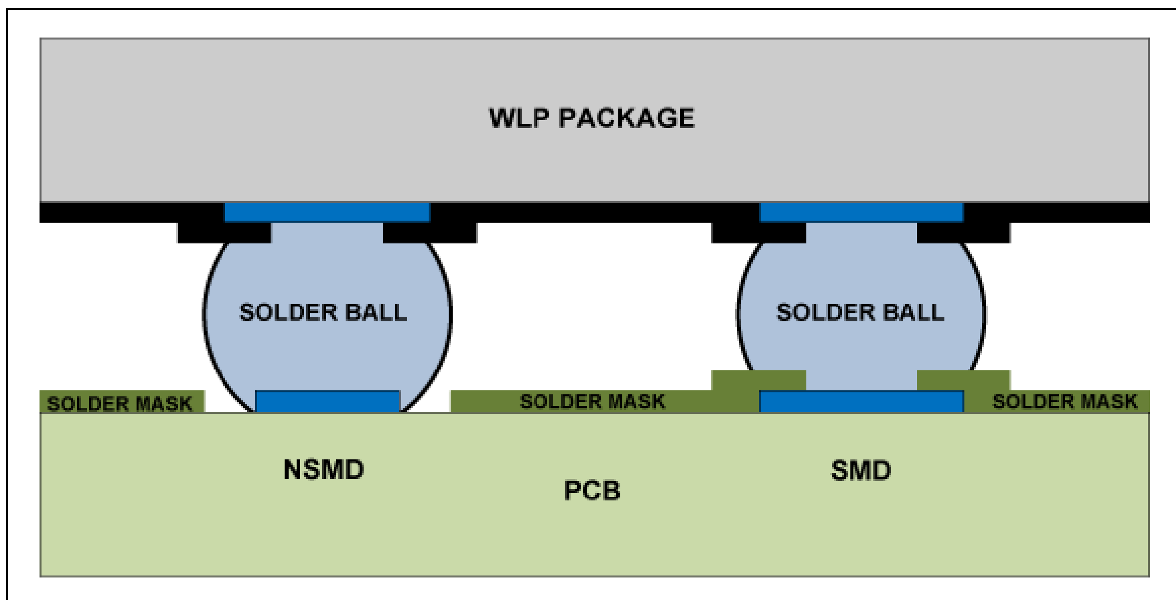

Figure 8. NSMD (Left) and SMD (Right)

Figure 8 illustrates NSMD pads on left: the solder ask opening is larger than the copper pad. SMD pads on right: the solder ask opening is smaller than the copper pad. [10]

1.5 Lead-free PCB Surface Finish

Surface finish can be defined as a coating, either metallic or organic in nature, which is applied to a PCB in order to assure solder ability of the metal under plate. Most of surface finish dissolves into the solder paste during reflow or wave soldering.

The typical 6 surface finishes and their thickness areas are listed in below Figure 9

Finish	Typ. Layer Thickness [μm]
HASL (SnAg) *(Hot Air Solder Leveling)*	> 5
Electroless Tin	0.3 - 1.2
Electroless Silver	0.2 - 0.5
Electroless Ni / Immersion Au *(ENIG)*	3 - 7 / 0.05 - 0.15
Galvanic Ni/Au	> 3 / 0.1 - 2
OSP *(Organic Solderability Preservatives)*	Typical 1

Figure 9. Surface Finish Thickness [11]

1.5.1 HASL

HASL was the most significant technology in past decades. It has a number of attributes that PCB fabricators and assembly houses prefer. And more, both leaded and lead-free are available for this technology. The PCB assembly people like HASL because

it can withstand multiple reflow cycles. The advantages and disadvantages are listed in Figure 10.

HASL (Hot Air Solder Level)	
Advantage	**Disadvantage**
Easily Applied	Contains Lead
Easily Reworked	Huge Co-Planarity Difference
Length Industry Experience	Not Suited for High Aspect Ratios
Good Bond Strength	PWB Dimensional Stability Issues
Long Shelf Life	Bridging Problems on Fine Pitch Assemblies
Easy Visual Inspection	Inconsistent Coating Thickness

Figure 10. Advantages and Disadvantages of HASL

1.5.2 OSP

OSP's weak point is it can only sustain a couple of reflow cycles. Any more than that, the PCB incurs thermal damage. The strong point is it has low cost. The advantages and disadvantages are listed in Figure 11.

OSP (Organic Solderability Preservative)	
Advantage	Disadvantage
Flat, Coplanar pads	Limited Thermal Cycles
Reworkable	Cannot be Reworked at CM
Doesn't Affect Finished Hole Size	Limited Shelf Life
Shor, Easy Process	
Low Cost	Panels Need to be Routed and Electrically Tested Prior to Coating
Good Soldermask Integrity	

Figure 11. Advantages and Disadvantages of OSP

1.5.3 ENIG

ENIG continues to be a well-accepted surface finish, even though the extra cost gold incurs. It has excellent co-planarity and medium fabrication cost. Its co-planarity and solder joint integrity are excellent too. It has good RoHS compliant, which is very important in nowadays. It also can sustain multiple reflows and has a good shelf life. The advantages and disadvantages are listed in Figure 12.

ENIG (Electroless Nickel/Immersion Gold)	
Advantage	Disadvantage
Planar Surface	Not Wire-Bondable
Consistent Thickness	Expensive
Multiple Thermal Cycles	Black Pad Issues
Long Shelf Life	Waste Treatement of Nickel
Solders Easily	Cannot be Reworked at PCB Fabricator
Good for Fine Pitch Product	Not Optimal for Higher Speed Signals

Figure 12. Advantages and Disadvantages of ENIG

1.5.4 ENEPIG

ENEPIG is a surface finish for PCB that has been around for a decade but is only recently coming back into vogue. Because the high price of palladium had kept it out of reach for most products. ENEPIG works well with both lead free and Sn63-Pb37 alloys. ENEPIG is called the "Universal" surface finish because it can be used for almost all assembly processes. The advantages and disadvantages are listed in Figure 13.

ENEPIG (Electroless Nickel/Palladium-Immersion Gold)	
Advantage	Disadvantage
Palladium Prevents Nickel from Passivating in the Presence of the "Porous" Gold Deposit	Added Cost Results
Presence of the "Porus" Gold Deposit	Dip Tank Process
Alumimum Wire Bondable	Evidence that Palladium Poisons the Solder Paste after Reflow
Planar Surface	Waste Treatement
Good for Fine Pitch Product	Expensive

Figure 13. Advantages and Disadvantages of ENEPIG

1.5.5 ImAg

Immersion Silver is a very standard finish on PCB and is RoHS compliant. The advantages and disadvantages are listed in Figure 14.

ImAg (Immersion Silver)	
Advantage	Disadvantage
Good for Fine Pitch Product	High Friction Coefficient
Planar Surface	Some Systems Cannot Throw Into Microvias with Aspect Ratios>1:1
Inexpensive	Tarnishing Must be Controlled
Eliminates Nickel	
Long Shelf-Life	
Can be Reworked	

Figure 14. Advantages and Disadvantages of ImAg

1.5.6 ImSn

Immersion Tin comes in second in terms of popularity. It has excellent co-planarity, that means it provides a consistently flat surface and could match for fine-pitch devices very well. The cost is acceptable, but it has a limited shelf life. It should be used within three to six months. However, the called "tin whiskers" phenomenon has historically plagued immersion tin. These electrically conductive, wispy-looking, hair-like formations could cause short circuits and subsequent failure. [12] The advantages and disadvantages are listed in Figure 15.

ImSn (Immersion Tin)	
Advantage	Disadvantage
Good for Fine Pitch Product	Handling Concerns
Planar Surface	Panels Must be Routed and Tested Prior to Coating
Eliminates Nickel	Contains Thiourea, a Known Carcinogen
Can be Substitute for Reflowed Solder	Limited Rework Cycles at CM
Inexpensive	Horiziontal Process Needs Nitrogen Blanket
	Too Viscous for Small Holes

Figure 15. Advantages and Disadvantages of ImSn

1.6 Solder Paste

Solder paste consists of solder alloy and a flux system. (Figure 16) Normally the volume is split into about 50% alloy and 50% flux and solvents. In term of mass, this means approximately 90 weight% alloy and 10 weight% flux system and solvents. The flux system has to remove oxides and contaminants from the solder joints during the

soldering process. The activation level of the used flux decides the capability of removing oxides and contaminants.

Figure 16. Solder Paste Sample

1.7 Solder Alloys

A solder is a fusible metal alloy with a melting point or melting range of 90 ℃ to 450 ℃ (200 ℉ to 840 ℉), used in a process that called soldering where it is melted to join metallic surfaces. It is especially useful in electronics. Alloys that melt between 180 ℃ and 190 ℃ are the most popular. Figure 17 gives us the melting point of batch of solder alloys.

Solder Alloy	Melting Point (°C)	Melting Point (°F)
5Sn-95Pb	307	585
0.5Sn-92.5Pb-2.5Ag	280	536
Sn/5Sb	243	469
100Sn3	232	450
99.3Sn-0.7Cu	227	440
96.5Sn-3.5Ag	221	430
Sn/3.0Ag/0.5Cu	219	426
Sn/3.8Ag/1.0Cu	217	423
Sn/3.5Ag/1.0Cu/3Bi	213	415
50In-50Pb	209	402
45Sn-55Pb	204	400
55Sn-45Pb	193	379
60Sn-40Pb	186	368
63Sn-37Pb	183	361
62Sn-36Pb-2Ag	179	354
97In-3Ag	143	289
Sn/57Bi	139	282
52In-48Sn	118	244

Figure 17. Melting Point of Solder Alloy

Tin/lead alloy is a fundamental solder, with a history dating back to the early days of radio. This alloy family consists of three basic compositions that have melting points in the 183 ℃ (361 ℉) region:

• 63Sn/37Pb: the eutectic composition with a melting point of 183 ℃ (361 ℉). The term "eutectic" indicates that the composition produces an alloy with a distinct melting point, versus a melting range.

The presence of lead, and its potential environmental impact led the industry to look for lead-free alternatives. Lead-free solder alloys Legislation in Europe banned lead-containing solders, with a few exceptions, effective on 01, July 2006. Lead-free alloy development has largely focused on a group of alloys that have become known by the

acronym "SAC" for its Sn/Ag/Cu (tin-silver-copper) composition. SAC alloys have compositions that range from 3.0% to 4.0% silver and from 0.5% to 0.8% copper, with the balance tin. They are generally regarded as eutectic, or nearly eutectic, at ~217 ℃ (422 ℉). [13]

1.7.1 Sn-Ag-Cu Solder Alloy

From reliability standpoints, Sn/Ag/Cu alloys have been chosen as the replacement for Sn-Pb solder. Table 3 indicates the properties of SAC 105, SAC 305 and Sn63-Pb37.

Table 3. Details of Three Solder Alloys

Alloy Type	Tin-Lead/ Pb-free	% Metal Loading				Melting Temperature		
		Tin (Sn) %	Lead (Pb) %	Silver (Ag) %	Copper (Cu) %	Eutectic (°C)	Solidus (°C)	Liquidus (°C)
SAC105	Pb-free	98.5	-	1	0.5	-	220	225
SAC305	Pb-free	96.5	-	3	0.5	-	217	221
Sn63-Pb37	Tin-Lead	63	37	-	-	183		

In the SAC system, the addition of Cu could make the melting temperature lower and improve the wettability. [14] Figure 18 is the top view (2-D) of the ternary phase diagram of Sn–Ag–Cu. [15] This red box area indicated is the near eutectic region. Most of the SAC alloy compositions currently in use are within this region.

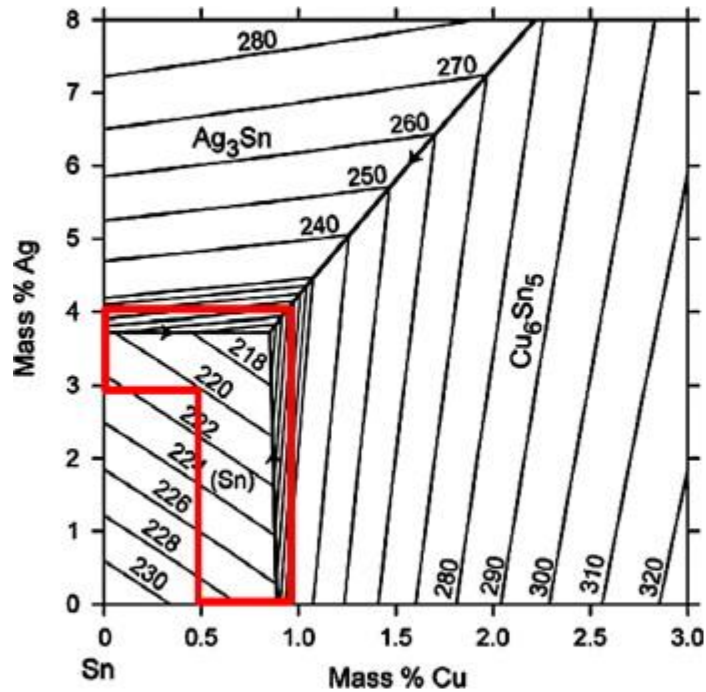

Figure 18. Sn-Ag-Cu Tenary Phase Diagram

The SAC105 alloy could provide improved reliability to stress and vibration over the SAC405 and SAC305 alloys. As Table 4 shows, the elastic modulus of SAC105 is 11% lower than SAC405.

Table 4. Elastic modulus measured by ultrasonic stress wave propagation

Alloy	SAC405	SAC305	SAC105	Sn/Pb
E [GPa]	53.3	51.0	47.0	40.2

And the SAC305 has the best wettability, low melt point, anti-fatigue and high reliability. It is widely manufactured as solder preform/wire applicate in electronic package soldering. [16]

1.8 SMT Assembly

Surface Mount Technology (SMT) uses an assembly process in which the components are soldered to the board. In contrast to conventional through-hole technology processes, the SMT components are placed directly on the surface of a PCB

instead of being soldered to a wire lead. By eliminating the need for leads inserted through-holes in the board, several advantages are developed:

(1) Smaller components can be made with closer leads

(2) Packing densities can be increased

(3) Components can be mounted on both sides of the board

(4) Smaller PCBs can be used

(5) Drilling of through-holes is eliminated during board fabrication

The areas that SMT components used on the board's surface typically range from 20% to 60% compared to through-hole components.

The limitations of SMT are:

(1) Surface mount components are more difficult to handle and assemble by humans because of smaller size;

(2) Much more expensive than leaded components;

(3) Inspection, testing and rework of the circuit assemblies are more difficult.

1.8.1 Assembly Process

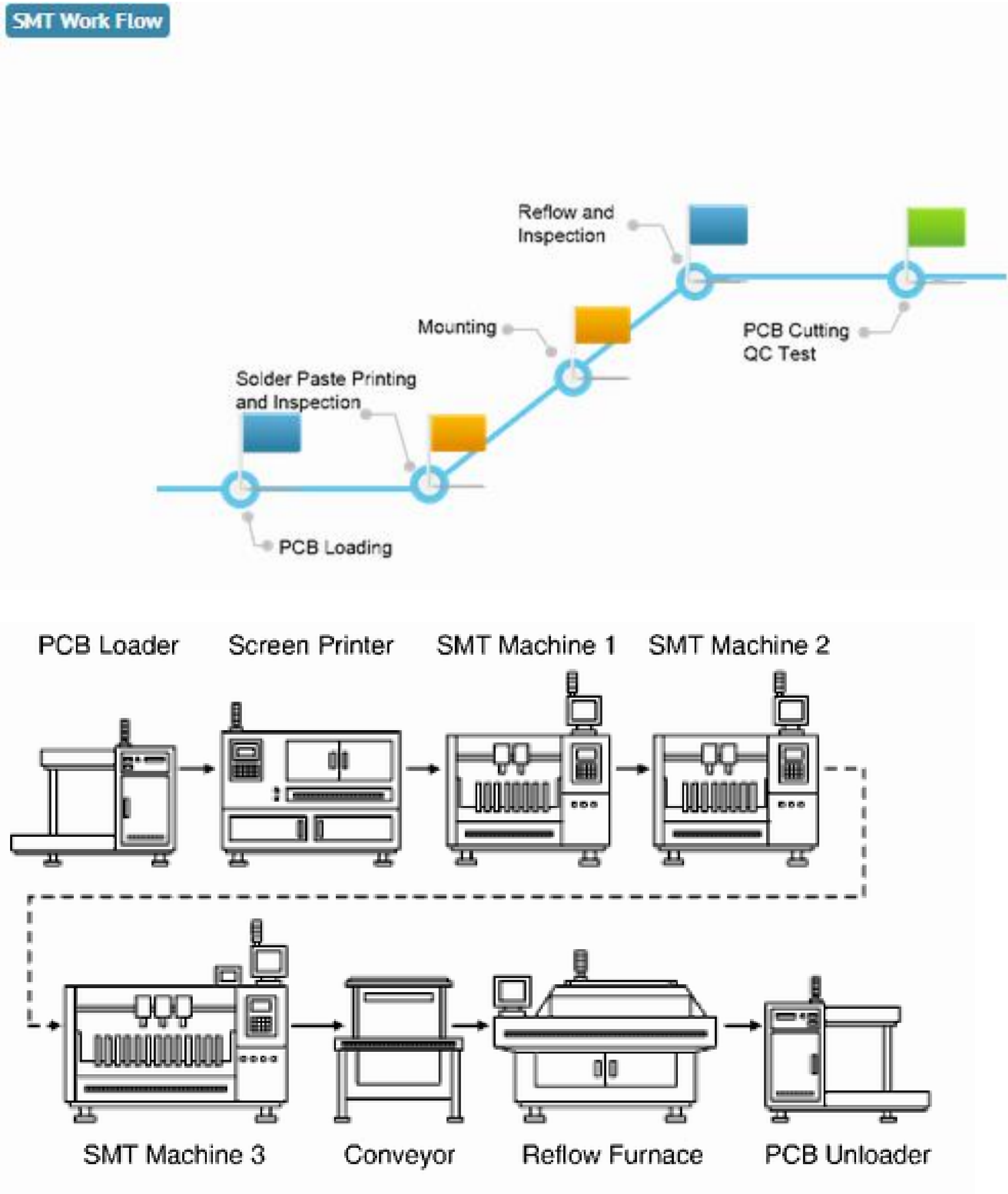

Figure 19. SMT Assembly Process Flow [17]

Step 1: Applying Soldering Paste

Applying soldering paste is one of the first steps in the SMT assembly process. The soldering paste is "printed" on the boards using the silk-screen method. Depending on the design of the board, different stainless-steel stencils for "printing" the paste onto the board and various product-specific pastes are used. After the paste is on the boards, a 2D-soldering paste inspection is performed to ensure that the paste is evenly and correctly applied. Once the accuracy of the soldering paste application has been confirmed, the boards are transferred to the SMT assembly line, where the components are soldered. [18]

Step 2: Component Placement and Assembly

The electronic components to be assembled come in trays or reels, which are then loaded into the SMT assembly machine. During the loading process, intelligent software systems ensure that components are not inadvertently switched or misloaded. The machine then automatically removes each component with a vacuum pipette from its tray or reel and places it in its correct position on the board. After the SMT assembly is completed, the boards are moved on to the reflow ovens for soldering.

Step 3: Component Soldering

The reflow-soldering process is used for series production orders. During this process, the boards are placed in a nitrogen atmosphere and are gradually warmed up with heated air until the soldering paste melts and the flux vaporizes, which fuses the components to the PCB. After this stage, the components become permanently affixed to the board after cooling off, which completes the SMT assembly process.

Addition: Automatic Optic Inspection (AOI) und Visual Check

In order to ensure the quality of the assembled boards, AOI visual inspections are performed. The AOI system automatically checks each board and compares the appearance of each board with the correct, pre-defined reference image using several cameras. In case deviations are identified, the machine informs the operator of the potential problem, who then corrects the mistake or removes the board from the machine for further inspection. The AOI visual check ensures consistency and accuracy in the SMT assembly production process. [18]

1.9 Reflow-Soldering

Reflow-soldering determines the yield and quality of PCBA (PCB Assembly) to a very large extent. Generally, the standard reflow-soldering processes consist of four steps:

1. Forced convection
2. Vapor phase
3. Infrared drying (with restrictions)
4. Typical temperature profiles are suitable for board assembly.

During the reflow process, each solder joint has to be exposed to temperatures above the melting point of solder for a sufficient time to obtain the optimum solder joint quality, whereas overheating the PCB with its components should be avoided.

Figure 20 shows a general forced convection reflow profile for soldering SMD package. Table 5 shows an example of the important parameters of such a soldering profile for tin-lead and lead-free alloys.

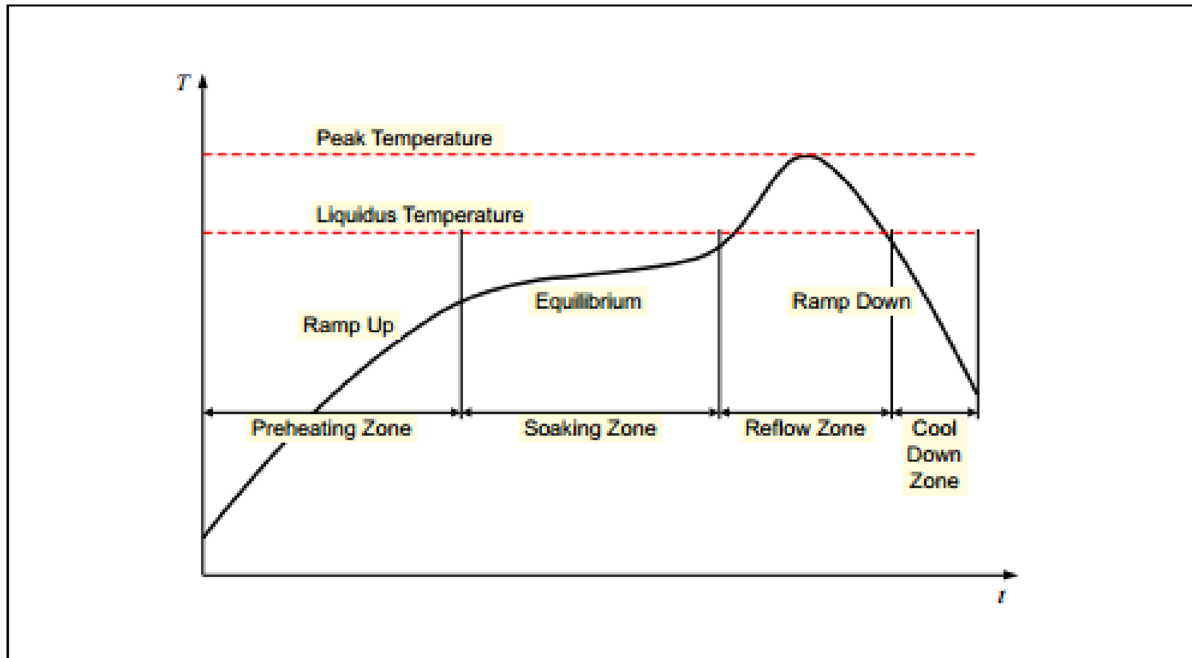

Figure 20. General Reflow Solder Profile

Table 5. Example of Reflow Solder Profile

Parameter	Tin-lead Alloy (SnPb or SnPbAg)	Lead-free Alloy (SnAgCu)	Main Influences coming from ...
Preheating rate	2.5 K/s	2.5 K/s	Flux system (Solder paste)
Soaking temperature	140 - 170°C	140 - 170°C	Flux system (Solder paste)
Soaking time	80 s	80 s	Flux system (Solder paste)
Peak temperature	225°C	245°C	Alloy (Solder paste)

1.10 Accelerated Life Testing

Traditional life data analysis involves analyzing times-to-failure data obtained under normal operating conditions in order to quantify the life characteristics of a product, system or component. To obtain such times-to-failure data may be very difficult or impossible for many reasons. The reasons for these challenges include the long life times of today's consumer products, the small time period between design and release, and the large challenge of testing products that are used continuously under normal conditions. Given these challenges and the need to observe failures of products to better understand their failure modes and life characteristics, reliability practitioners have attempted to

devise methods that force these products to fail more quickly than they would under normal conditions of use. In other words, the practitioners tried to accelerate their failures. Over the years, the phrase-accelerated life testing has been used to describe all such practices.

• Temperature cycling: The accelerated thermal cycling is generally used to compare the performance of different packages. The test conditions are accelerated by using cycle times and temperatures over and above what the actual use requires.

• Thermal shock: The thermal shock testing consists of two main types. The first type is an air chamber in which the specimen is alternately exposed to hot and cold air. The other type consists of a liquid bath in which the specimen is alternately exposed to hot and cold liquid.

• Drop: The drop test examines the mechanical integrity of the package and/or assembly under a mechanical shock. It uses machines to generate shock with such methods as free fall and elastic rebound. For special (military) purpose products, a common method is MIL standards half sine shock testing. [19]

• Vibration: The vibration test shakes circuit boards by using sine wave testing to random wave testing and shock testing, which provides testing that more closely resembles the actual environment.

1.11 Outline of the Dissertation

This dissertation is divided into the following chapters:

- Chapter 1: Introduction to Surface Mount Technology, package component types, board substrates, solder paste and SnPb/Pb-free soldering alloys, board finishes, and SMT processes.

- Chapter 2: Literature review on the lead-free solders development; microstructural changes of solder joints; and elevated vibration, drop, and thermal aging effects.
- Chapter 3: Description of the test vehicle, SMT assembly process, and experimental setup.
- Chapter 4: Description of the data analysis of different solder alloys, different package sizes, and different surface finishes under aging and thermal cycling.
- Chapter 5: Description of the failure analysis of BGA Component under aging and thermal cycling.
- Chapter 6: Summary and conclusion.

Chapter 2

Literature Review

2.1 Introduction

Solder plays a crucial role in the assembly and interconnection of electronic products. As a joint material, solder provides electronic, thermal and mechanical continuity. Owing to the realization of the harmful influence of lead on the environment and human health, many Pb-free solder-alloys have been developed to replace SnPb solders in electronic applications [20] [21]. [22], [23], [24], [25], [26] and [27]. SAC solder has been proposed as the most promising substitute for lead-containing solders because of its relatively low melting temperature, its superior mechanical properties, and its relatively good wettability.

Several studies performed the thermal-mechanical properties of SAC alloy. Microstructure evolution and deformation caused by global CTE mismatch between components and printed circuit boards, and local CTE differences in various phases or grains in the solder [28] were the two primary factors that reduce package reliability.

Most studies pay attention to the mechanical property change and microstructural evolution of solder joints subjected to accelerated mechanical test conditions such as drop and vibration tests. Thermal cycling or thermo-mechanical fatigue testing of solder joints is very important for the reliability of solder joints. Because of large difference in the coefficient of thermal expansion (CTE) of the different constituents in the packaged assembly, stresses and strains vary with temperature leading cyclic strain or inelastic energy damage and fatigue failure of the solder joints [29]. However, only limited attention has been paid to the effect of package characteristic lifetime reliability under long term isothermal aging at elevated temperatures, which is one of the topics in this

dissertation. The reason is the test has high requirement for the equipment, time period and labor hours. Most studies also have the limitation of package size and die size variation. This paper puts real electronic packages, with large deviations in experimental designs, die sizes, package sizes, ball counts, and pitch sizes as considerable variations. Furthermore, surface finish effect is less talked about under long term aging/cycling condition.

2.2 Effect of IMC

2.2.1 General Information

Hosford, et al. and Smallman, et al., [30], [31] found the microstructural characteristics of an alloy determine its mechanical performance. Therefore, understanding the microstructural characteristics of the SAC alloy is essential to understand the mechanical performance and reliability of SAC solder joints.

J.C. Suhling performed the formation of intermetallic compounds between the primary elements Sn and Ag, and Cu affect all the properties of the SAC alloys. According to the binary phase diagram shown in Figure 21, there are two possible intermetallic compounds that may be formed: Ag_3Sn forms due to the reaction between Sn and Ag as shown in Figure 21a and Cu_6Sn_5 forms due to the Sn and Cu reaction as shown in Figure 21b [23].

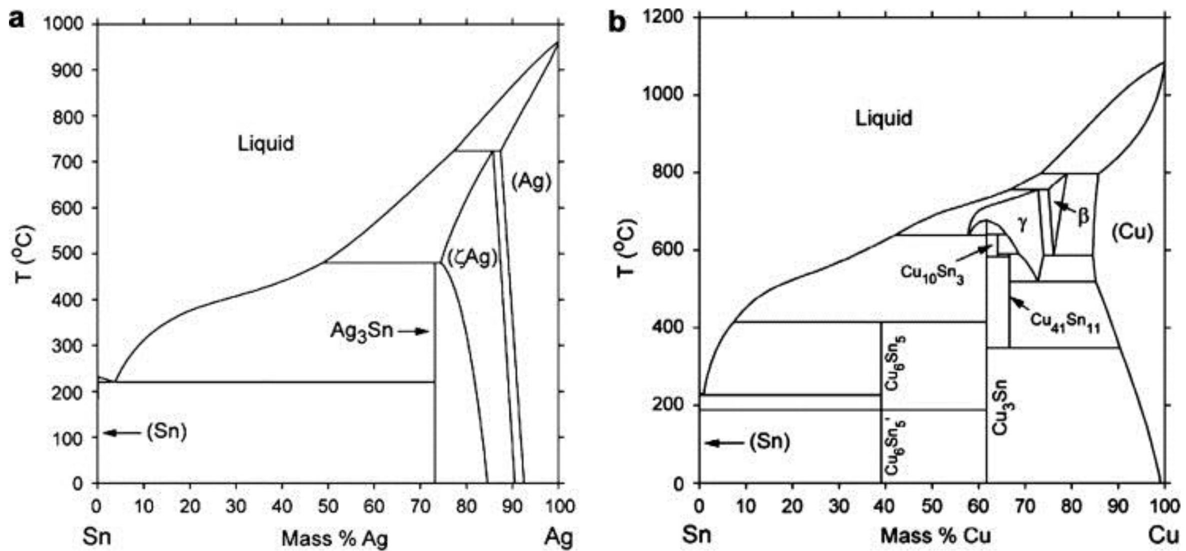

Figure 21. Binary phase diagram (a) Sn–Ag and (b) Sn–Cu

2.2.2 Effect of Ag_3Sn IMC

Shnawah et al. [31] investigated the as-soldered microstructure or initial microstructure of Sn–xAg–Cu. They found that the microstructures of Sn–xAg–Cu alloy consisted of a β-Sn matrix with dispersoids of fine Ag_3Sn and coarsened Cu_6Sn_5 intermetallic compounds (IMCs). They concluded high Ag content SAC solder (SAC305/SAC405) yields large numbers of Ag_3Sn IMC particles and small sizes of primary Sn grains based on Figure 22. This showed that the number or volume fraction of the fine Ag_3Sn IMC particles in the bulk alloy microstructure of SAC solder alloy tends to increase with increasing Ag content. On the other hand, low Ag content SAC alloy (SAC105) gives rise to more primary Sn phase (large Sn grains) and decreases number of Ag_3Sn IMC particles.

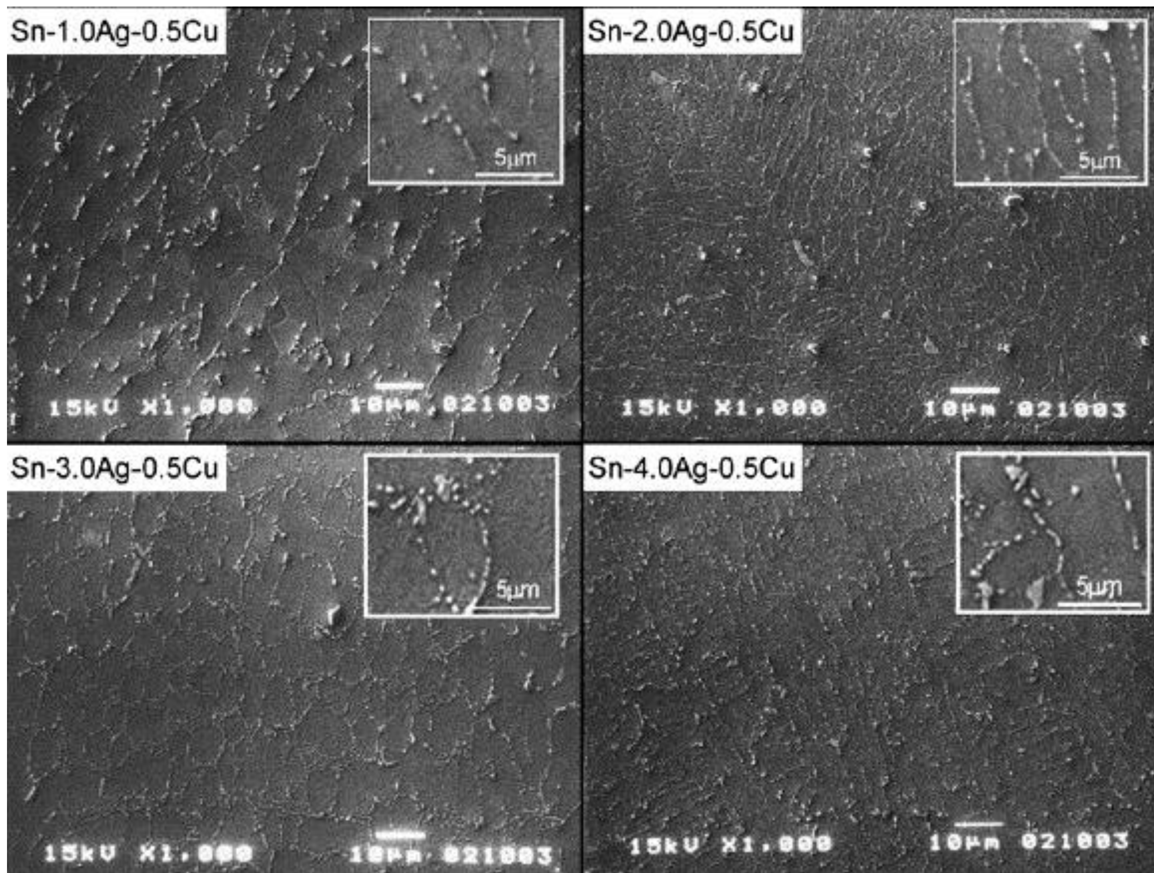

Figure 22. The initial microstructure of Sn–xAg–Cu bulk solders.

Kim et al. [32] reported that the formation of large Ag3Sn could be attributed to the solder composition, and there was little effect from substrates. They observed large Ag3Sn for high Ag content solder joints, the shapes of which were dendrite-like and hopper crystal-like plates. The formation sites of large Ag3Sn plates were at the top of the interfacial reaction layer and the voids.

Chen et al. [33] showed that three types of Ag_3Sn compounds during solidification at different cooling rates are found to be particle-like, needle-like and plate-like. If large Ag_3Sn plates form at the stress concentration region, cracks can initiate and propagate along the interface between the Ag_3Sn and the solder, which deteriorate the reliability of solder joint. However, Anderson et al.[34] indicated fine Ag_3Sn precipitates can pin the

grain boundaries in the solder, stabilize the microstructure and strengthen the matrix. Ag_3Sn particles could be evenly distributed among the eutectic or along the Sn-rich phase boundary in SnAgCu systems.

In Tsai et al.'s research work, [35] the Ag_3Sn and Cu_6Sn_5 IMC particles possess much higher strength than the bulk material in SAC alloy, while primary Sn has the lowest elastic modulus and lowest yield strength among the constituent phases in SAC solder, which is provided by Daewoong et al.[36] . Fine IMC particles in the Sn matrix can therefore strengthen the alloys.

2.2.3 Effect of Cu-Sn IMC

Cu is extensively used as the contact metallization in conventional electronic assemblies particularly on printed circuit boards (PCBs) and increasingly as the interconnection layer on semiconductor devices in electronics industry, while Sn-based alloys are universally used as interconnection materials [37], [38] and [39]. The resulting Cu–Sn intermetallic compounds formed during soldering process shows an important role in the wettability of solders [40].

The intermetallic layer appears to be comprised of two compounds of different compositions. Zhang et al. [41] presented the research work with SnAgCu solder and bare Cu substrates of reaction couples aged at 125 ℃ for different aging times. They found the accelerated growth of the intermetallic compound layer with the aging time during isothermal aging. Binary intermetallic compound layers were formed at the solder joints on copper substrate. Cu6Sn5 forms first at the interface under thermal condition for SAC solder. Cu_3Sn will form later between Cu and Cu_6Sn_5 by solid-state reaction to satisfy the requirements of local equilibrium. In their EPMA analysis results, the planar

intermetallic layer next to the solder possesses a composition (at.%) of Cu:Sn = 6.1:5, which corresponds to the Cu_6Sn_5 phase. The composition of the intermetallic layer next to the copper is Cu:Sn = 3:1, which corresponds to the Cu_3Sn phase.

Tu and Thompson [42] propose that the growth rate of Cu_6Sn_5 in bimetallic Cu–Sn thin film is linear, and the reduction rate of Cu_6Sn_5 due to the growth of Cu_3Sn is parabolic. Formation of the intermetallic compound (IMC) layers at the interface is an indication of good bonding between solder and the metal pad. However, Gan et al. investigated excessive intermetallic growth and the brittle nature of the intermetallic layer can be detrimental to the mechanical reliability of the joint [43].

Moreover, recent investigations [44],[45] and [46] had reported that the growth of Cu–Sn IMC layer had a degraded effect on the solder joint reliability, with increasing thickness of the Cu–Sn IMC layer, the thermal fatigue life, tensile strength and fracture toughness of solder joints will decrease. As a result, the interfacial reaction may be directly related to the solder joint reliability in the electronic package.

2.2.4 Effect of IMC Thickness Growth

Generally, the thickness of the IMC layer at the interface between the solder and substrate is very important in determining the reliability of the whole package because an excessively thick IMC layer is sensitive to stress and sometimes provides initiation sites and paths for the propagation of cracks. Therefore, as the growth of the IMC layer could degrade the reliability of the solder joint, it is essential to study the formation and growth of the IMC layer. [47]

Trend 1: IMC layer

Ramkumar et al. [48] gave the intermetallic compounds growth maps for five different finishes on lead-free 0201 (L 0.02 in.; W 0.01 in.) package. The test condition is isothermal aging at 150 ℃ up to 500 h. It showed the average IMC thickness with ENIG finishes slightly growing during aging due to the nickel barrier of the IMC layer only. (Figure 23)

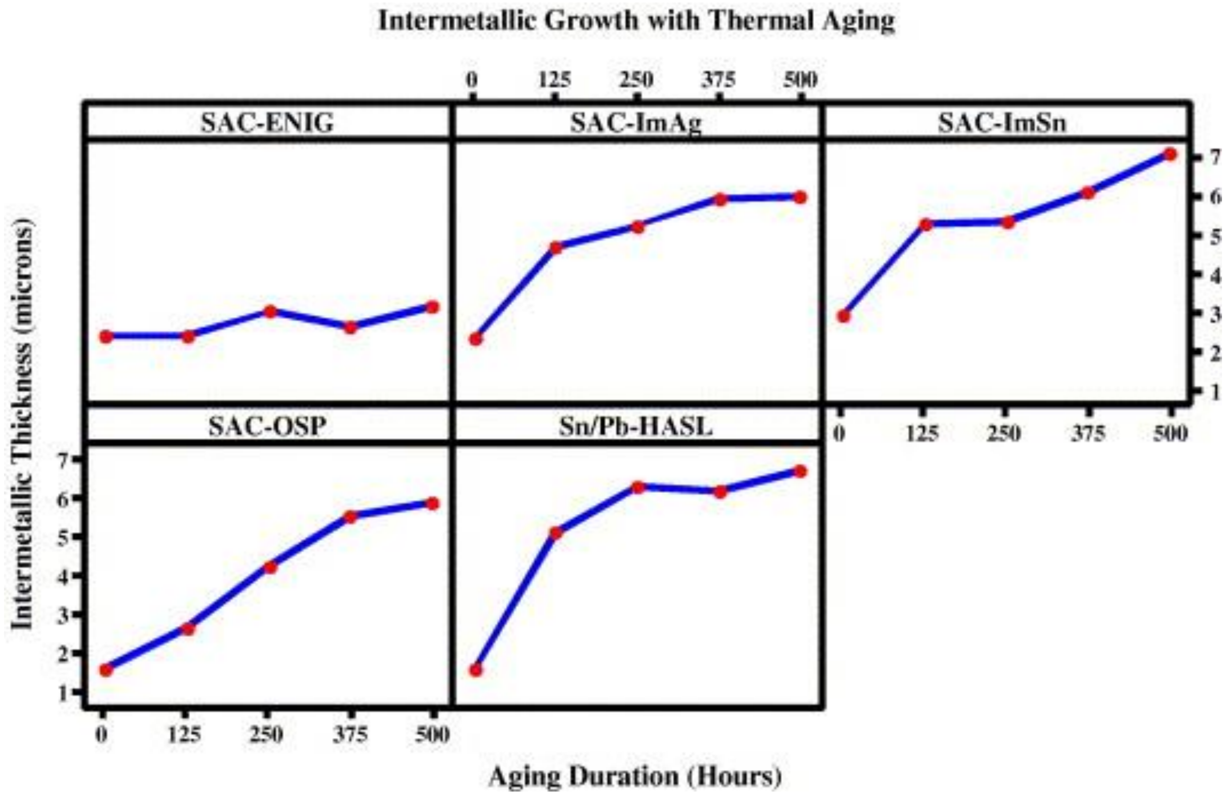

Figure 23. Intermetallic growth with isothermal aging

Trend 2:

For the IMC layer growth, Zhang et al. [45] showed the reaction happened inside of Cu3Sn/Cu6Sn5 IMC. They presented an equation:

$$\mathbf{Cu_6Sn_5 + Cu \rightarrow Cu_3Sn}$$

This explained that the interfacial reaction happens after Cu atoms arrive at the interface of Cu_3Sn/Cu_6Sn_5 by diffusion through the grain boundaries of the Cu_3Sn layer. By this reaction, Cu_6Sn_5 is converted to Cu_3Sn at the interface.

2.2.5 Effect of IMC with different Surface Finish

Berthou et al. and Pang et al. [49] illustrated that the composition of the IMC layer depends on PCB finish. For ImSn, a first layer Cu_6Sn_5 intermetallic is formed at the PCB/solder joint interface. Then, during aging a second layer of Cu_3Sn is formed at the IMC layer/PCB interface, which reduces the mechanical behavior of the solder joint. For ENIG finish, the IMC layer is of CuSn type with a small proportion of nickel: layer $(Ni, Cu)_6Sn_5$. The nickel layer will act as a diffusion barrier by preventing the formation of the Cu3Sn layer. Phosphorus is also present, due to the process deposition of the nickel layer.

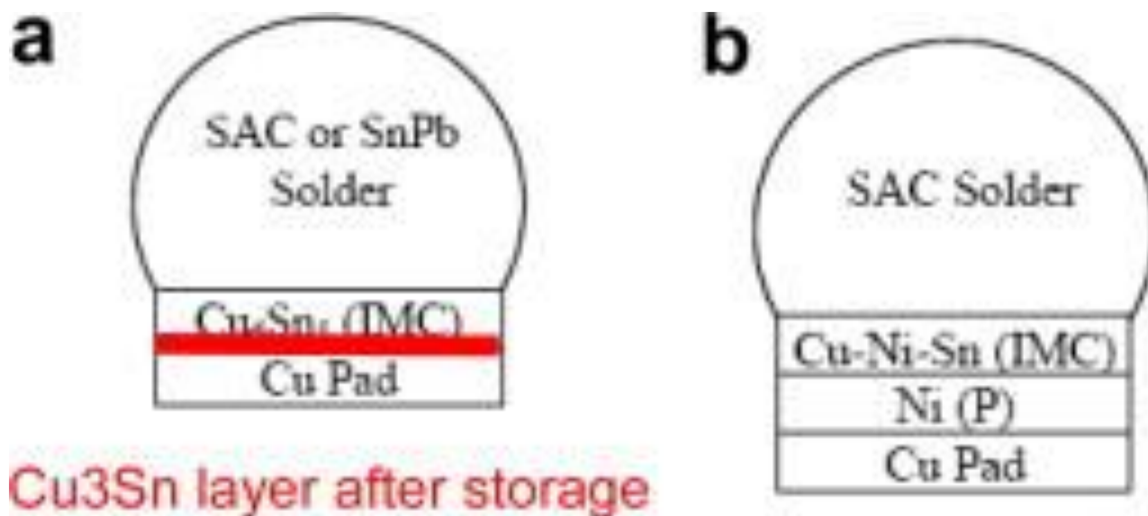

Figure 24. IMC Layer of ENIG (a) and ENEPIG (b)

2.2.6 Effect of Sn Recrystallization

Berthou et al. [49] performed an accelerated thermal cycling test for Chip resistors 1206 and BGA with SAC305 solder. The cycling temperature was −55/+125 ℃, with

ramp and dwell time of 20 min. Cross-sections were performed in accordance with the failure analysis method, at $T = 0$, 500, 750 and 1000 thermal cycles. The evolution of the microstructure was observed on BGA SAC solder ball after 1000 thermal cycles. An observation with cross polarized light permits to see the recrystallization of the Sn macro-grain into small Sn grains (Figure 25).

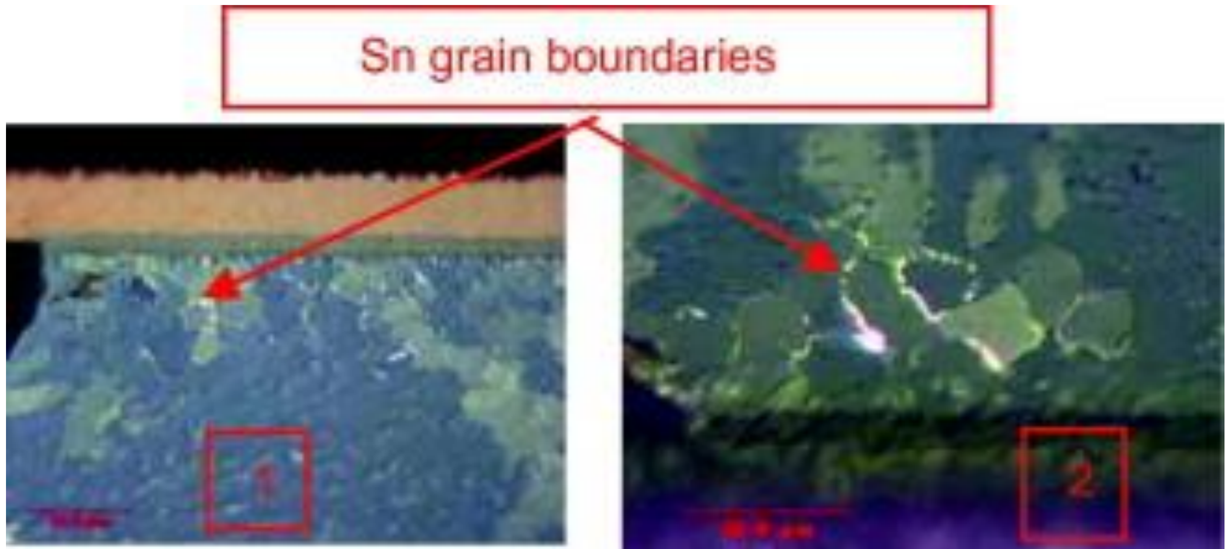

Figure 25. Sn grain boundaries under cross polarized light, zone (1) and (2).

In the paper, they proposed the evolution of SAC solder joint in thermo-mechanical fatigue in Figure 26.

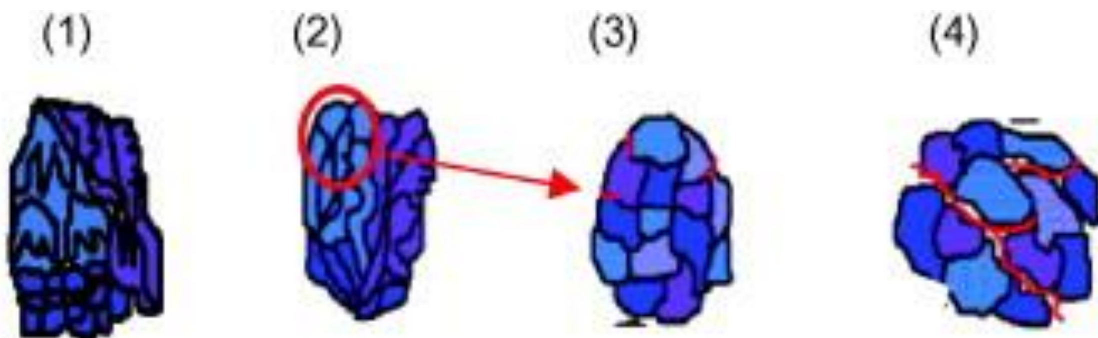

Figure 26. Recrystallization

Creep/stress relaxation is accompanied by a recrystallization phenomenon. In step (1), the dendritic structure is fine and regular with polarized light microscopy, so it is possible to see the number of dendrite (β-Sn phase) groups having the same crystallographic orientation.

(2) The number of tin macro-grains is higher than in the first step, and the dendritic structure is rougher.

(3) The crack initiates along these Sn grain boundaries.

(4) Finally, the crack propagates through the recrystallized zone along tin grain boundaries until electrical opening in solder joint. [50-55]

2.3 Drop Test Effect for ENIG, ENEPIG finishes

Ha et. al. [56-57] studied the effects of different PCB surface finishes, as ENIG and ENEPIG, after reflow and thermal aging (1,000h at 125°C). In this study, they used Sn-3.0Ag-0.5Cu BGA balls with a diameter of 450mm and a rigid PCB (FR-4), which is an SMD (Solder Mask Defined) type board. The drop test board was fixed to the drop table of the drop tester (SD-10, LAB, USA) at each corner with the mounted packages facing downward, following JESD22-B111. The drop table was then released at a certain height and dropped freely to impact on the strike surface repetitively, each time creating a half-sine impact acceleration pulse with a peak acceleration of 900G (1G =9.81 m/s) and an impact duration of 0.7ms (Figure 27). The drop test condition corresponded to the JEDEC drop test condition F. When the resistance increases by more than 100ohms from the initial resistance at the time of shock and results in 0ohms, it is then regarded as a failure. Moreover, when such an increase in resistance is observed at least 3 times out of 5 in the shock test, it is regarded as a failure.

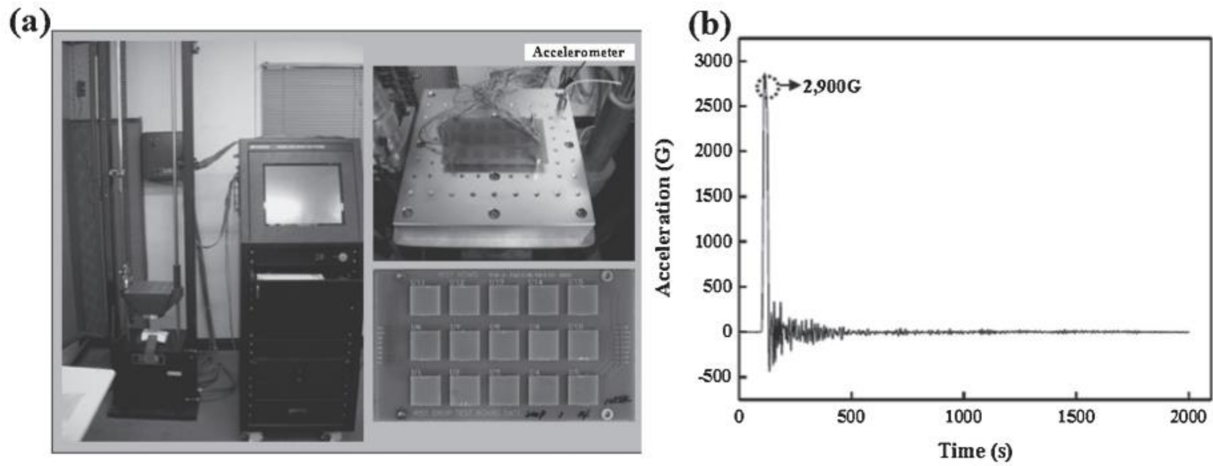

Figure 27. Drop Test Setup

See Figure 28 for the results of the drop test. The ENEPIG board has greater reliability after reflow than the ENIG board and shows excellent characteristics under all conditions after thermal aging. The ENEPIG board is least sensitive to temperature and therefore shows better reliability before and after thermal aging. Moreover, Figure 28 illustrates that the Pd layer causes the ENEPIG board to have greater reliability in the drop test than the ENIG board, because of its superior characteristics.

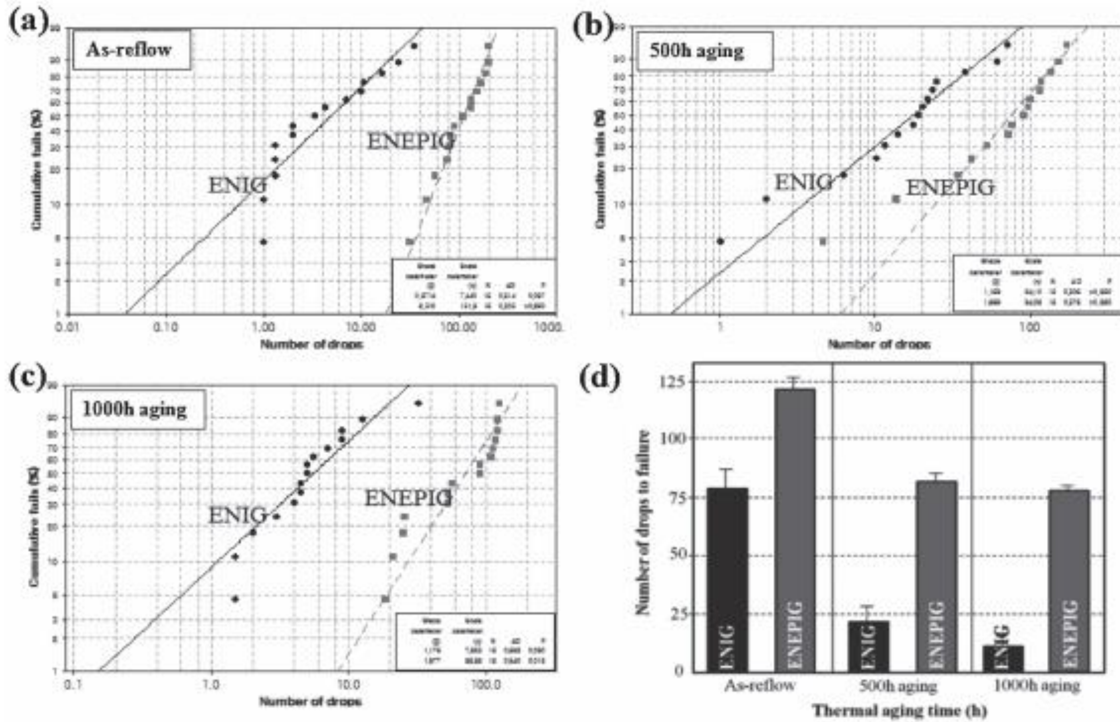

Figure 28. Weibull Life Time Analysis

2.4 Vibration Test for ENEPIG/ImAg Finishes

Surface finishes are used to preserve and promote solderability of exposed copper metallization on printed wiring boards [58-60]. In Menoon et. al.'s study [61], the durability of solder interconnects that are formed between BGAs and ENEPIG finished pads using SnPb and SAC305 solders under harmonic vibration loading is examined. ENEPIG test specimens with two thicknesses of palladium were evaluated (Table 6). Isothermal preconditioning levels at 100 ℃ for 24hrs and 500hrs were included to evaluate the impact of intermetalic evolution on the durability of the soldered interconnects. Tests specimens created with immersion silver (ImAg) finished printed wiring boards were also included for comparison. The failure data found that the durability of interconnects formed with ENEPIG finish has comparable or better durability than the durability of interconnects formed with ImAg finish irrespective of the

solder. The tests indicate that the use of a thicker palladium layer reduced the degradation in durability that occurred from isothermal aging.

Table 6. Test Vehicle Surface Finish

Surface Finish	Material	Thickness
ImAg	Silver (Ag)	0.2 µm
ENEPIG-A	Nickel (Ni)	5 µm
	Palladium (Pd)	0.05 µm - 0.10 µm
	Gold (Au)	30 nm - 50 nm
ENEPIG-B	Nickel (Ni)	5 µm
	Palladium (Pd)	0.15 µm - 0.20 µm
	Gold (Au)	30 nm - 50 nm

The cycles to failure were estimated by multiplying the time to failure with the measured cyclic frequency. The cycles to failure data were fit to 2-Parameter Weibull distributions to obtain characteristic life (η) and shape parameter (β). These Weibull results are shown in Table 7. The characteristic lives for the ImAg and the ENEPIG samples were similar in the case of the SnPb solder. However, in the case of the SAC305 solder, the characteristic lives of the ENEPIG samples exceeded those of the ImAg samples. This drop may be due to the gold or palladium impacting the formation of the interfacial IMC layer and changes to the bulk solder. The drop in characteristic life with increased aging time was more significant in the ENEPIG finish with the thinner palladium layer [62].

Table 7. Weibull Parameters (a) SnPb Solder (b) SAC 305 Solder

Solder Type	SnPb			
Aging Condition	100°C/24 hrs		100°C/500 hrs	
Weibull Parameters	η	β	η	β
ImAg	2.4E+06	0.7	4.9E+06	0.7
ENEPIG-A	5.6E+06	0.8	1.0E+06	1.0
ENEPIG-B	6.7E+06	0.6	2.1E+06	1.3

(a)

Solder Type	SAC305			
Aging Condition	100°C/24 hrs		100°C/500 hrs	
Weibull Parameters	η	β	η	β
ImAg	6.2E+05	0.7	5.8E+05	0.5
ENEPIG-A	2.4E+07	0.8	3.8E+06	0.6
ENEPIG-B	1.0E+07	0.8	3.5E+06	0.6

(b)

2.5 Thermal Aging and Cycling

A wide variety of SAC solders containing different levels of Ag has been studied and is currently in use for a wide range of applications in the electronics industry. Henshall et. al. [63] concluded that the content level of Ag in SAC solder alloys is of advantage or disadvantage depending on the requirements of application, package, and reliability. Syed et. al. [64] mentioned the best level of Ag content for drop performance is not necessarily the best level for optimum temperature cycling reliability. Hence, the

SAC alloys are limited in their potential applications in the portable electronic products in which thermal cycling and drop/impact are the primary requirement for board level solders joint reliability. [65]

Shnawah et al. [31] evaluated the SAC105 and SAC305 solder ball joints for BGA interconnections under temperature cycling and drop impact tests (Figure 29). The data indicated that lower Ag content solder balls perform better under drop impact loading conditions, while temperature cycling reliability suffers as Ag content decreases. In other words as also seen in Figure 29a, SAC105 solder balls showed better performance than SAC305 under drop loading conditions. However, the trend is reversed for temperature cycle test (Figure 29b).

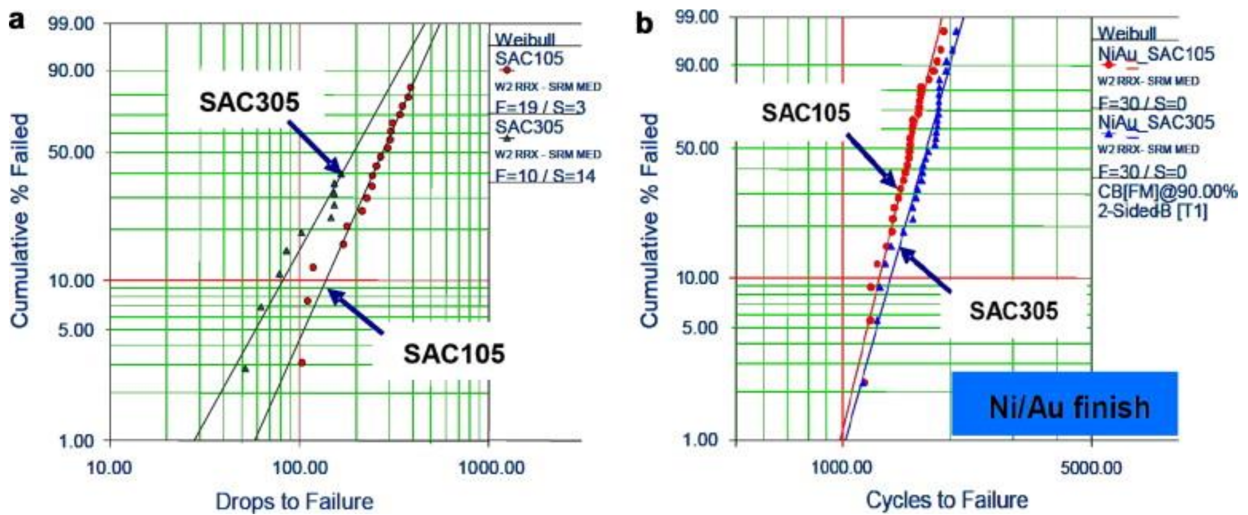

Figure 29. (a) Drop impact test and (b) Temperature cycling test.

Chapter 3

Test Introduction

3.1 Introduction

Lots of studies [34-65] demonstrate that Pb-free solder reliability undergoes significant changes over time, which leads to our studies here of the effect of aging on Pb-free solder reliability. Drop and vibration tests were conducted by many researchers. Isothermal aging effects on lead-free solders have been extensively investigated and showed aging effects significantly degrade the mechanical properties of lead-free solders. However, limited work has been done on the effects of aging on board-level thermal performance of lead-free solder; limited studies have been done on the different surface finishes for various packages. Aging effect on different most popular SAC105 and SAC305 with ENIG and ENEPIG finishes is still unknown; limited work were studied the reliability for long reliability >=6 months; limited work were studied to analysis the different acceleration factors of the reliability on aging effects and the trends of aging on different package designs. In order to break through those limitations, the TV-7 research project was introduced. In previous studies, Zhang, et al. [66-71] concluded that a direct and deleterious effect on packaging reliability results during long-term isothermal aging for fine-pitch ball grid array (BGA) packages with Sn-1.0Ag-0.5Cu (SAC105), Sn-3.0Ag-0.5Cu (SAC305), and Sn-37Pb solder ball interconnects.

The purpose of this work is to discover the role of isothermal aging on the reliability of Sn-Ag-Cu (SAC) assemblies. Different surface finishes mixed with various types and sizes of packages were employed in our test vehicles. A full experiment matrix with varying aging temperatures and solder alloys was considered, followed by accelerated

thermal cycling to generate Weibull plots showing how the package reliability depends on aging time and temperature.

3.2 Test Vehicle Design and Assembly

3.2.1 Test Vehicle

The assembled test vehicle is shown in Fig. 30. The assembly test boards were four-layer FR-4 glass epoxy PCBs with dimensions 100.076 x 67.056 mm having a glass transition temperature (Tg) of 170°C. Each test board was populated with 5x5mm, 10x10mm, 15x15mm, and 19x19mm, 7×7mm CSP, 5×5mm MLF and a series of 2512 resistors.

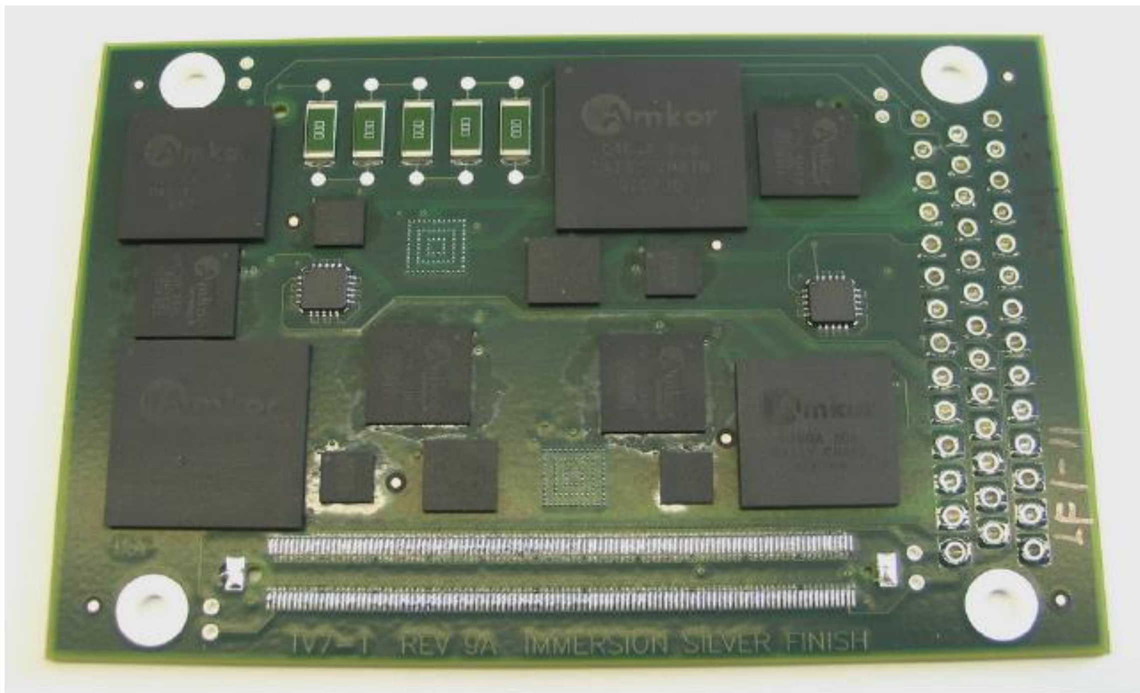

Figure 30. Test vehicle.

The boards in the test used non solder mask design (NSMD) pads for easier analysis of aging on the reliability. The Sn termination resistors (passive devices) measured 6.3

mm x 3.2 mm. Industry-standard naming conventions of resistor sizes described the length and width of its body in hundredths of an inch. The resistors used in this research are thus referred to as 2512. They were mounted in banks of five resistors placed in series. All test components provided by Practical Components were daisy chained for continuous sampling of component reliability through the accelerated life tests. The detail information of components is listed as Table 8.

Table 8. Component Matrix

Package Type	Body Size (mm)	Die Size (mm)	Ball/Lead Count	Pitch (mm)	Ball Allignment
BGA	19X19	12.0X12.0	288	0.8	Perimeter
BGA	15X15	12.7X12.7	208	0.8	Perimeter
BGA	10X10	5.0X5.0	360	0.4	Perimeter
BGA	5X5	3.2X3.2	97	0.4	Full Array
CSP	7X7	5.9X5.9	84	0.5	Perimeter
QFN	5X5	4.5X4.5	20	0.25	

3.2.2 Surface Finish

To help identify the board with different finishes, we apply two different colors for the PCB board. The green one is ENIG, the red one is ENEPIG (Figure 31).

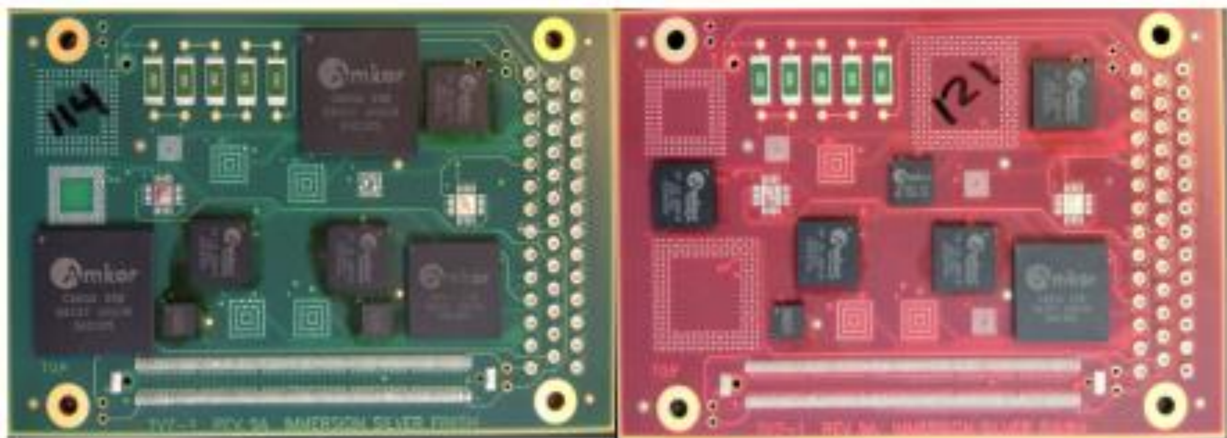

Figure 31. ENIG (Left) and ENEPIG (Right)

Rutherford Backscattering Spectroscopy (RBS) is conducted for ENIG and ENEPIG to measure the thickness of metallic layers, see Figure 32. The ENIG finish consists of two metallic layers: a thin gold coating over the thicker nickel coating deposited via electroless process directly onto the PCB copper pad. The additional 0.15 um of Pd layer from ENEPIG improves the wettability and acts as a diffusion barrier [66-67].

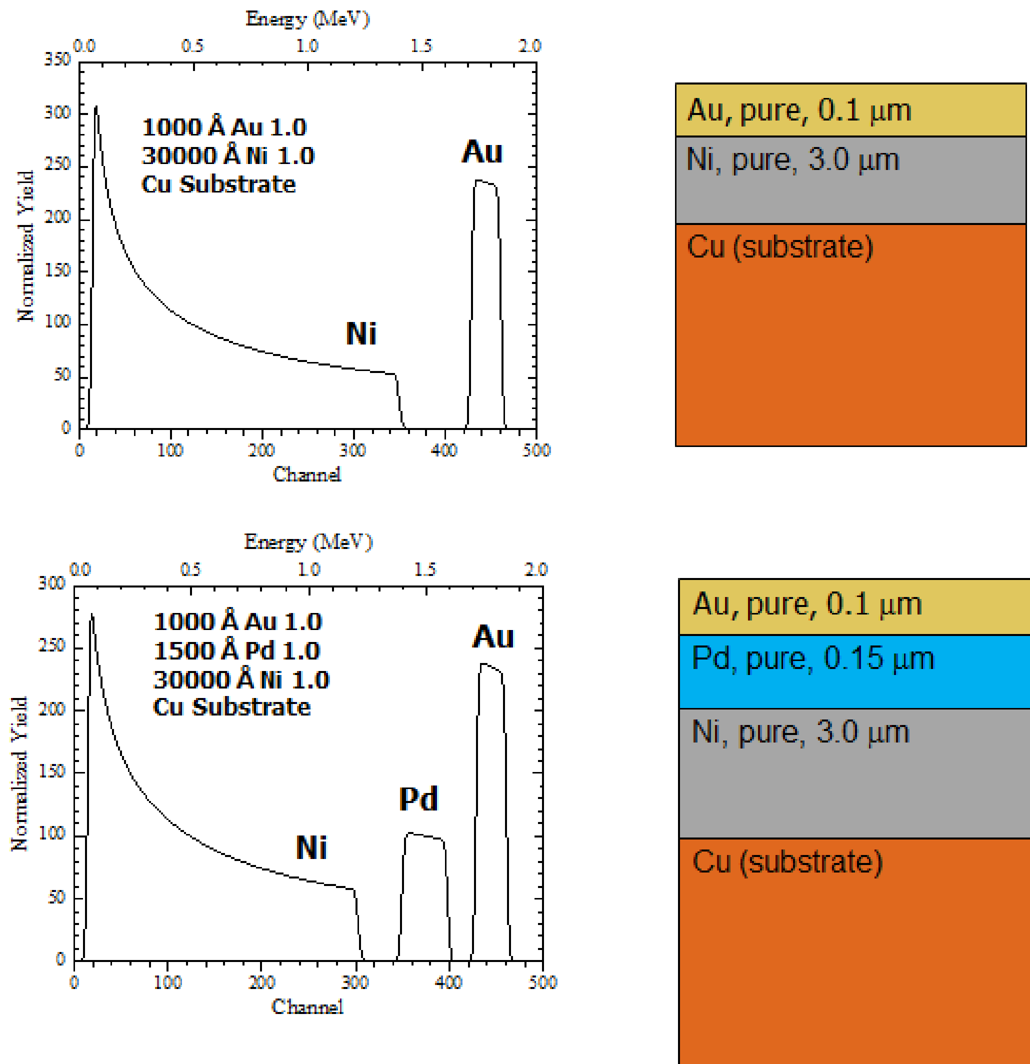

Figure 32. RBS Analysis for ENIG and ENEPIG

3.2.3 Solder Paste and Stencils

No-clean-type 3-Kester 256 paste (Sn-37Pb) and SAC 305 solder paste were the two main solder pastes we selected for testing. For the lead-free test vehicle, the components were built onto the PCB with no clean Senju305 M31-GRN360-k1MK-V (Table 9).

Table 9. Lead-free Solder Paste Parameters

Item	ECO M31-GRN360-K1MK-V Specification	Test method
Alloy Composition	Ag:3.5, Cu:0.75, Sn:Balance	J-STD-006
Powder Shape Powder Grain Size	Spherical Type 3 (25~45µm)	J-STD-005-3.3.3, STM-12, J-STD 005-3.3

We applied the E-FAB Electroform stencil for our test, the thickness of which is 0.115 mm (0.0045 in). The solder paste print machine used was MPM UP2000 HiE.

Solder paste printing machine: MPM UP2000 HiE

Figure 33. Printing Machine

3.2.4 SMT Assembly Processes

All the test vehicles were fabricated in Continental AG – Huntsville Electronics Division. Before assembly, there is a 12 hour "bake out" process in an oven at 150 ℃ to remove moisture and prevent damage to the components during reflow. The stencil and the PCB were positioned in the screen printer and the solder paste was pressed through the stencil with a rubber squeegee. The board was transferred out and inspected for correct alignment of the solder paste to the PCB pad sites.

Next, the PCBs were put into two placement machines: Assembleon MG-1 and Universal GSM-1. MG-1 used a tape and real feeder to place small components: resistors, 5mmBGA, MLF, CSP and 10mmBGA; GSM-1 used a tray feeder to pick and place 15mm BGA and 19mm BGA components. Once the machine stared to receive boards, the programmed algorithm began and all the electronic components were picked and placed onto the test vehicle in order. The board was then checked again in case of skewed package placement. Figure 34 shows the Continental Electronics prototype manufacturing lab.

Figure 34. The Continental Electronics prototype manufacturing lab

Figure 35 shows the 13-zone Rehm V7 convection reflow oven used for reflow. The oven supplies a nitrogen gas environment during reflow and has a conveyor speed of 33.5 inch/min. The temperature was monitored and the SAC alloys melting temperature was ~ 217 ^{o}C. The peak temperature was 245–247 ^{o}C for PBGAs and 252 ^{o}C for resistors. The time duration for PBGAs in the oven above the melting point was around 52 to 55 seconds, and 61 seconds for resistors. In the Sn-37Pb assemblies' thermal profile, the peak temperature of PBGAs was between 224 to 229 ^{o}C. Resistors had a peak temperature of 231 ^{o}C. The time duration for PBGAs in the oven above the melting point was around 60 to 65 seconds, and 67 seconds for resistors. By comparing two processes, there was a difference of 21 ^{o}C in the peak temperature of PBGAs [68]. The Pb-free-reflow profiles used for the assembly are shown in Figure 36.

Relfow Oven: Rehm V7

Figure 35. Reflow Oven

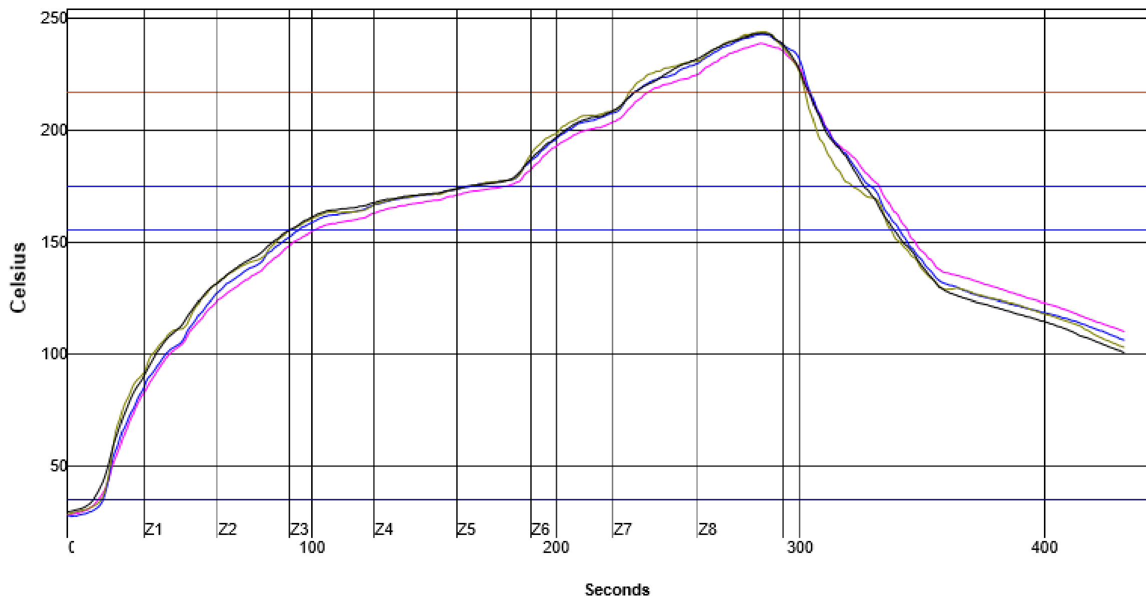

Figure 36. Reflow Profile (X-axis: Time-Second; Y-axis: Temperature-Celsius)

Figure 36 maps the reflow profile. The conveyor speed is 26.0 inch/min. Preheat temperature is from 35-155°C at the time period 0-100 seconds. Soak time is from 155-175°C at the time period 100-200 seconds. The low limit of peak temperature is 235°C. And the high limit of peak temperature is 245°C. The total time above SAC melting temperature 217 ^{o}C is about 90 seconds.

3.2.5 Inspection Test Vehicle

A transmission X-ray tomography system was used to inspect the quality of the solder joints in the assemblies. This type of system is good for detecting problems such as insufficient solder, solder ball bridging, pad skewing, and voids in joints.[69] Figure 37 shows a couple of cases of pad skewing and solder bridging and how they would look in such a system. We found very few cases of misaligned assembly.

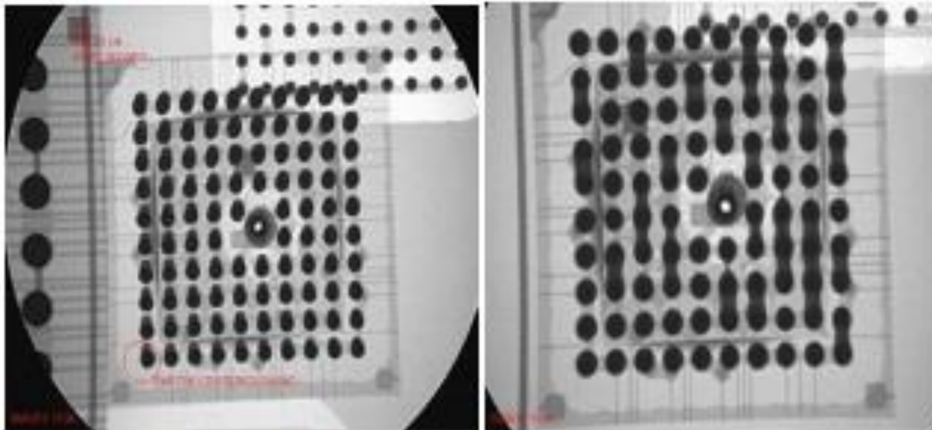

Figure 37. Skewed Pad on the Left and Solder Bridging on the right

3.3 Thermal Test

3.3.1 Test Matrix and Test Conditions

The test vehicles were grouped in time periods of 0, 6, and 12 months and subjected to 125°C aging temperature. The full matrix is shown in Tables 10. Our thermal testing

design followed mainstream industry standards recommended by the Institute for Interconnecting and Packaging Electronic Circuits (IPC) and the Joint Electron Device Engineering Council (JEDEC).[70] For the thermal cycling reliability test, thermal cycling (TCT) was carried out from -40°C to 125 °C per JEDEC JESD22-A104B-Condition G. All tests were set for a 15 min dwell time and 30 min ramp time thermal profile, shown in Figure 38.

Table 10. Test Plan

	No Aging		21 Days		6 Month		12 Month		24 Month	
Thermal Cycle -40°C~ +125°C	ENIG		ENIG		ENIG		ENIG			
	SnPb 10	SAC 5	SnPb 25	SAC 14	SnPb 15	SAC 15	SnPb 10	SAC 10		
	ENEPIG		ENEPIG		ENEPIG		ENEPIG			
	SnPb 5	SAC 5	SnPb 25	SAC 14	SnPb 15	SAC 15	SnPb 10	SAC 10		
	ImAg				ImAg		ImAg		ImAg	
	SnPb 5	SAC 8			SnPb 5	SAC 5	SnPb 5	SAC 5	SnPb 5	SAC 5

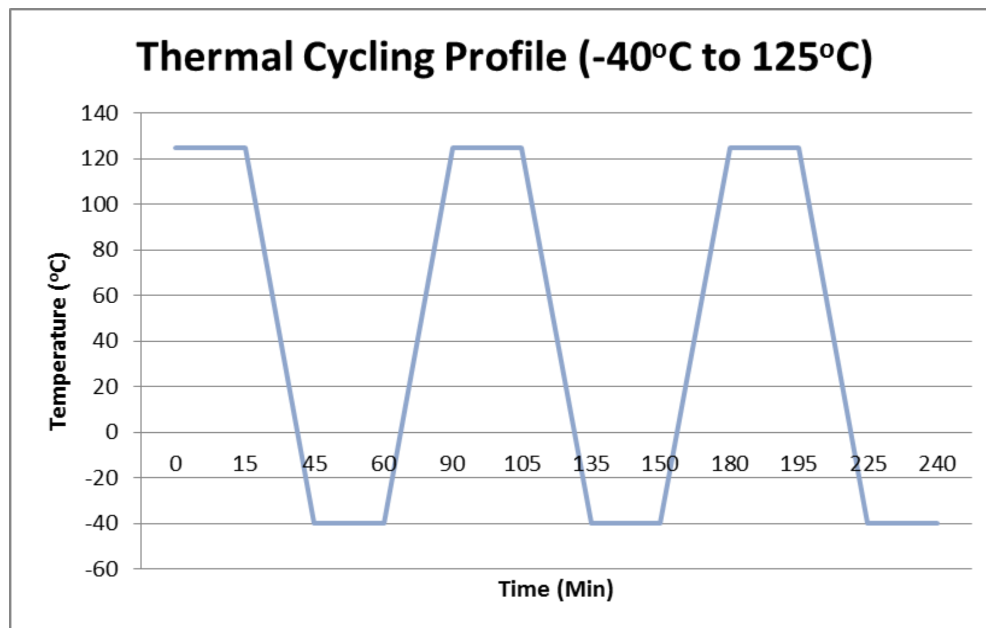

Figure 38. Thermal Cycling Profile

3.3.2 Data Acquisition System

The boards were placed vertically in the accelerated thermal cycling furnace and wired to a switch scanning system which allows for continuous monitoring of the various daisy chain networks was throughout the cycling using a high accuracy digital multimeter coupled with a high performance switching system controlled by LabView software. Based on IPC-9701, the practical definition of solder joint failure is an interruption of electrical continuity > 1000 Ohms. In this study, failure was defined to be the point when the daisy chain resistance was > 300 Ohms for five repeated resistance measurements. [71] Figure 39 shows the schematic design of the monitoring system.

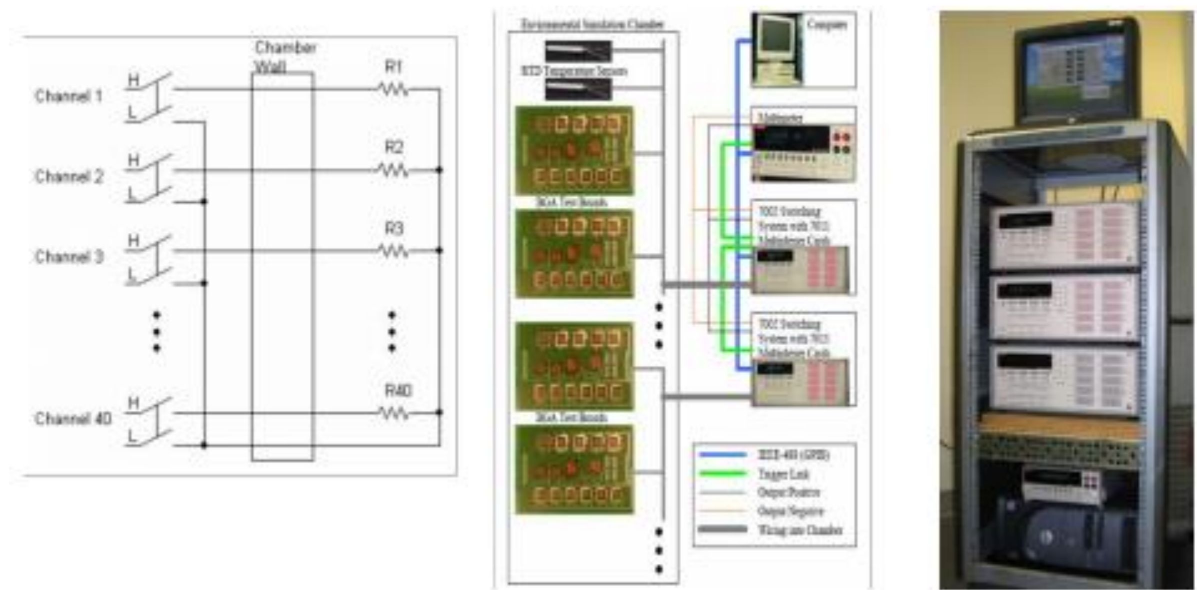

Figure 39. Schematic Design of the Monitoring System

3.4 Failure Analysis

All samples for microscopic examination were cross-sectioned and polished with SiC polishing paper (240, 320, 400, 600, 800, 1200), followed by 0.1um and 0.05um micron diamond suspension fine polishing. [72]After polishing, a thin gold or carbon film was sputtered on the surface of samples for the prevention of electrical charging

during SEM observation. SEM and energy dispersive X-ray spectroscopy (EDX) was used to investigate the microstructure of the joints.

The back-scattered electron (BSE) imaging mode was used in most of the electron micrographs to highlight the various microstructural features in the solder joints. Figure 40 demonstrated the schematic explanation of SEM functions. SEM uses a focused beam of high-energy electrons to generate a variety of signals at the surface. When the primary electron beam interacts with the specimen, the electrons lose energy within an absorption volume known as the interaction volume. Its size depends on the electron beam energy, the atomic number of the material, and the specimen density. The secondary electrons generated through the electron-surface interaction are collected by a scintillator, photomultiplier, and head amplifier detector system and directed to a cathode-ray tube monitor and/or digital image system.

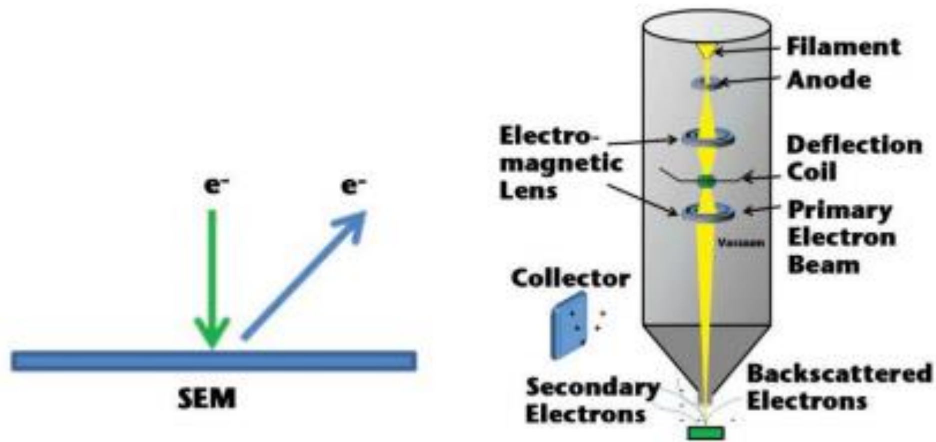

Figure 40. (a): SEM schematic showing the ion attack to release surface ions; (b): SEM schematic for beam signal

EDX is used with the SEM to acquire the elemental composition of the thin film and/or solder material. EDX rests upon the fact that each element has a unique atomic structure which emits distinctive X-rays after electron irradiation. The primary electron

beam possesses sufficient energy to ionize a core level of the target atom, which subsequently relaxes by an electron transition from an upper energy level to the vacated level. In the process, X-ray energy of a distinctive energy is emitted and detected by the X-ray detector in the SEM. Since each atom has a unique set of energy levels, the spectrum of X-ray energies allows determination of the elements in the absorption volume [72].

Chapter 4

Reliability Data Analysis

The failure life of electronic packages is characterized with a Weibull distribution. The characteristic life (η) is the point (i.e. number of cycles) at which 63.21% of the population is expected to fail. The slope (β) of the Weibull distribution distinguishes different classes of failure modes. The least squares method estimates the characteristic life and slope of the Weibull distribution. The r^2 value indicates the quality of the data fit.

4.1 Data Analysis of Aging Effect

The list of Weibull plots below generally depicted the reliability performance of 19mm, 15mm, 10mm, and 5mm BGA package subjected to 24 months 125°C aging.

a) Immersion Ag, SAC 305

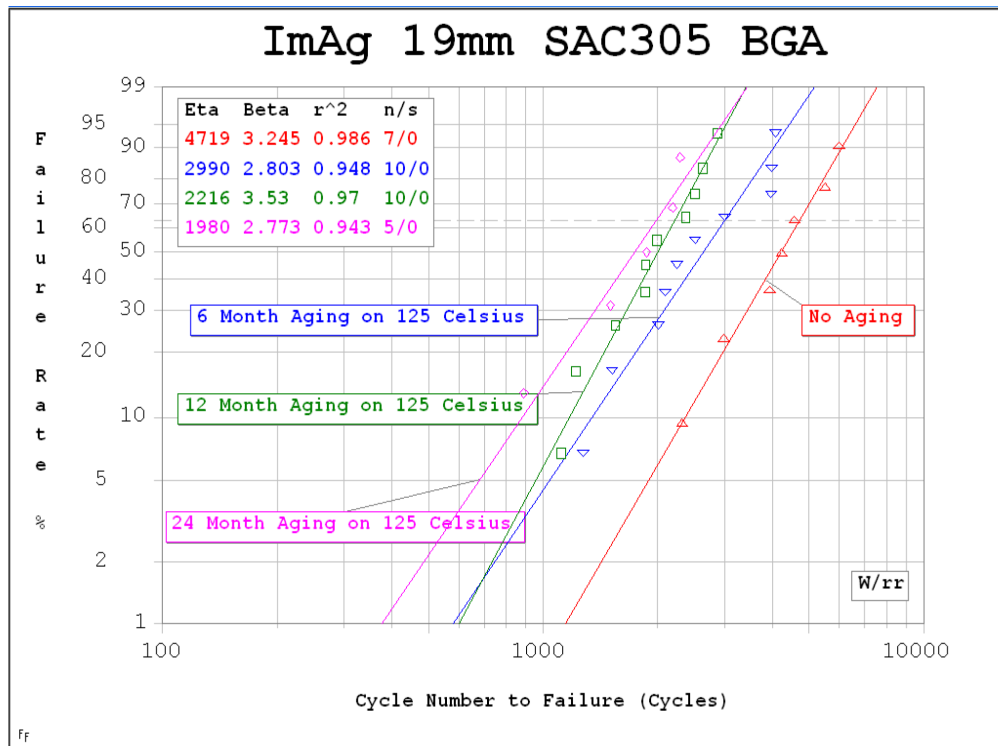

(a)

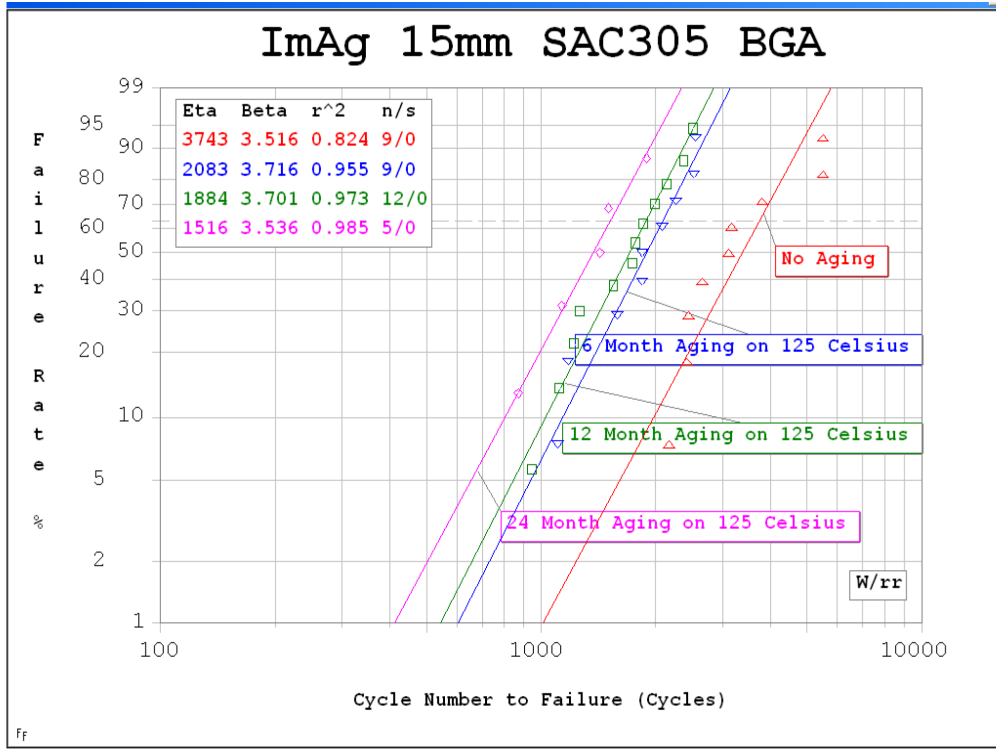

(b)

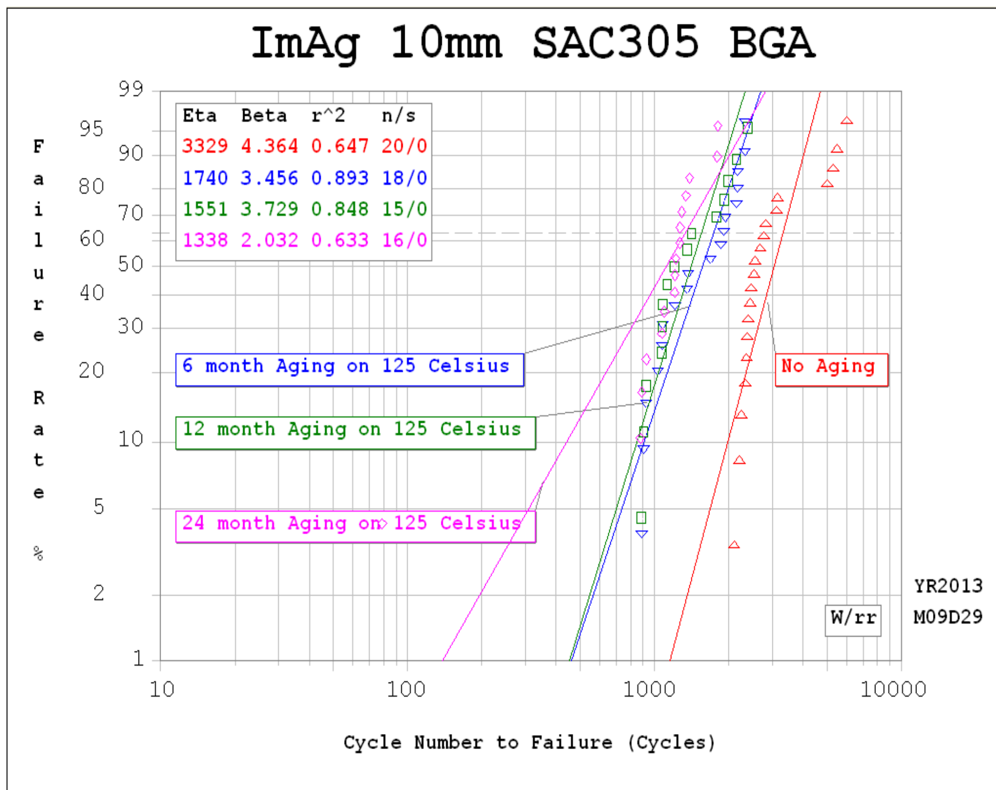

(c)

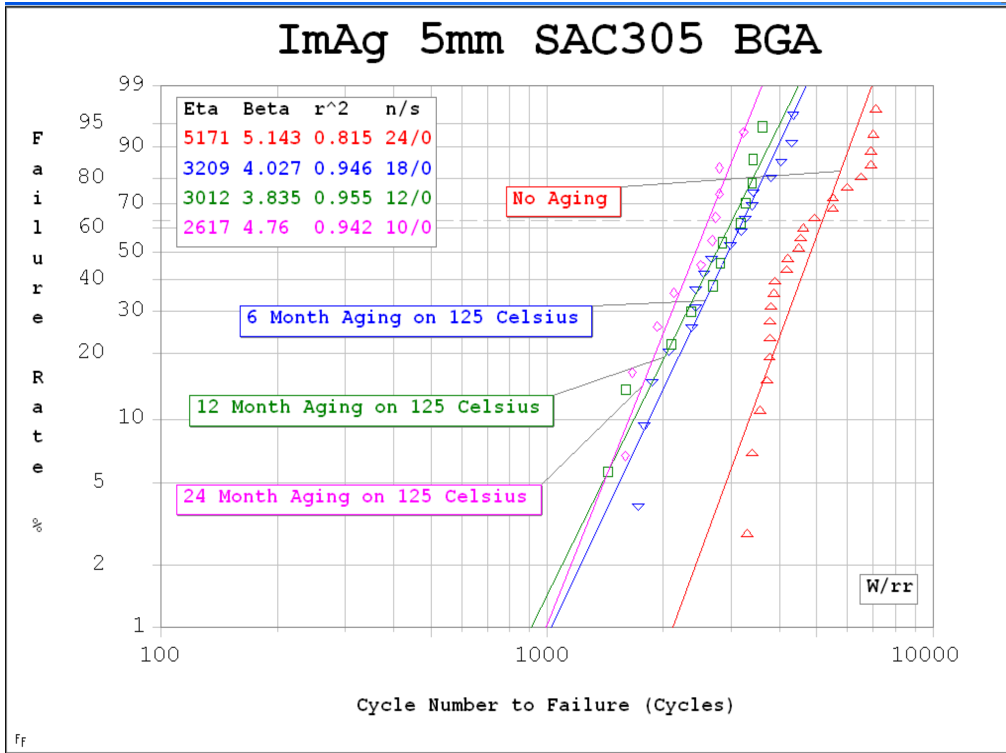

(d)

Figure 41. Weibull Plot for up to 24 Month Aging at 125°C for Immersion Ag, SAC305 BGA with Various Package Size: (a) 19mm, (b) 15mm, (c) 10mm and (d) 5mm.

As Figure 41 shows, after aging at 125°C for 6 month, 12 month and 24 month, the characteristic lifetime for 19mm SAC305 solder on ImAg drops from 4719 to 2990, 2216 and 1980 cycles respectively. The characteristic lifetime for 15mm SAC305 solder on ImAg drops from 3743 to 2083, 1884 and 1516 cycles. The characteristic lifetime for 10mm SAC305 solder on ImAg drops from 3329 to 1740, 1551 and 1338 cycles. The characteristic lifetime for 5mm SAC305 solder on ImAg drops from 5171 to 3209, 3012 and 2617 cycles. The thermal cycling test profile was set to run with a 15 min dwell time and 30 min ramp time with the temperature from -40°C to 125°C.

b) **Immersion Ag, SAC 105**

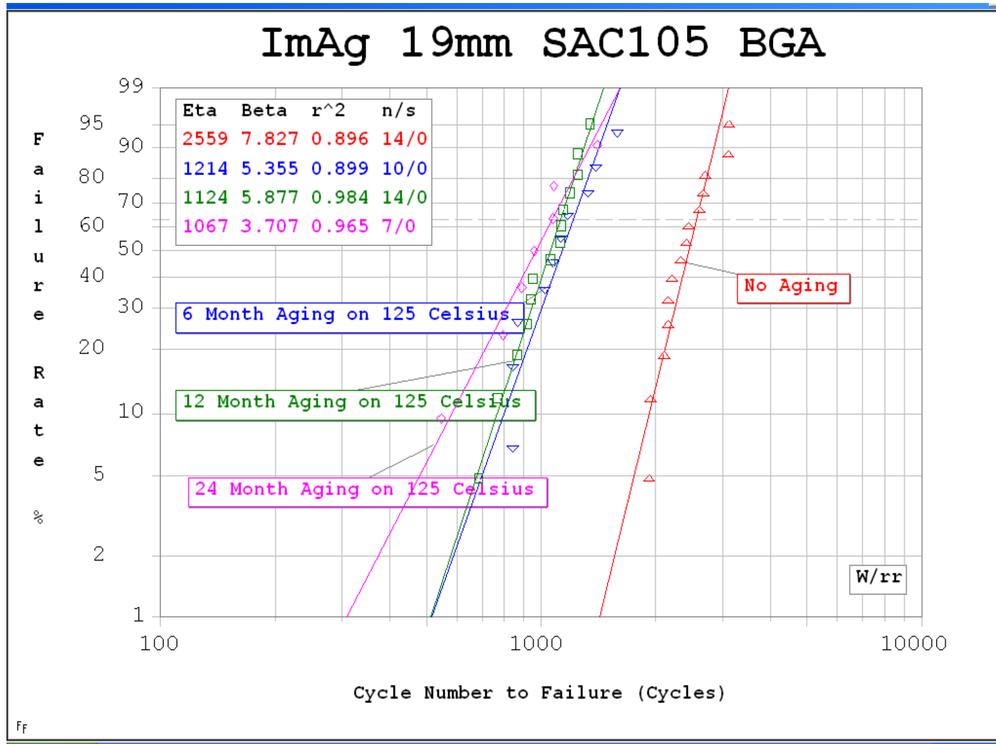

(a)

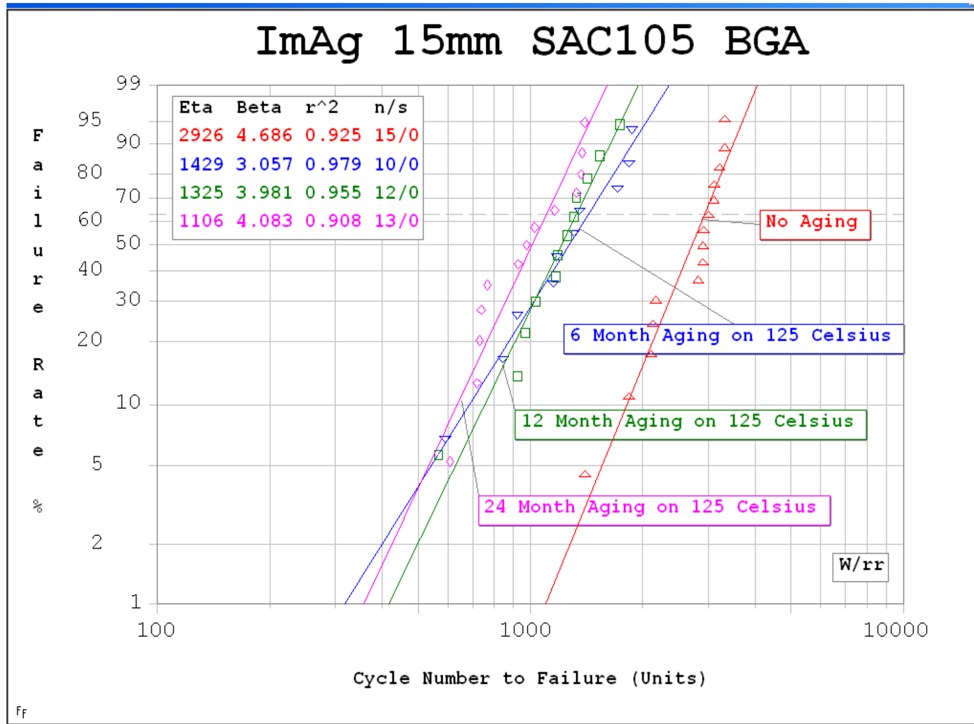

(b)

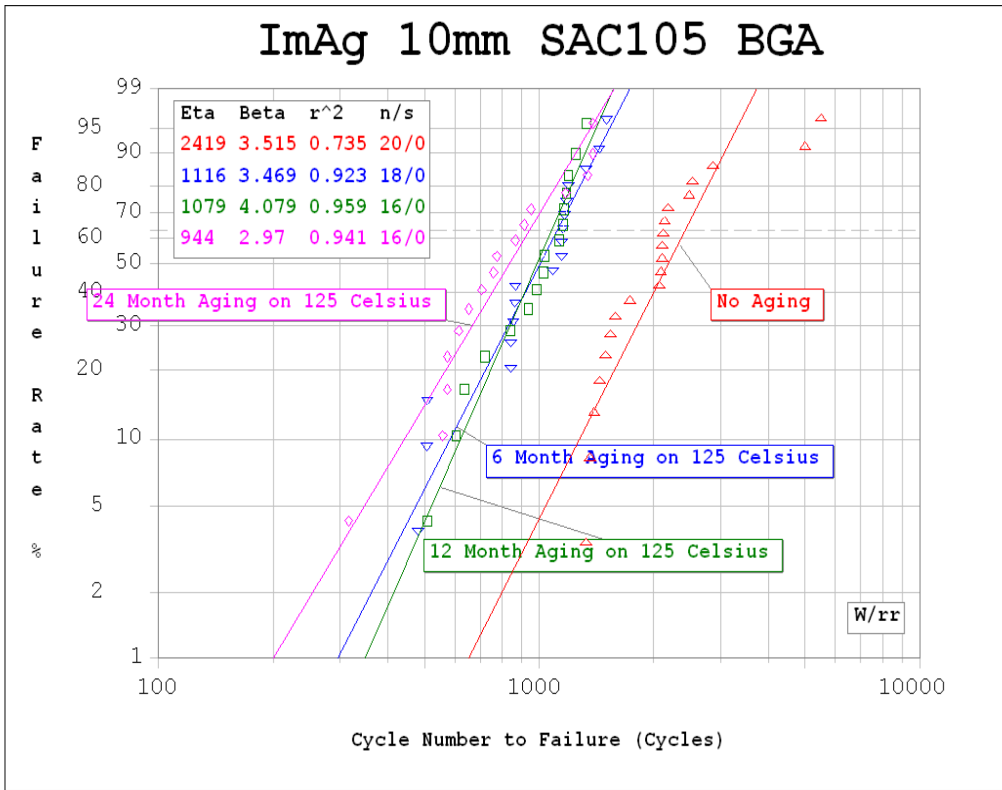

(c)

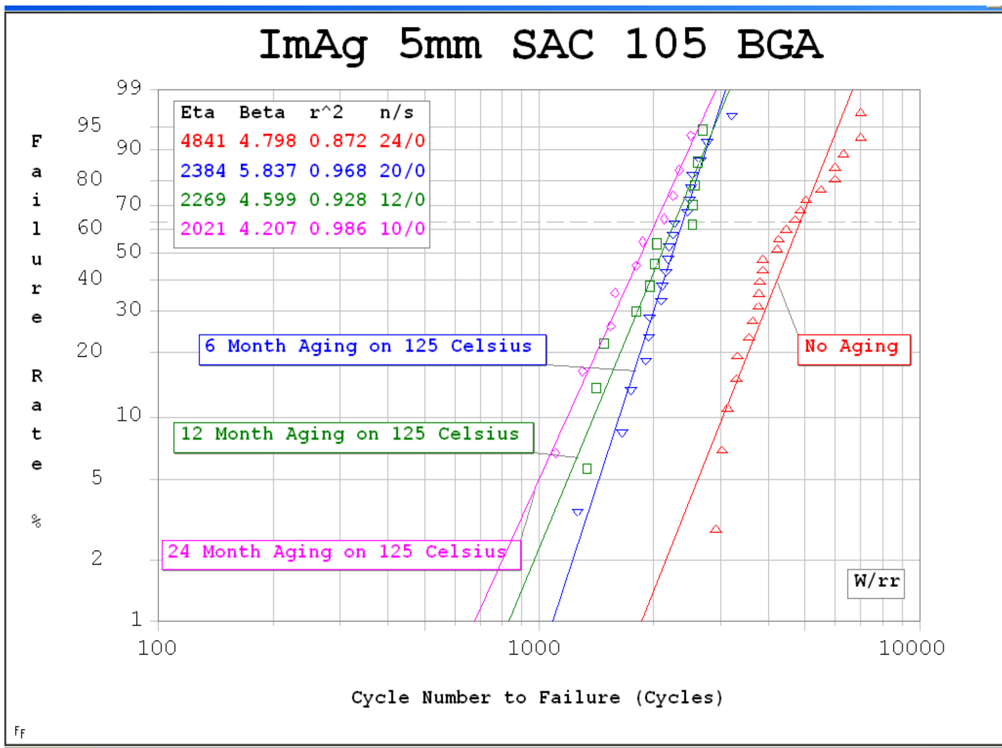

(d)

Figure 42. Weibull Plot for up to 24 Month Aging at 125°C for Immersion Ag, SAC105 BGA with Various Package Size: (a) 19mm, (b) 15mm, (c) 10mm and (d) 5mm.

As Figure 42 shows, after aging at 125°C for 6 month, 12 month and 24 month, the characteristic lifetime for 19mm SAC105 solder on ImAg drops from 2559 to 1214, 1124 and 1067 cycles respectively. The characteristic lifetime for 15mm SAC105 solder on ImAg drops from 2926 to 1429, 1325 and 1106 cycles. The characteristic lifetime for 10mm SAC105 solder on ImAg drops from 2419 to 1116, 1079 and 944 cycles. The characteristic lifetime for 5mm SAC105 solder on ImAg drops from 4841 to 2384, 2269 and 2021 cycles. The thermal cycling test profile was set to run with a 15 min dwell time and 30 min ramp time with the temperature from -40°C to 125°C.

Table 11. Characteristic Life for BGA for Different Aging Times (aging at 125°C; M = months)

	SAC105 19mm	SAC105 15mm	SAC105 10mm	SAC105 5mm	SAC305 19mm	SAC305 15mm	SAC305 10mm	SAC305 5mm
NA	2559	2916	2419	4841	4719	3743	3329	5171
6M	1214	1429	1116	2384	2990	2083	1740	3209
12M	1124	1325	1079	2269	2216	1884	1551	3012
24M	1067	1106	944	2021	1980	1516	1338	2617

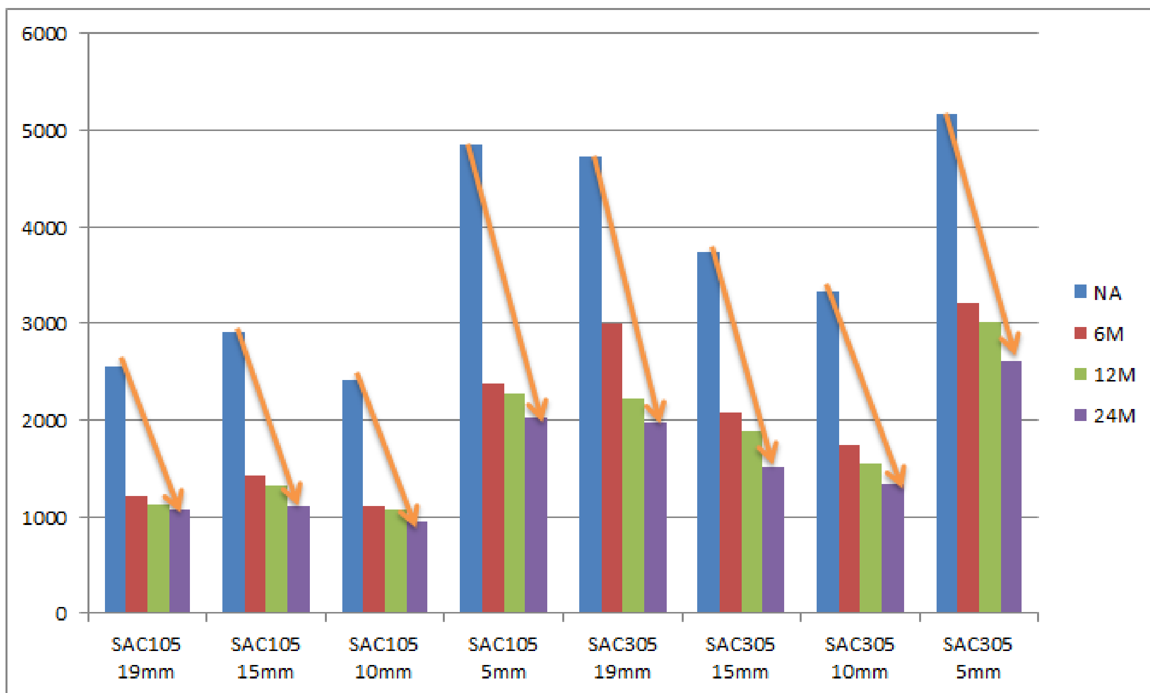

Figure 43. Characteristic Life Time for BGA for Different Aging Times

From Figure 41, 42, 43 and Table 11, we could easily find the Weibull characteristic lifetime is dramatically reduced during isothermal aging at 125°C for SAC105/305 on a variety of package sizes.

Table 12. Degradation Rate of Each Aging Group (M = months)

Aging Period	19mm SAC105	19mm SAC305	15mm SAC105	15mm SAC305	10mm SAC105	10mm SAC305	5mm SAC105	5mm SAC305
0 to 6 M	52.6%	36.6%	51.1%	44.4%	53.9%	37.4%	50.8%	37.9%
0 to 12M	56.1%	53.1%	54.7%	49.7%	55.4%	53.4%	53.2%	41.7%
0 to 24 M	58.3%	58.0%	62.2%	59.5%	61.0%	59.8%	58.3%	49.4%

Table 13. Degradation Rate Differences with Aging Time (M = months)

Aging Period	19mm SAC105	19mm SAC305	15mm SAC105	15mm SAC305	10mm SAC105	10mm SAC305	5mm SAC105	5mm SAC305
0 to 6 M	52.6%	36.6%	51.1%	44.4%	53.9%	37.4%	50.8%	37.9%
6 to 12M	3.6%	16.4%	3.6%	5.3%	1.5%	16.0%	2.4%	3.8%
12 to 24 M	2.2%	5.0%	7.5%	9.8%	5.6%	6.4%	5.1%	7.6%

The degradation rate for all tested alloys/pitch sizes is shown in Table 12. Differences between the degradation rates with aging time are shown in Table 13. From Table 13 we conclude that for each of the aging groups, during the first time period of 6 months the components reliability degrades in a very fast rate (over 50%). With additional aging time after 6 months, however, the degradation rate becomes slower and slower (< 10%) and eventually may approach an asymptotic value.

4.2 Data Analysis of Package Size Effect

Different Package Size BGA components have different reliability performances. In our test, the 19mm and 15mm BGAs have a pitch size of 0.8mm, while the 10mm and 5mm BGAs have a 0.4mm pitch size. The ball diameter for 19mm BGA is 0.38mm; for 15mm it is 0.36mm; for 10mm it is 0.18mm; and for 5mm it is 0.20mm. The 19mm,

15mm, and 10mm BGAs have a perimeter ball alignment, while 5mm BGA have full array ball alignment.

Table 14. Characteristic Life Time for Immersion Ag, SAC305 BGA with Different Package Sizes

	SAC305 NA	SAC305 6M	SAC305 12M	SAC305 24M
19mm	4719	2990	2216	1980
15mm	3743	2083	1884	1516
10mm	3329	1740	1551	1338
5mm	5171	3209	3012	2617

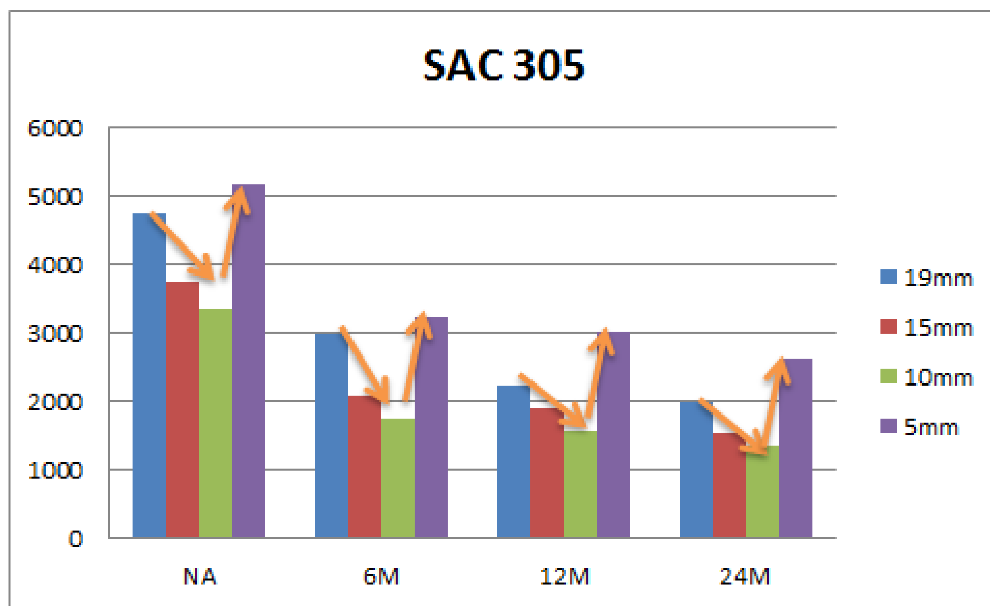

Figure 44. Degradation Chart for Immersion Ag, SAC305 BGA after Aging at 125°C with Varying Package Sizes.

Table 14 and Figure 44 disclose that, for perimeter ball alignments, the 19mm and 15mm BGAs always have higher characteristic lifetimes than the 10mm, which shows that packages with large solder balls have higher reliability. On the other hand, the 5mm BGA has the highest characteristic life, indicating that packages with full array ball alignments perform better than perimeter ball alignments under high temperature aging + thermal cycling conditions. This may suggest that the full array ball alignment has higher structural stability from the mechanical point of view, so that solder balls can endure

severe changes of stress and strain during thermal fatigue caused by CTE mismatches. However, there are lots of reasons could cause this, such as die/package size ratio, solder ball/pad structure, ball alignment and so on. Since there are a lot of variations for this test, further research are necessary to demonstrate the effect of ball alignment with same die size, package size and pitch size. I suggest running the ball alignment test for 15mm and 5mm with same die/package ratio and the ball alignment test for 5mm with different die size in the next step.

4.3 Data Analysis of Pb-Free Effect

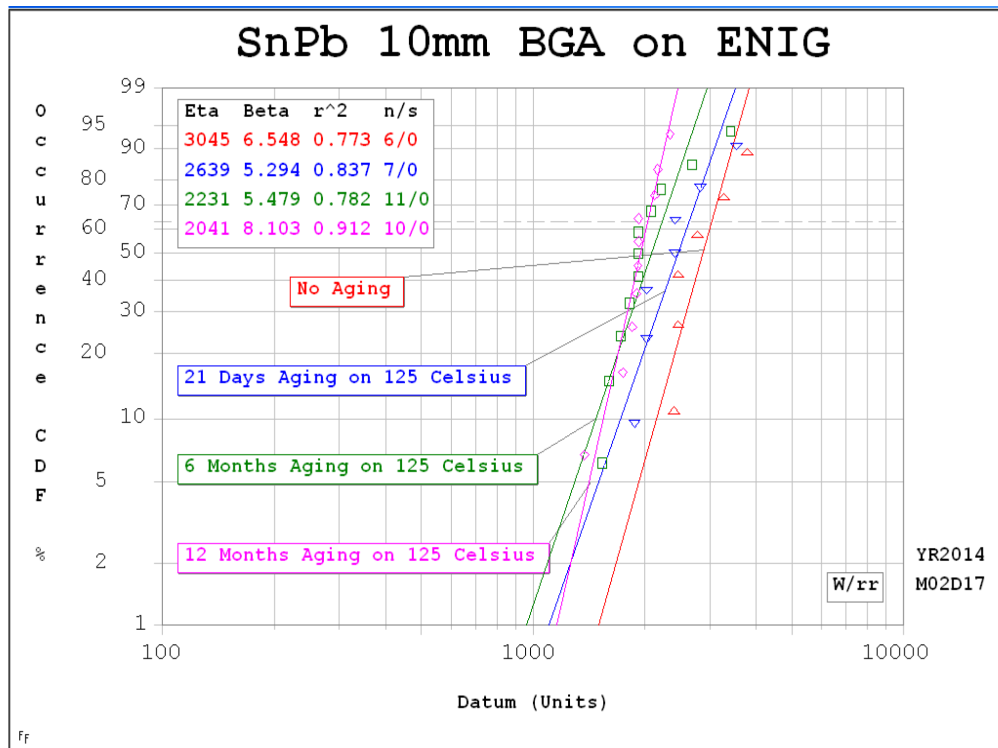

(a)

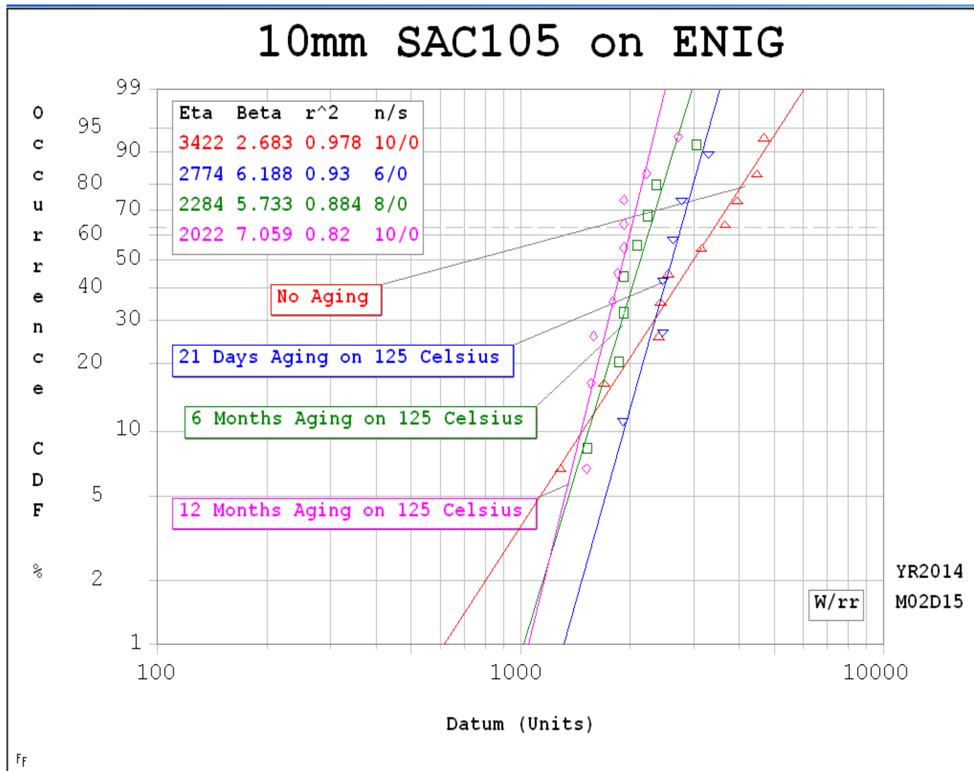

(b)

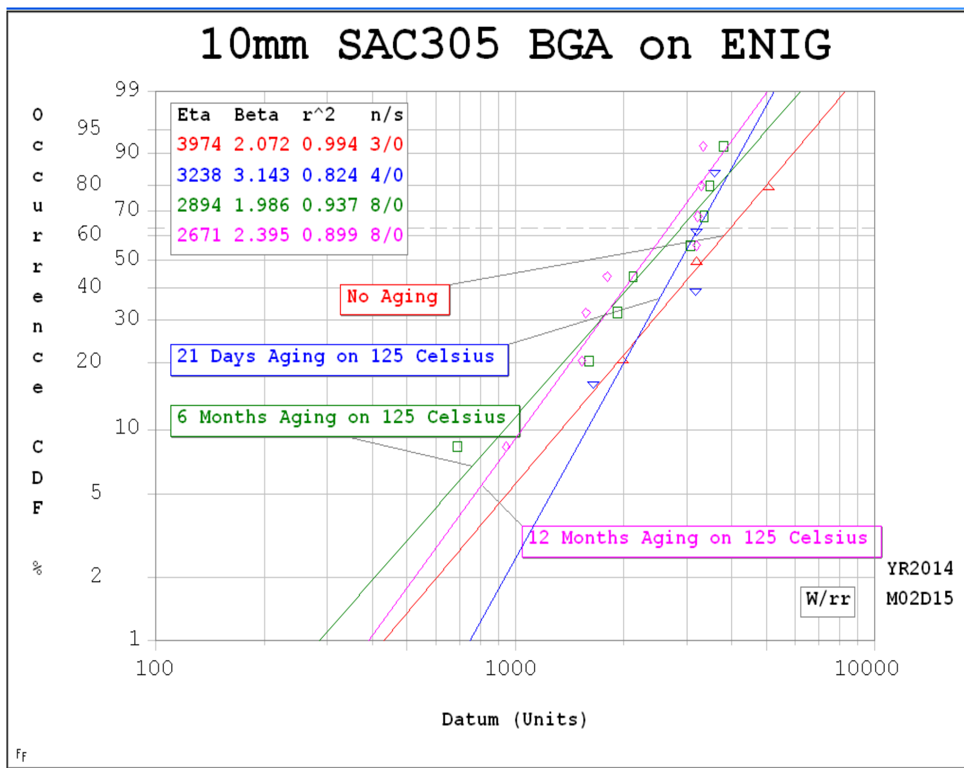

(c)

Figure 45. Weibull Plot for 10mm BGA Package on ENIG Plating after Aging at 125oC (a) SnPb (b) SAC105 (c) SAC305

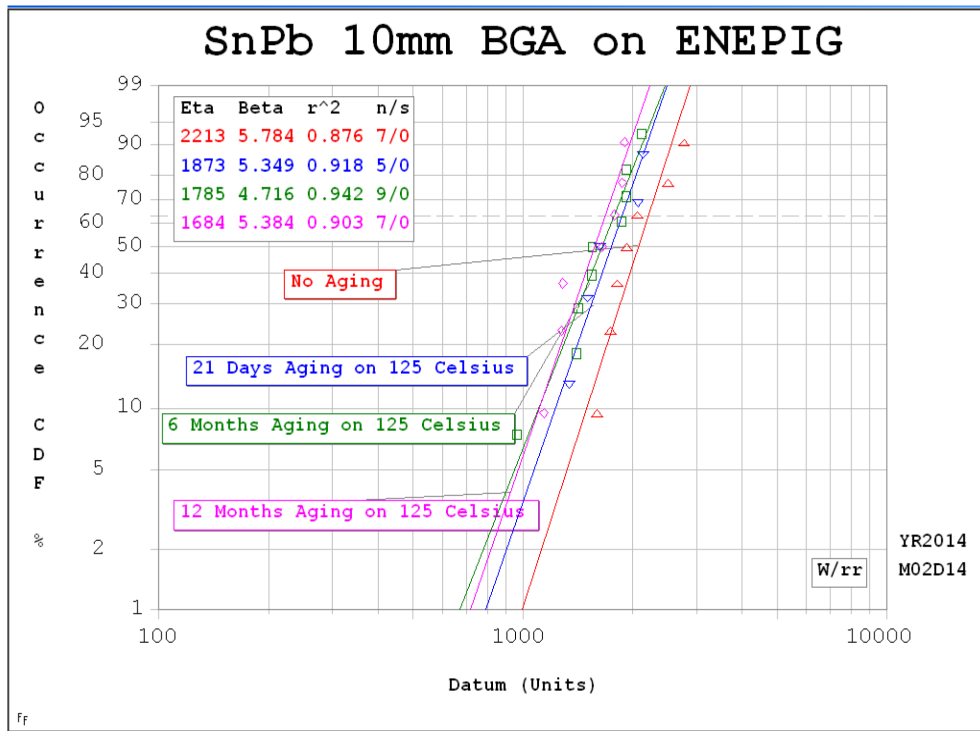

(a)

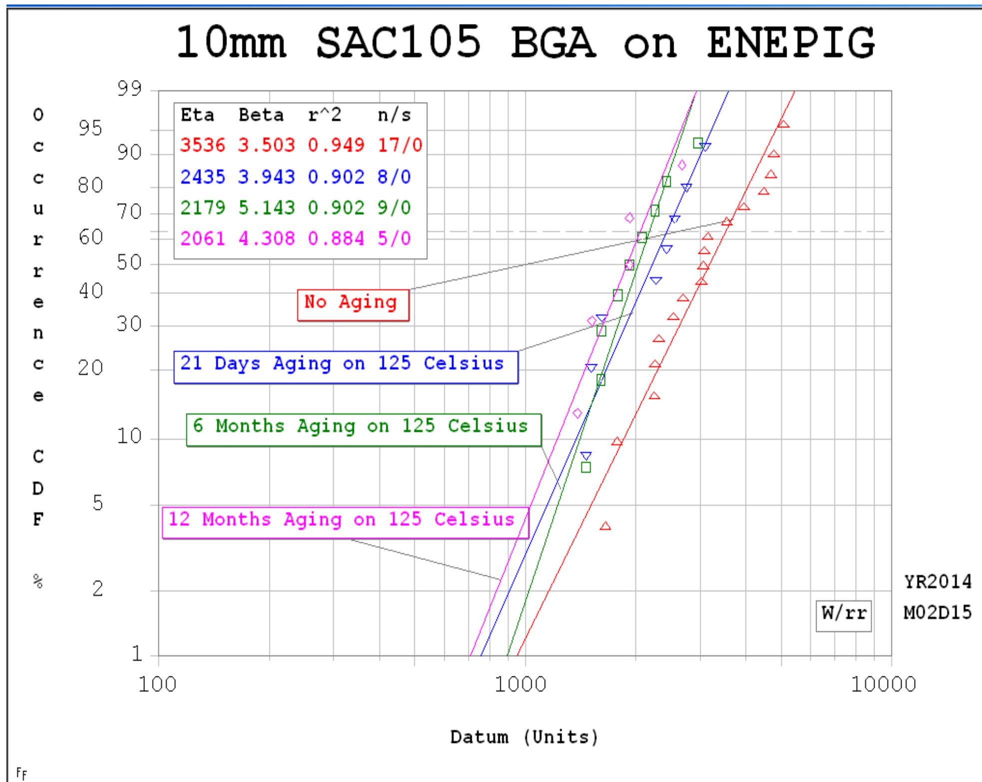

(b)

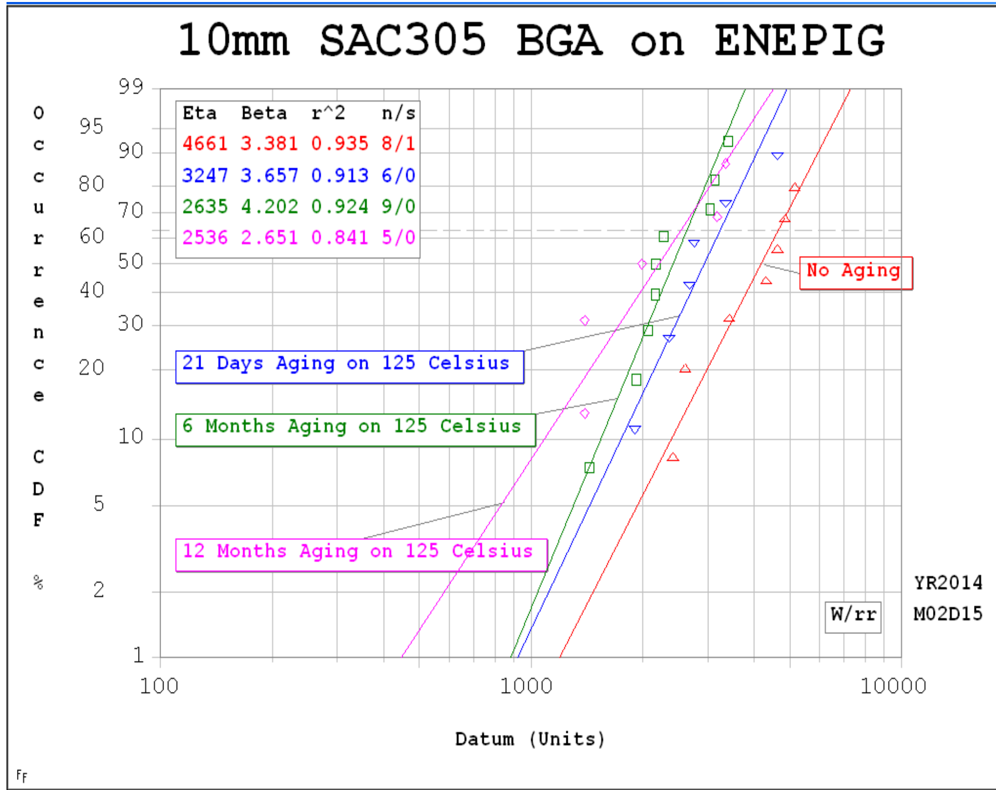

(c)

Figure 46. Weibull Plot for 10mm BGA Package on ENEPIG Plating after Aging at 125°C (a) SnPb (b) SAC105 (c) SAC305

Table 15. Characteristic Life Time for SnPb, SAC105 and SAC305 BGA with 10mm package size and ENIG, ENEPIG Plating after Aging at 125°C

10 mm PBGA		SnPb	SAC105	SAC305
ENIG	NA	3045	3422	4661
	6M	2231	2284	2894
	12M	2041	2042	2671
ENEPIG	NA	2213	3536	3974
	6M	1785	2179	2635
	12M	1684	2061	2536

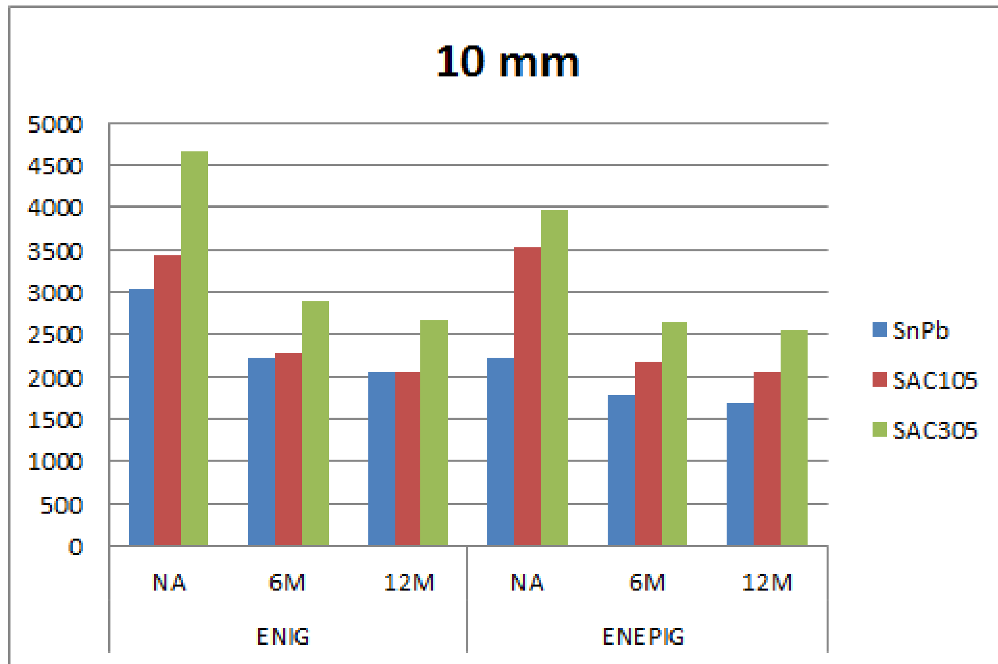

Figure 47. Characteristic Life Time for SnPb, SAC105 and SAC305 BGA with 10mm package size and ENIG, ENEPIG Plating after Aging at 125°C

From Figure 46, 47 and Table 15, we could find that for 10mm BGA packages with ENIG or ENEPIG finished, the ranking of life time performance with thermal aging and cycling is that: **SAC 305 > SAC 105>SnPb**.

According to Zhou Hai and Jiawei Zhou's previous research work, Ag_3Sn IMC reduces/redirects the crack growth which results in enhanced joint structural strength. This helps to explain the superior thermal fatigue performance of SAC305 (higher Ag content material) than SAC105.

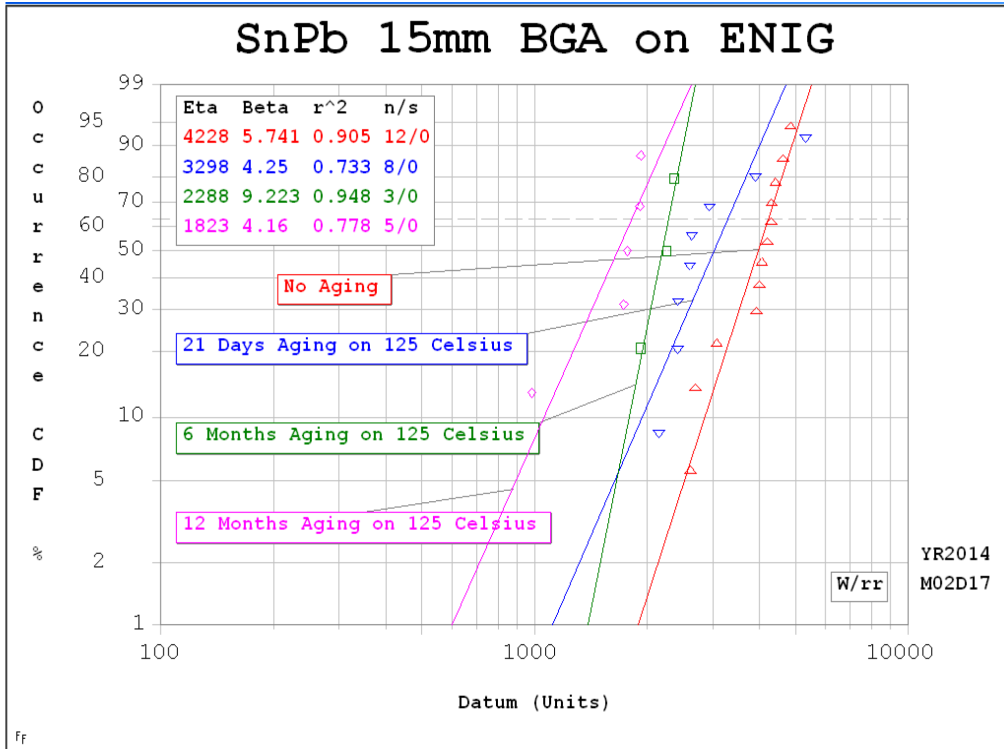

(a)

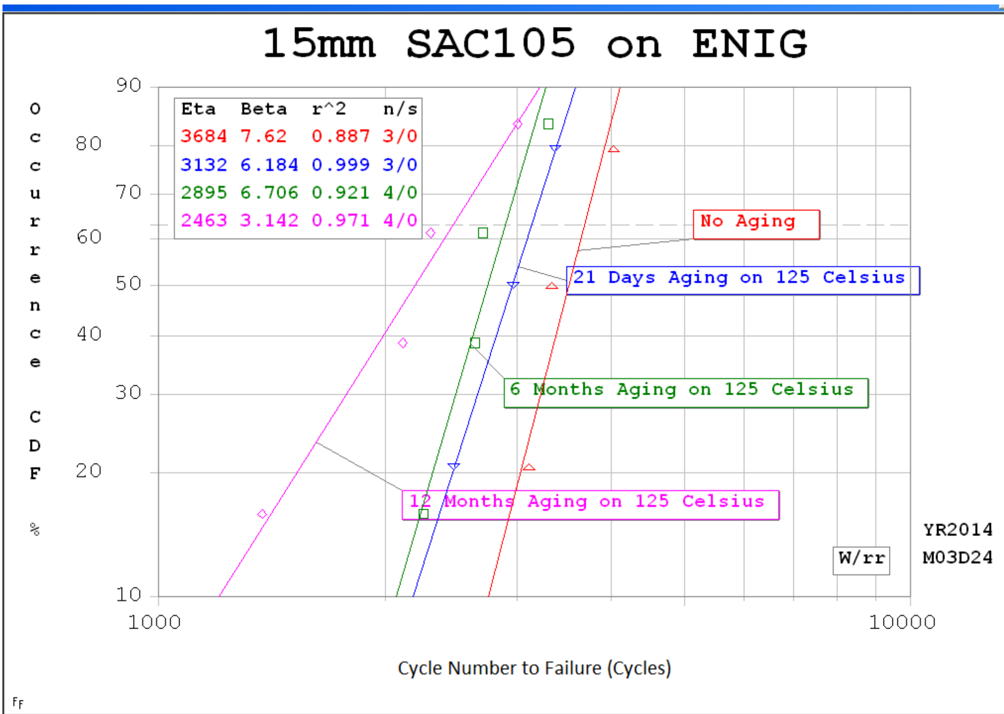

(b)

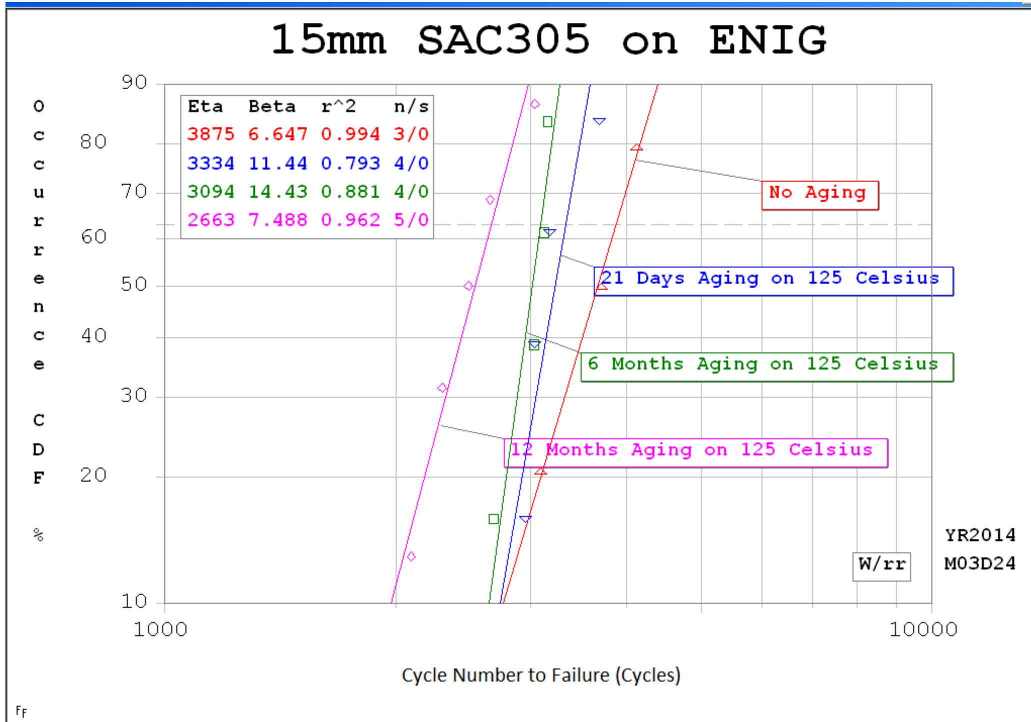

(c)

Figure 48. Weibull Plot for 15mm BGA Package on ENIG Plating after Aging at 125°C (a) SnPb (b) SAC105 (c) SAC305

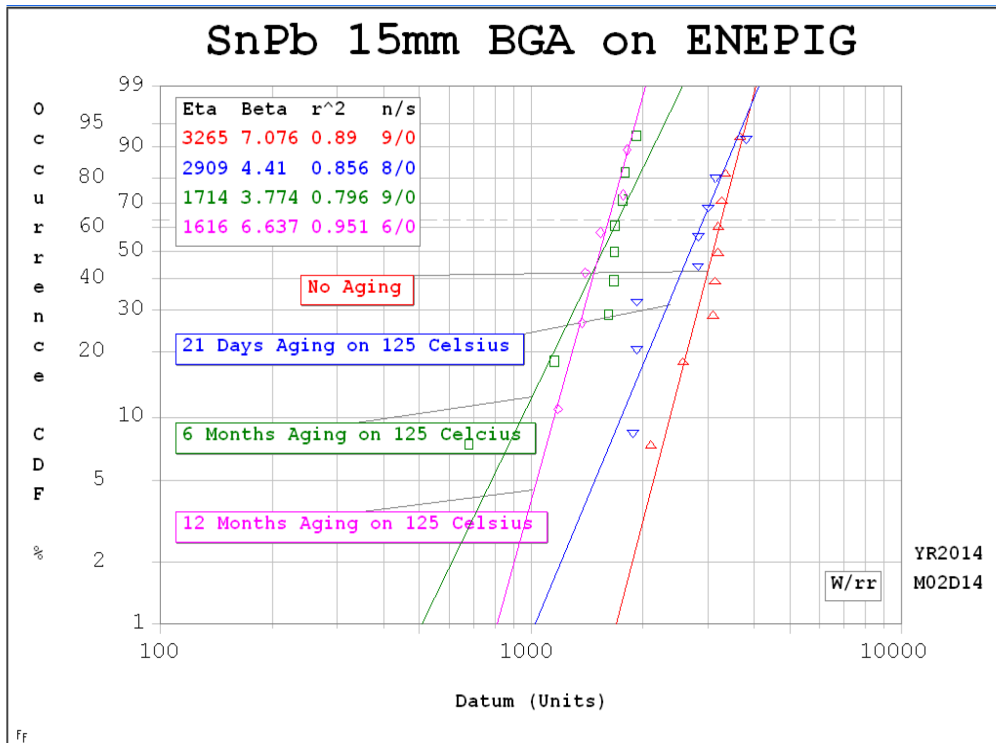

(a)

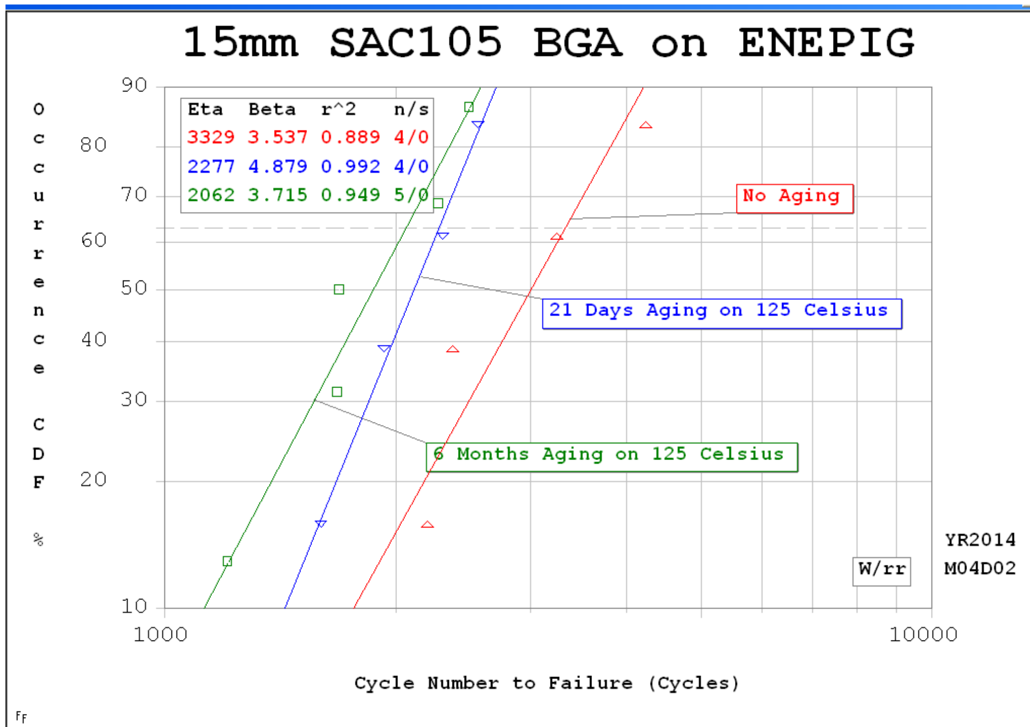

(b)

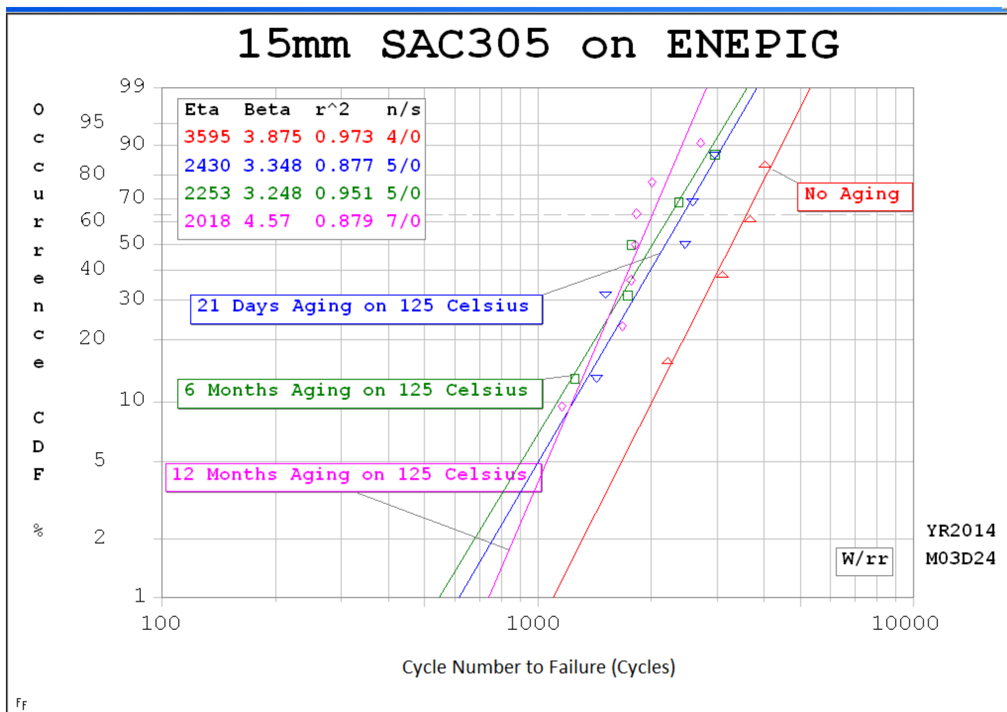

(c)

Figure 49. Weibull Plot for 15mm BGA Package on ENEPIG Plating (a) SnPb (b) SAC105 (c) SAC305

Table 16. Characteristic life comparison (η) for SnPb, SAC105 and SAC305 BGA with 15mm package size and ENIG, ENEPIG Plating

15 mm PBGA		SnPb	SAC105	SAC305
ENIG	NA	4228	3604	3875
	6M	2288	2895	3094
	12M	1823	2463	2663
ENEPIG	NA	3265	3329	3595
	6M	1714	2062	2253
	12M	1616		2018

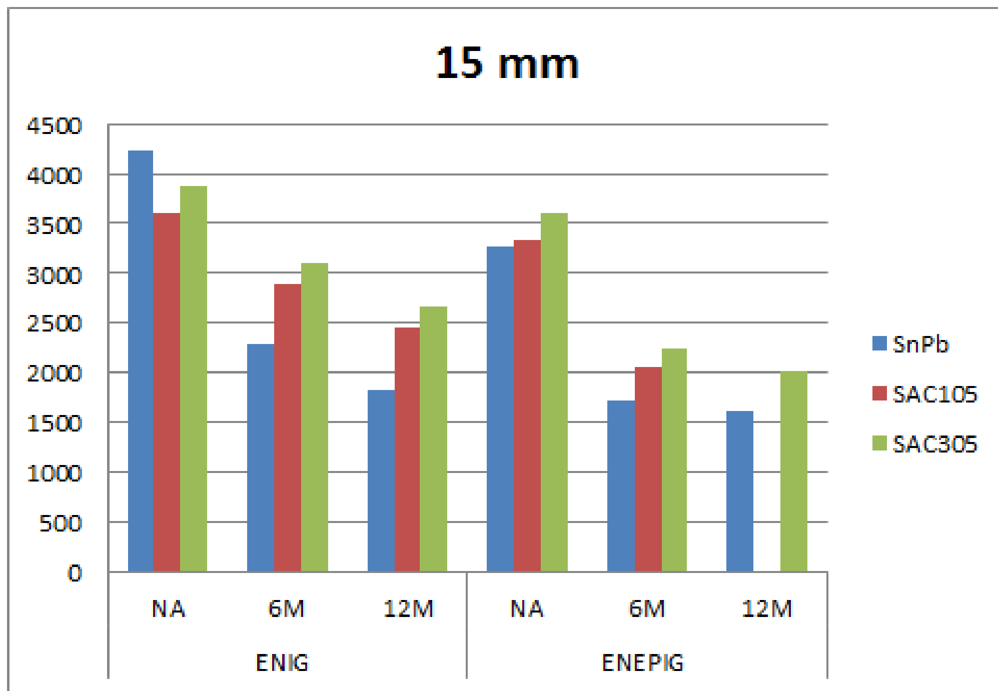

Figure 50. Characteristic life comparison (η) for SnPb, SAC105 and SAC305 BGA with 15mm package size and ENIG, ENEPIG Plating

From Figure 48, 49, 50 and Table 16, we could conclude that for 15mm BGA packages with ENIG or ENEPIG finished, the ranking of life time performance with thermal aging and cycling is that: **SAC 305 > SAC 105>SnPb** in most cases, except ENIG no aging group.

4.4 Data Analysis of Surface Finish Effect

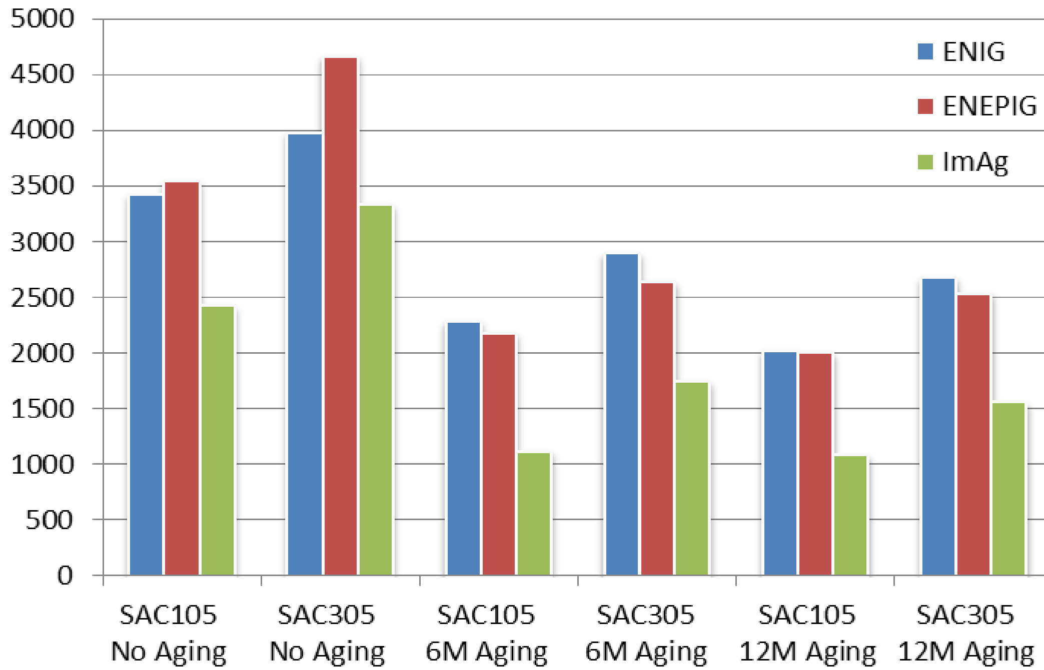

Figure 51. Characteristic life comparison (η) for 10mm BGA finished with ENIG, ENEPIG & ImAg subject to 125°C/12 months aging.

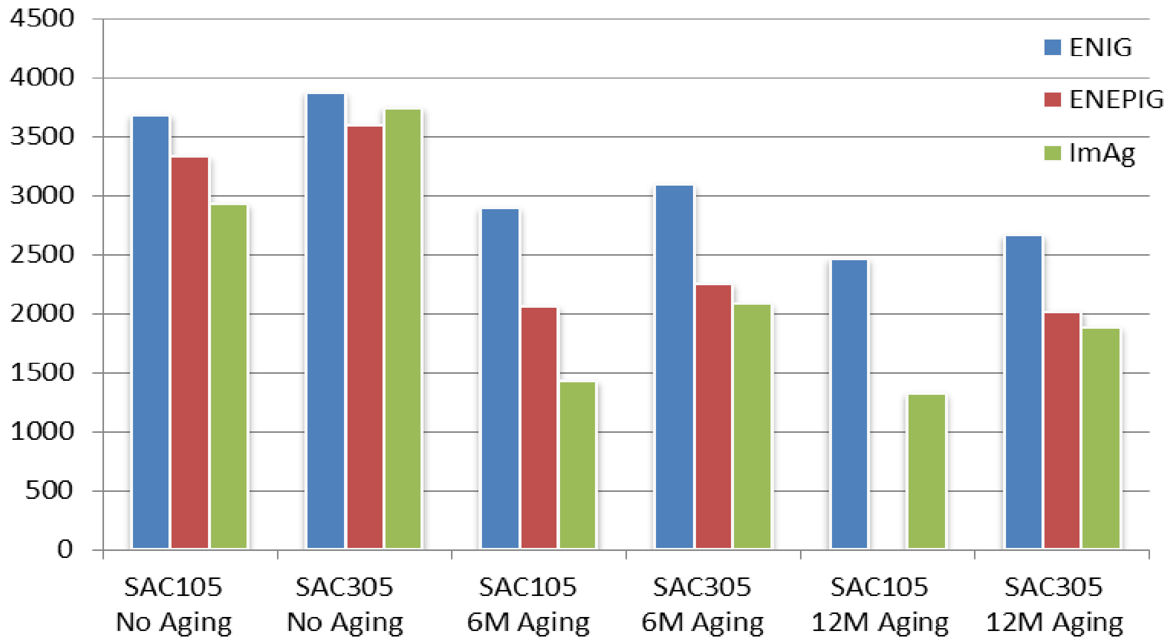

Figure 52. Characteristic life comparison (η) for 15mm BGA finished with ENIG, ENEPIG & ImAg subject to 125°C/12 months aging.

Based on the Weibull characteristic life (η), Figures 51 and 52 give a comparison of the reliability performance among ENIG, ENEPIG & ImAg board side surface finishes for 15mm packages (0.8mm pitch) and 10mm packages (0.4mm pitch) at 125°C aging. In most cases, the rank of the characteristic lifetimes for both SAC105 and SAC305 with different surface finishes **after aging** can be ordered as: **ENIG> ENEPIG> ImAg**. The data suggests that ENIG is the best surface finish for applications involving long-term isothermal aging. ENEPIG ranks second, followed by ImAg. To better illustrate, we provide more detailed analysis for the 15mm package.

No Aging Group of 15mm Package:

For SAC105, the characteristic lifetime is reduced from 3684(ENIG) to 2926(ImAg), which is a 20.6% degradation. For SAC305, the characteristic lifetime is reduced from 3875(ENIG) to 3595 cycles (ENEPIG) which is a 7.2% degradation. In this non-aged case, ENIG has a longer lifetime than ENEPIG/ImAg when applied on either SAC105 or SAC305.

Aging Group of 15mm Package (6 months & 12 months):

For SAC105, the characteristic lifetime with ENIG is 2895 cycles, which is twice the life of ImAg after aging at 125°C for 6 months. For SAC305, the characteristic lifetime with ENIG is 3094 cycles, which is 1.5 times the life of ImAg. The degradation of characteristic lifetime spanning the surface finishes is 50.1% for SAC105 and 32.7% for SAC305. For the 12 month aging data, the Weibull characteristic lifetime for SAC 105 dropped 46.2% and, for SAC305, the degradation was 29.3%.

Generally, the thickness of the IMC layer at the interface between the solder and substrate is very important in determining the reliability of the whole package because an

excessively thick IMC layer is sensitive to stress and sometimes provides initiation sites and paths for the propagation of cracks. [73] [74] Therefore, as the growth of the IMC layer could degrade the reliability of the solder joint. In the case of the ENEPIG surface finish board, the IMCs formed at the interface are composed of $(Cu,Ni)_6Sn_5$ and $(Ni,Cu)_3Sn_4$, as in the case of the ENIG board. Randy Schueller [75] presented the report that nickel served as a barrier layer to copper, though Ni could eventually also diffuse to the surface of gold and cause the same. This may help explain that ENIG and ENEPIG perform better than Immersion Ag.

According to Sang-Su Ha's research work [76], the Pd layer may control the diffusion of Ni at the time of the reaction between Ni and Sn in the solder and then the P-rich Ni layer and IMCs are formed to a limited extent after reflow. In other words, little Ni participated in the Cu-Ni-Sn IMC reaction and, thus, a thin P-rich Ni layer is formed. In the case of the 10mm no aging group, the Pd layer may act as a diffusion barrier to the interfacial growth of the IMC.

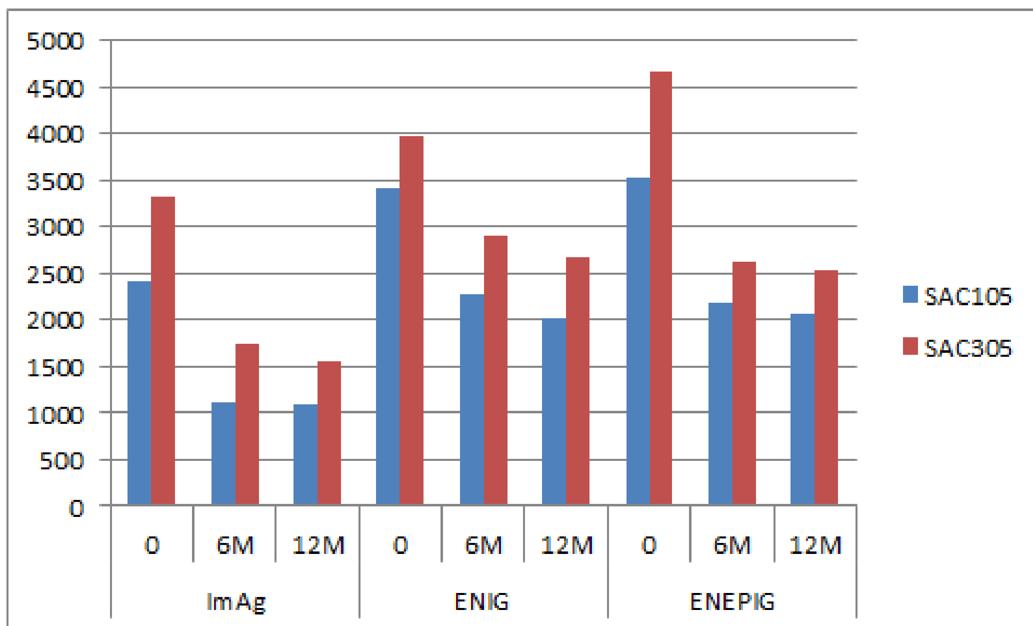

Figure 53. Characteristic life comparison (η) for 10mm BGA soldered with SAC105 & SAC305 subject to 125°C/12 months aging.

As Figure 53 shows, after aging at 125°C for 6 months, the characteristic lifetime for 10mm SAC305 solder on ENIG, ENEPIG and ImAg drops from 3974, 4661, 3329 cycles to 2894, 2635, and 1740 cycles respectively. And further, it reduced to 2671, 2536 and 1551 cycles subjected to 125°C aging for 12 months.

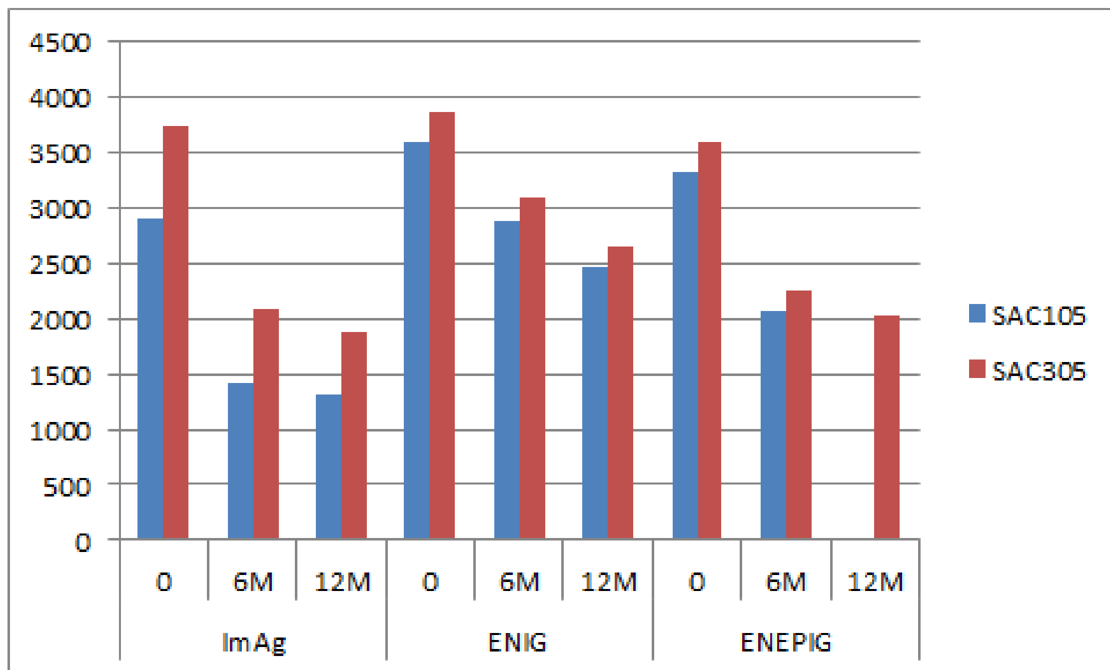

Figure 54. Characteristic life comparison (η) for 15mm BGA soldered with SAC105 & SAC305 subject to 125°C/12 months aging.

As Figure 54 shows, after aging at 125°C for 6 months, the characteristic lifetime for 15mm SAC305 solder on ENIG, ENEPIG and ImAg dropped from 3875, 3595, 3743 cycles to 3094, 2253, and 2083 cycles respectively. And further, it reduced to 2663, 2018 and 1884 cycles subjected to 125°C aging for 12 months.

Figures 53 and 54 provide a comparison of the reliability performance between SAC105 and SAC 305 for the 15mm package (0.8mm pitch) and 10mm package (0.4mm pitch) subject to 125°C aging. We conclude that SAC305 solder performs better than SAC105 in all cases, and illustrates the risk in using SAC105 solder balls in applications where thermal fatigue failure is a concern.

Table 17. Degradation Rate Comparison for 10mm BGA Package after Aging

10mm BGA Package	SAC 105		SAC 305	
	6 Months Aging	12 Months Aging	6 Months Aging	12 Months Aging
ENIG	33.2%	40.9%	27.2%	32.8%
ENEPIG	38.4%	43.4%	43.5%	45.6%
ImAg	53.9%	55.4%	47.7%	54.4%

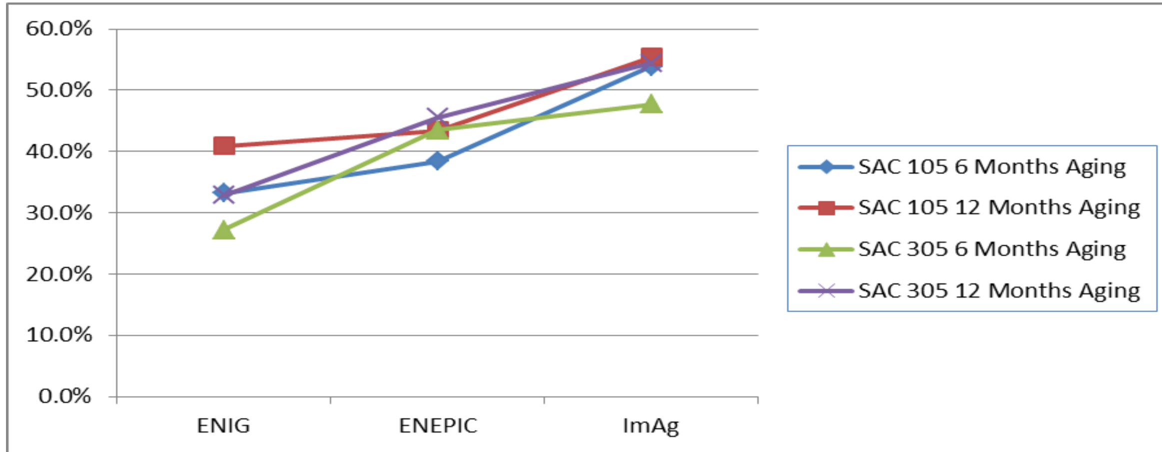

Figure 55. Degradation Rate Comparison for 10mm BGA Package after Aging

Chapter 5

Failure Analysis

5.1 IMC Analysis

Previous studies from Zhou et. al found the thickness of the IMC layer at the interface between the solder and substrate is very important in determining the reliability of the whole package. Formation of the intermetallic compound (IMC) layers at the interface is an indication of good bonding between solder and the metal pad. However, an excessively thick IMC layer is sensitive to stress and sometimes provides initiation places and paths for the propagation of cracks. Thus, it is essential to study the formation and growth of the IMC layer, as the growth of the IMC layer could degrade the reliability of the solder joint.

5.1.1 IMC Properties

Prior investigations in many laboratories have shown that the continuous growth of interfacial intermetallic compound (IMC) during isothermal aging strongly influences fatigue solder failures. As the brittle intermetallic layer consumes a larger fraction of the solder ball, cracks propagate along them, causing solder joint cracking and eventual failure under the high strain due to CTE mismatches. [77][78]

In Figure 56 and 57, large, plate-like Ag_3Sn phases are found regularly in SAC305 solder joints subject to isothermal aging alone, which is due to its higher Ag content. Zhang et. al observed that coarsened Ag_3Sn IMC reduces/redirects the crack growth which results in enhanced joint structural strength. This helps to explain the superior thermal fatigue performance of SAC305 (higher Ag content material) than SAC105.

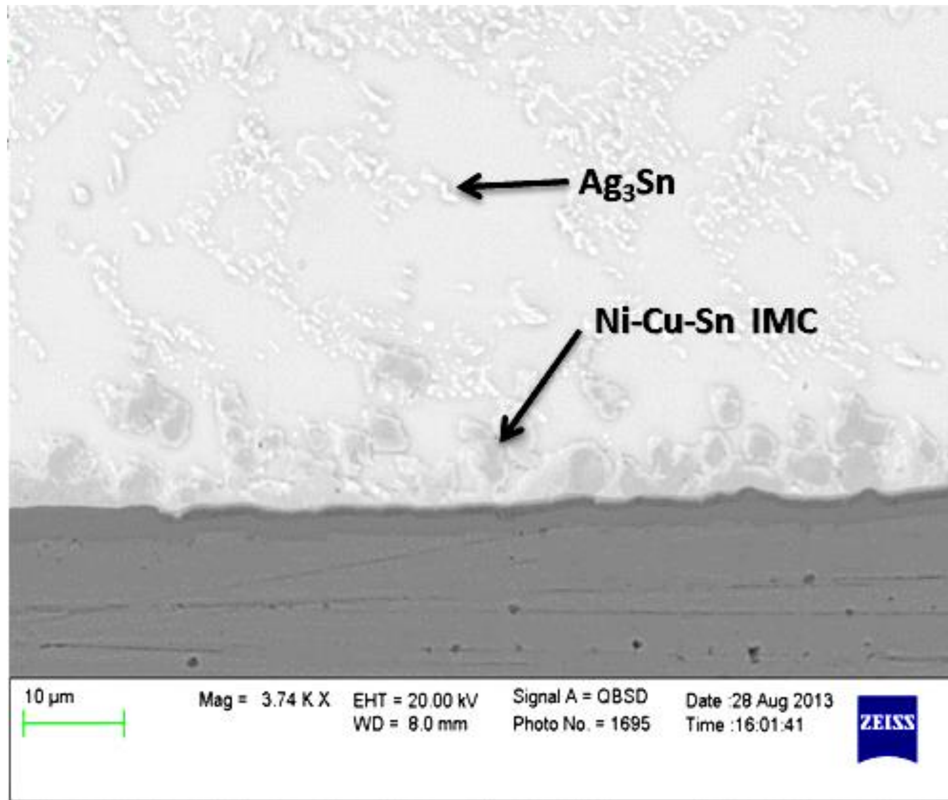

Figure 56. SAC305 solder joint on ENIG, no aging, BSE imaging.

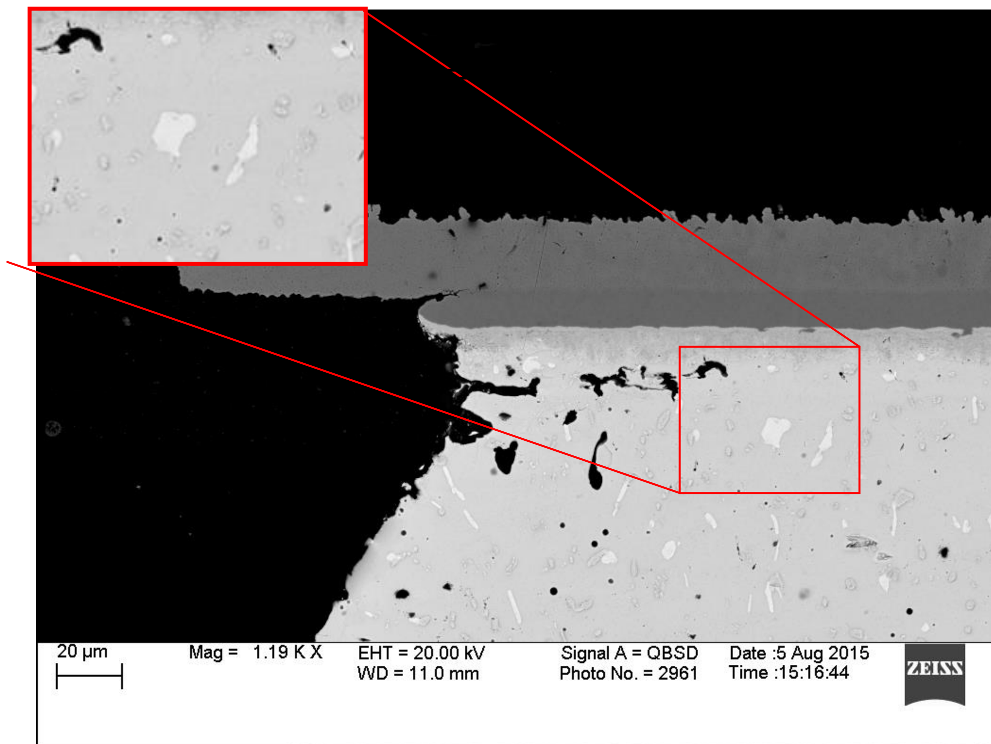

Figure 57. Plate-Like Ag_3Sn on 15mm SAC305 solder joint with ENIG, 6 month aging, BSE imaging

For the SAC solder immersion with Ag, a first layer Cu_6Sn_5 (η-phase) intermetallic is formed at the board/solder joint interface. Then, a second layer of Cu_3Sn (ε-phase) is formed at the IMC layer/board interface during aging which reduces the mechanical behavior of the solder joint. After the Cu atoms arrive at the interface of Cu_3Sn/Cu_6Sn_5 by diffusion through the grain boundaries of the Cu_3Sn layer, the following interfacial reaction happens:

$$\mathbf{Cu_6Sn_5 + Cu \rightarrow Cu_3Sn}$$

By this reaction, Cu_6Sn_5 is converted to Cu_3Sn at the interface [88].

For ENIG/ENEPIG finishes, as figure 58 shows, in the interfacial reaction between the Ni layer and SAC 105 /SAC 305, ternary IMCs consisting of Cu, Ni and Sn are observed. In our test, all components are finished with ENIG on the package side.

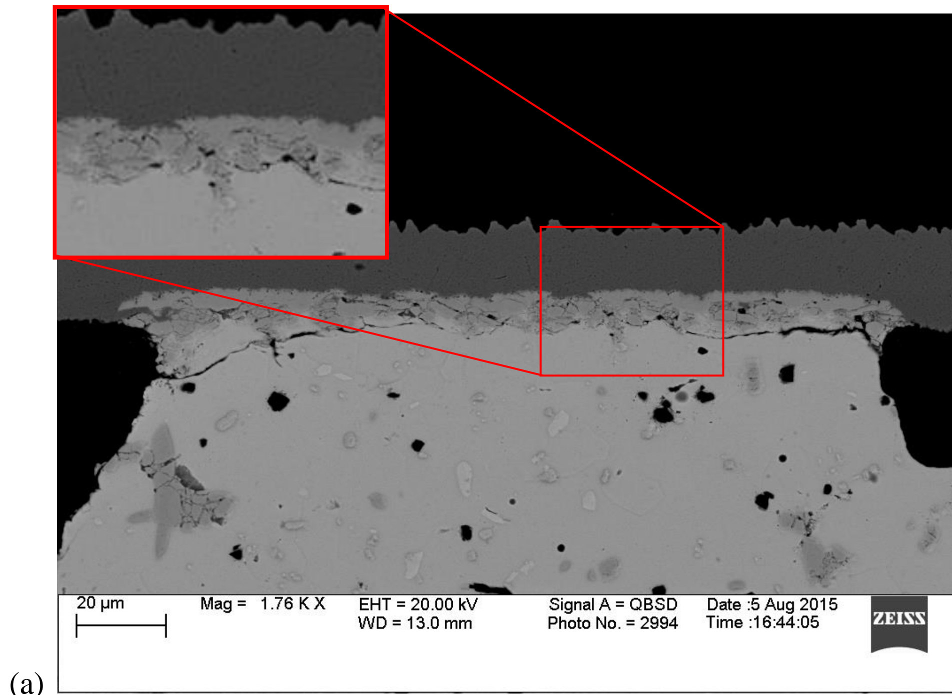

(a)

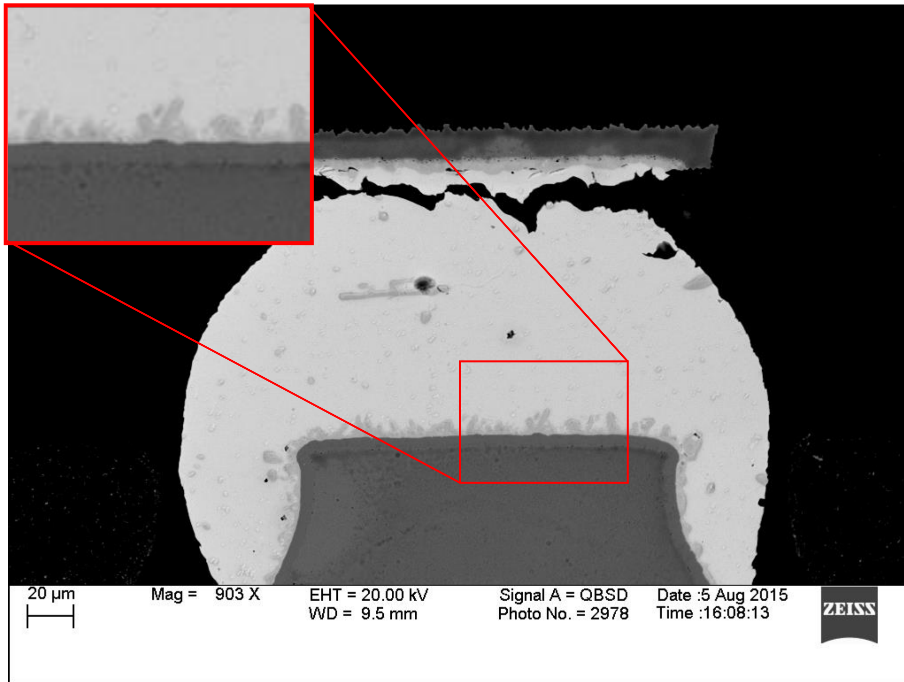

(b)

Figure 58. IMC Layer of 10mm SAC105 solder joint finished with ENIG at Package Side (a) and Board Side (b).

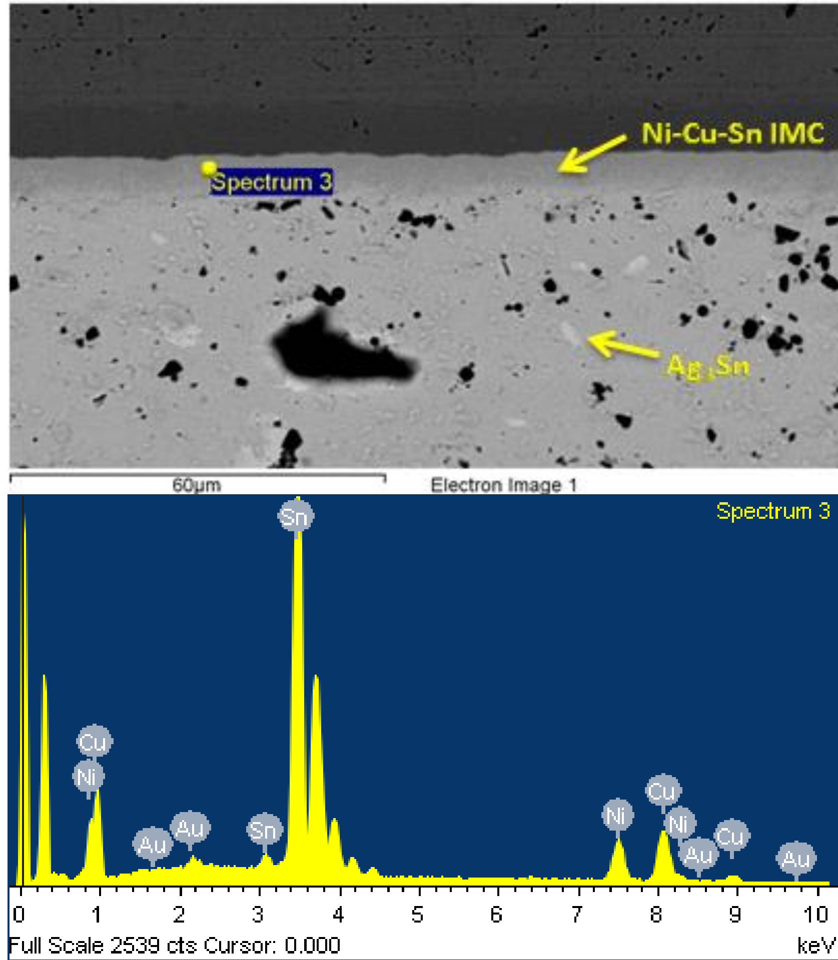

Element	Weight%	Atomic%
Ni K	10.15	16.61
Cu K	16.25	24.56
Sn L	71.42	57.78
Au M	2.17	1.06
Totals	**100.00**	

Figure 59. Package side IMC EDX for SAC305 (0.8 mm pitch) solder joint on ENEPIG, 6 months aging.

In SAC/ENIG/ENEPIG systems, the IMC layer is of Cu-Sn type with a small proportion of nickel: $(Ni,Cu)_6Sn_5$ and $(Ni,Cu)_3Sn_4$. The nickel layer in ENIG/ENEPIG

systems acts as a diffusion barrier which inhibits Cu dissolution into the solder to ensure better reliability. It is expected to find a small fraction of Au in the IMC zone. [79]

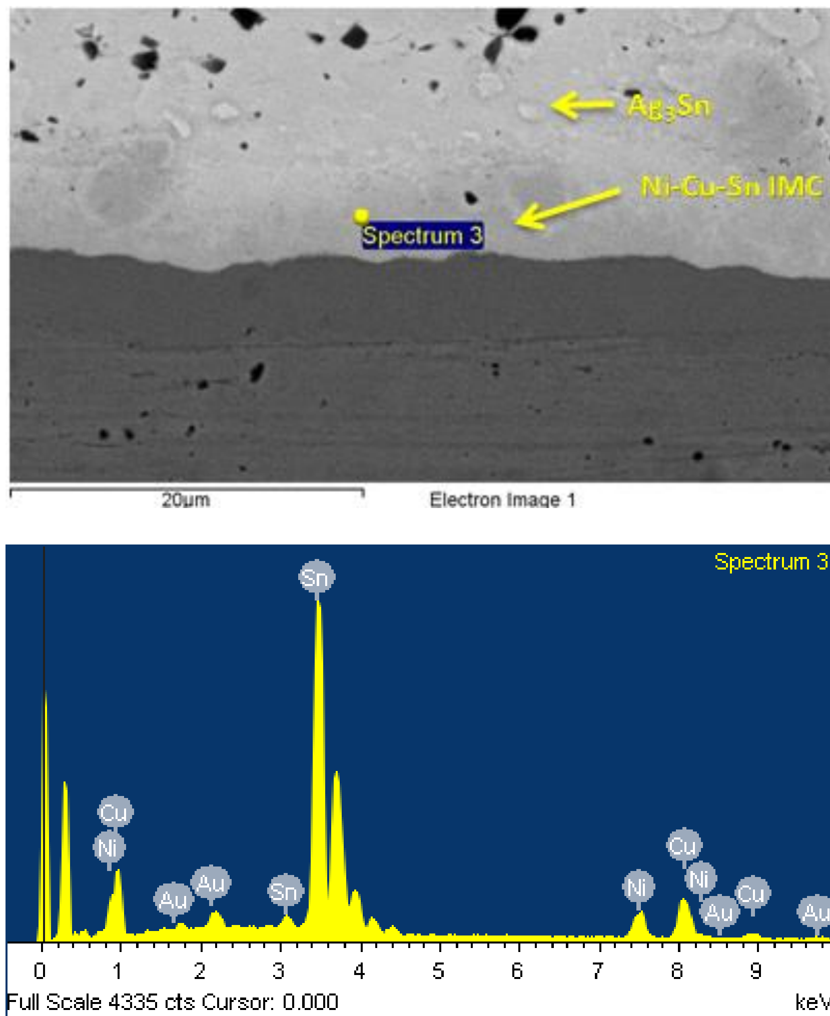

Element	Weight%	Atomic%
Ni K	8.22	13.78
Cu K	15.86	24.57
Sn L	71.87	59.62
Au M	4.05	2.03
Totals	**100.00**	

Figure 60. Board side IMC EDX for SAC305 (0.8 mm pitch) solder joint on ENEPIG, 6 months aging.

Figure 60 shows all the elements found at the board side. The percentage of elements is similar to the package side in Figure 59.

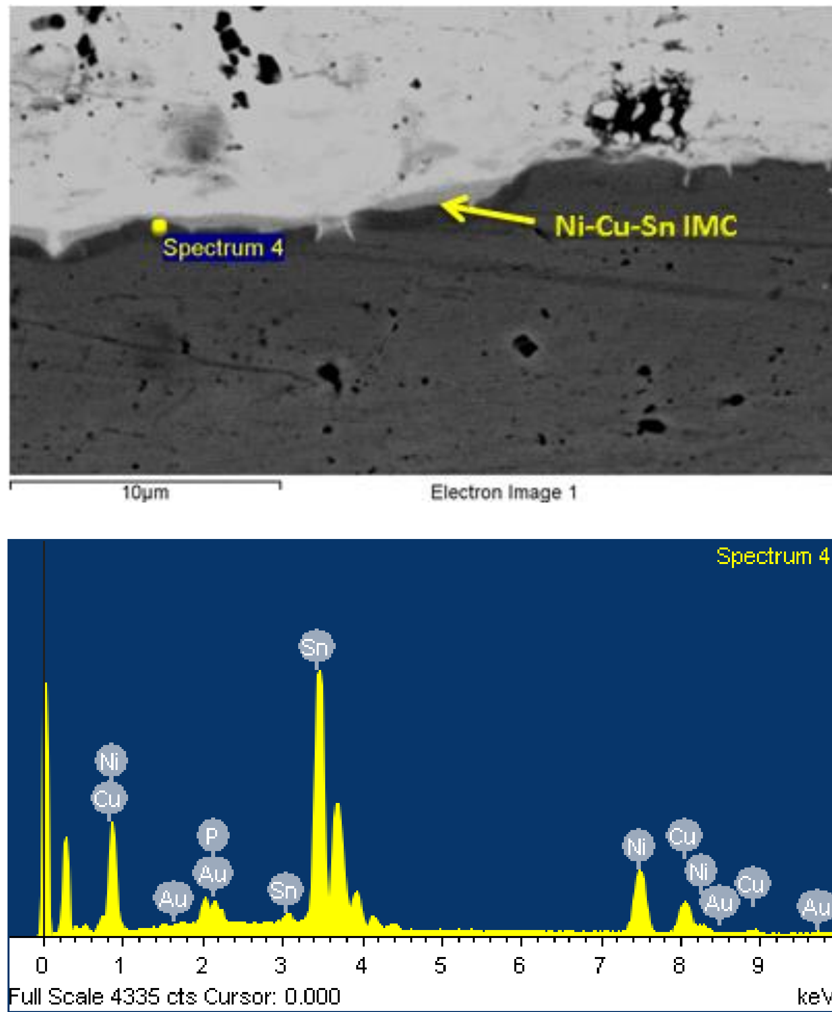

Element	Weight%	Atomic%
P K	1.93	5.46
Ni K	20.21	30.13
Cu K	13.25	18.25
Sn L	59.60	43.94
Au M	5.01	2.22
Totals	**100.00**	

Figure 61. Board side IMC EDX for SAC305 (0.8 mm pitch) solder joint on ENIG, 6 months aging.

Figure 61 shows that phosphorus is often observed at the interfaces due to the process deposition of the nickel layer. [80]

5.1.2 IMC Thickness Analysis

Five IMC thickness measurements (Table 18 & Table 19) were averaged along the intermetallic layer for 10 groups five solder balls located at a left corner, left middle, center, right middle and right corner line under a package.

Table 18. 0.8mm pitch SAC305 Board Side IMC Thickness Growth during 125°C Aging

Surface Finishes (0.8mm pitch)	No Aging (µm)	6 month Aging (µm)	12 month Aging (µm)
ImAg	1.83	6.45	9.04
ENIG	2.37	3.89	5.99
ENEPIG	1.55	4.43	5.7

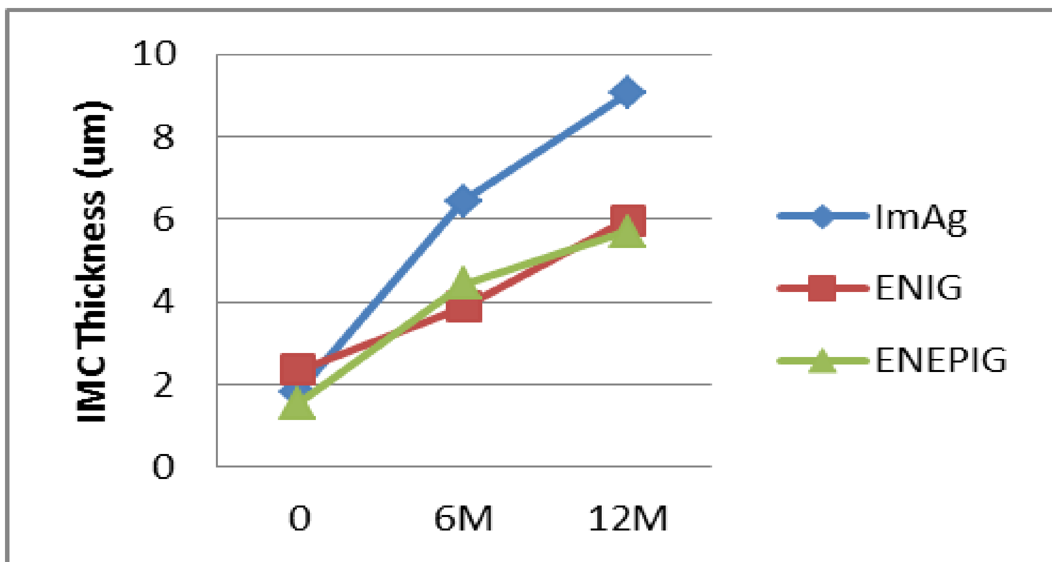

Figure 62. 0.8mm pitch SAC305 Board Side IMC Thickness Growth during 125°C Aging

Figure 62 shows that ENIG and ENEPIG have a smaller average IMC thickness than ImAg, which may be due to the prevention of the Ni layer barrier. It also shows that ENEPIG has a smaller average IMC thickness under the no aging condition than ENIG, which may be due to the additional presence of Pd in ENEPIG, assuming Pd provides an additional barrier to Cu diffusion. Eventually, after 12 months of aging, the board side IMC for both ENIG and ENEPIG finishes approaches a similar thickness. However, the fact that both ENIG and ENEPIG IMC thicknesses are increasing vs. aging time offers a partial explanation for the degraded reliability performance of SAC alloys on ENIG/ENEPIG over time and temperature. [81]

Table 19. 0.8mm Pitch SAC105/SAC305 Board Side IMC Thickness Growth with ENIG Finish

ENIG (0.8mm pitch)	No Aging (μm)	6 month Aging (μm)	12 month Aging (μm)
SAC105	3.74	5.17	5.39
SAC305	3.41	3.89	4.09

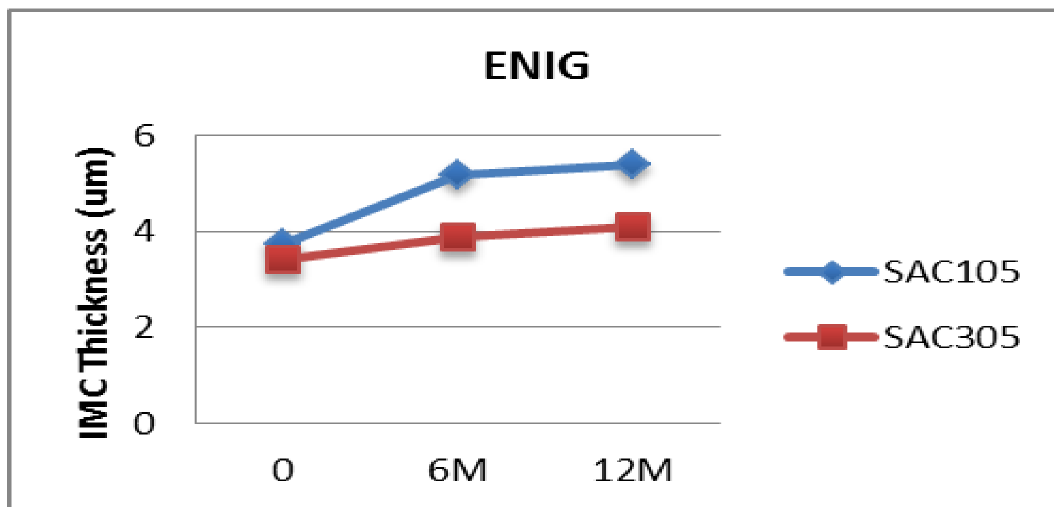

Figure 63. 0.8mm Pitch SAC105/SAC305 Board Side IMC Thickness Growth with ENIG Finish

In Figure 63, we find that the **IMC thickness of SAC305 is less than SAC105 with ENIG plating after 6 month and 12 month aging.**

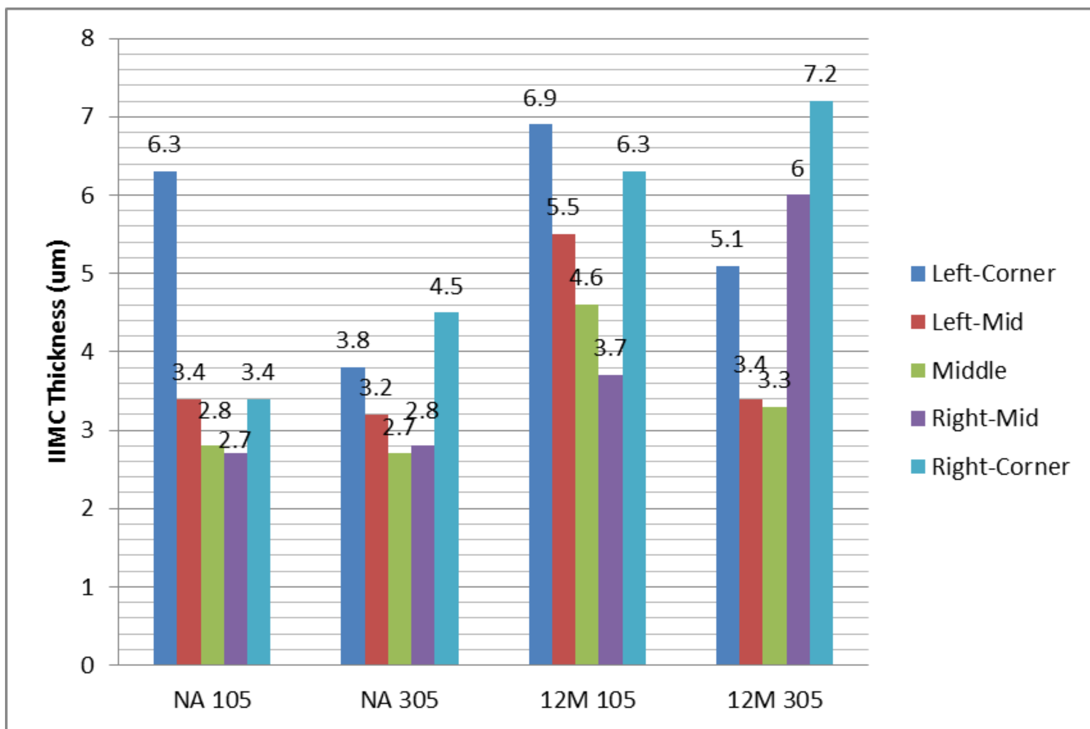

(a)

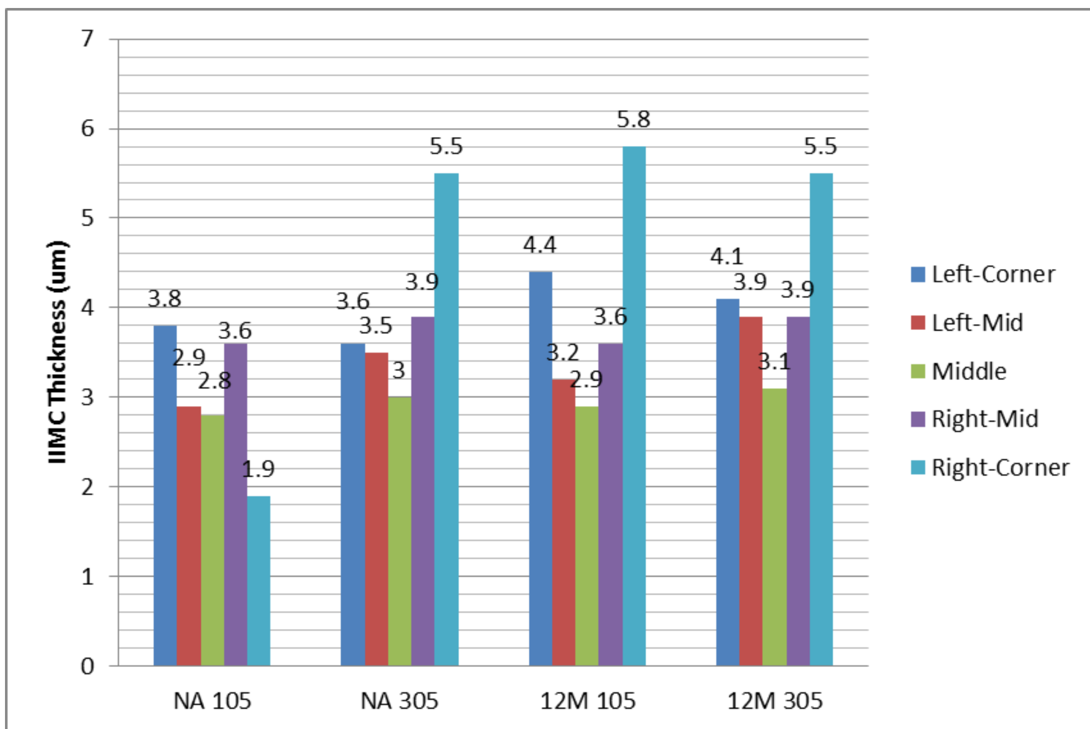

(b)

Figure 64. IMC thickness analyses for 15mm BGAs with ENIG finish. (a) Board Side (b) Package Side

As Figure 64 shows, the IMC is thicker at corner side solder balls than center balls in most cases.

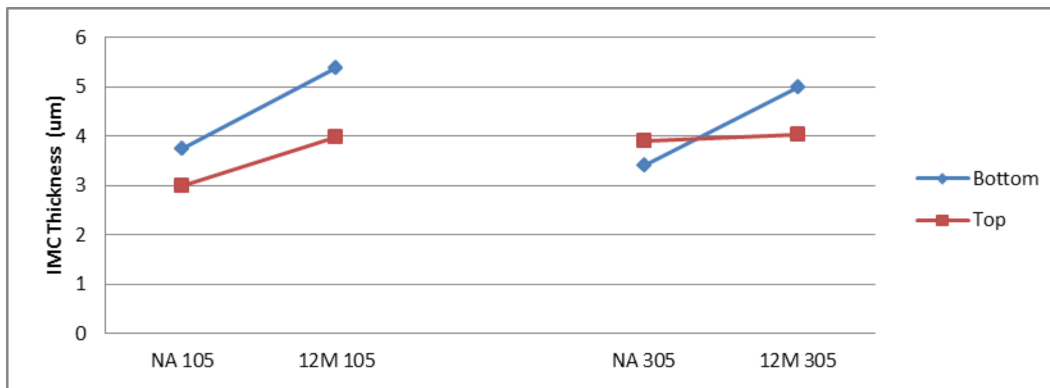

a) b)

Figure 65. IMC thickness growth with ENIG finish on package (top) and board (bottom) side for 15mm solder balls.

From Figure 65, we can find the aging effect on the IMC growth. The IMC thickness growth rate is higher at bottom side (board side) than top side (package side) solder balls, a finding which is observed in most of 15mm BGA samples of our test. There are lots of factors may effect on this, like Cu diffusion rate, ENIG layer thickness, solder joint structure, rigional temperature difference and so on. One possible explanation for this result is related to the thickness of Ni layer on package and board side. A thicker Ni barrier should be more effective to avoid Cu diffusion and lead to slower IMC growth rate. I suggest running different Ni layer thickness test on both sides on 15mm SAC 305 solder joints to find a best one which could balance reliability performance and material cost.

5.1.3 IMC Thickness Growth Effect

Moreover recent investigations [15] had reported that the growth of Cu–Sn IMC layer had a degraded effect on the solder joint reliability, with increasing thickness of the Cu–Sn IMC layer, the thermal fatigue life of solder joints will decrease.

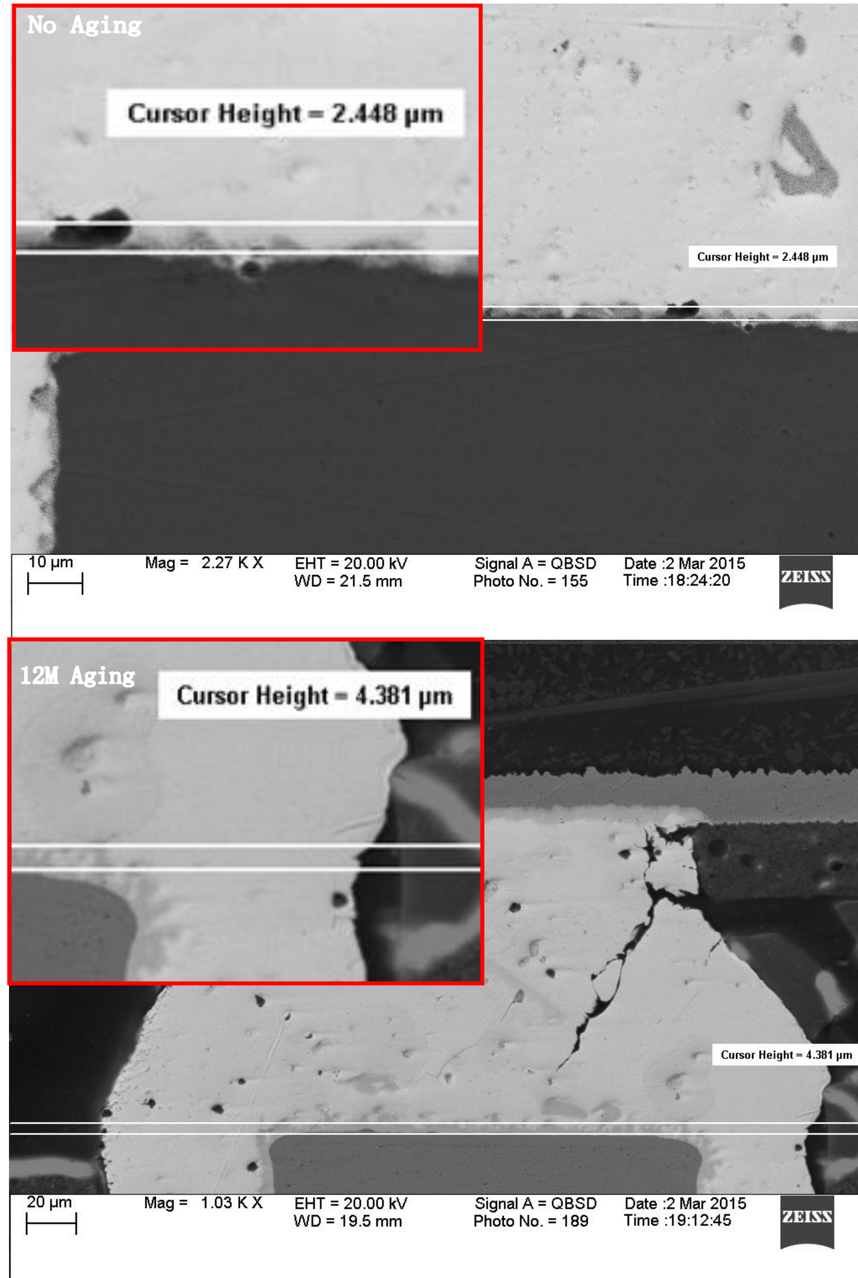

(a)

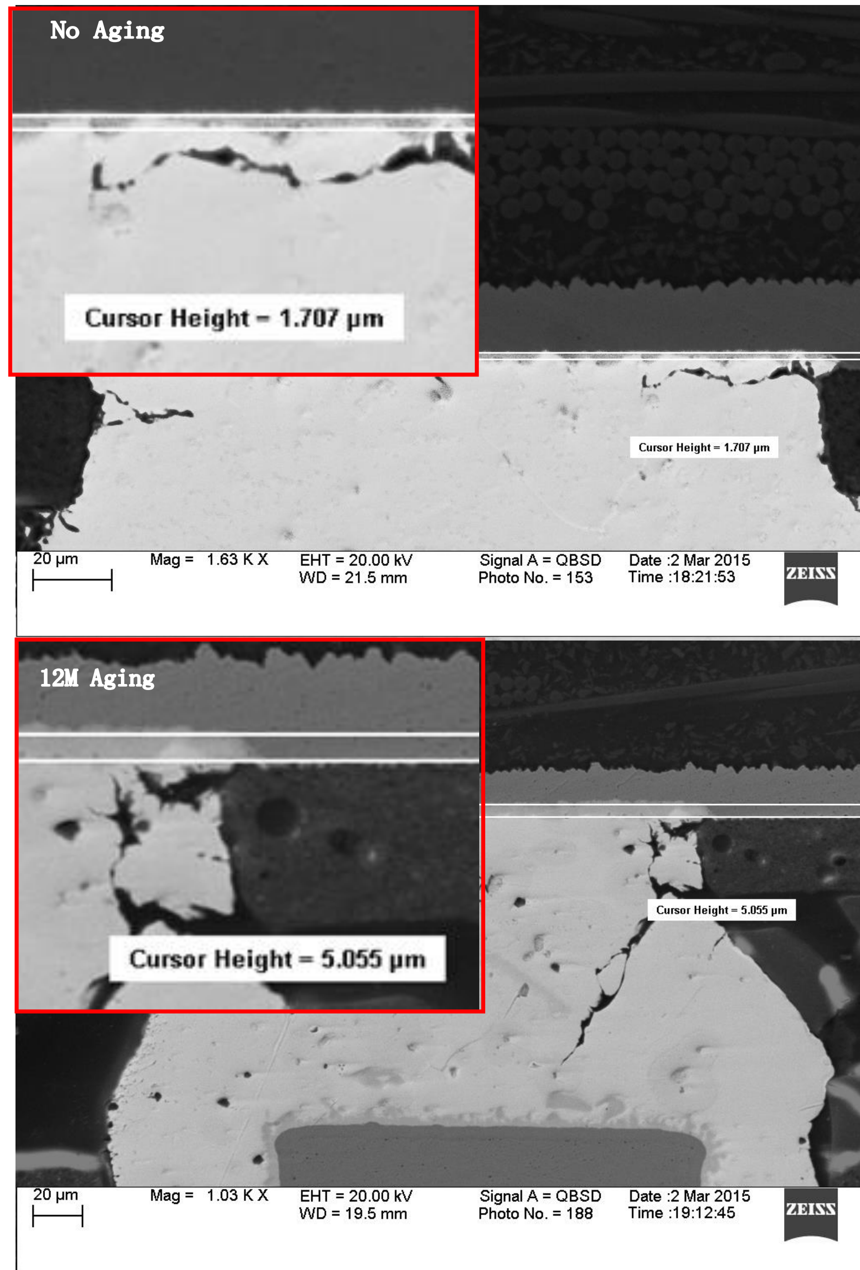

(b)

Figure 66. IMC Thickness Growths with the Effect of Aging for 10mm SAC 105 solder joints finished with ENIG (a) Board Side, (b) Package Side

Above figures show the IMC thickness growth after aging. (Figure 66)

5.2 Failure Mode

Figure 67 shows three typical failure modes for the 10mm package size, 0.4mm pitch BGA after thermal aging and cycling for SAC105 on ENEPIG and ENIG surface finishes, respectively. It looks like the microstructure deformation of finer pitch solder interconnections (0.4mm) is much more severe. The cracks are more likely initiated at the package side corner of the interconnection and then proceed along the IMC boundary, see Figure 67(a). Figure 67(b) shows a crack path with an angle downwards to the solder bulk after thermal aging and cycling. Occasionally, cracks may generate from the inside of solder ball (Figure 67(c)). [82][83]

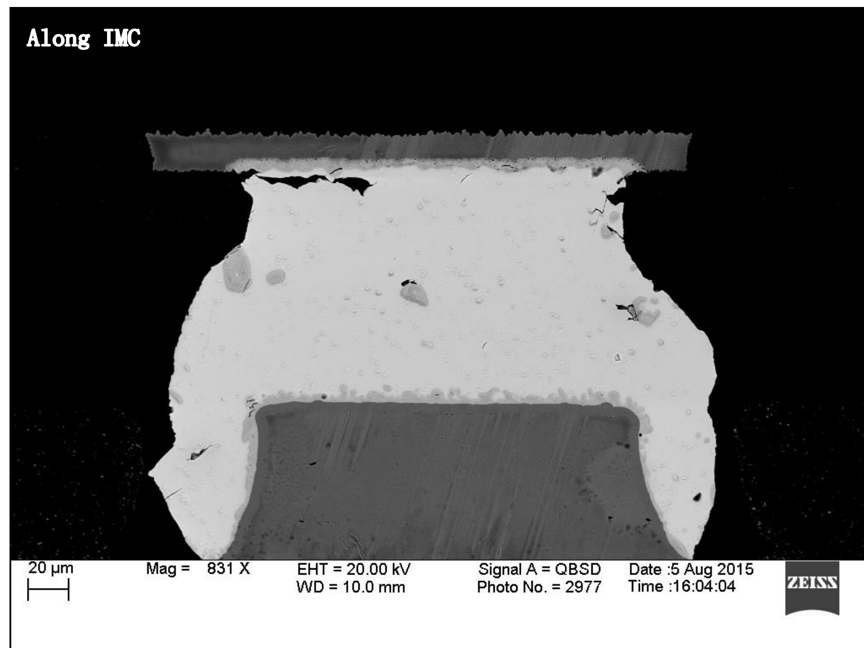

(a)

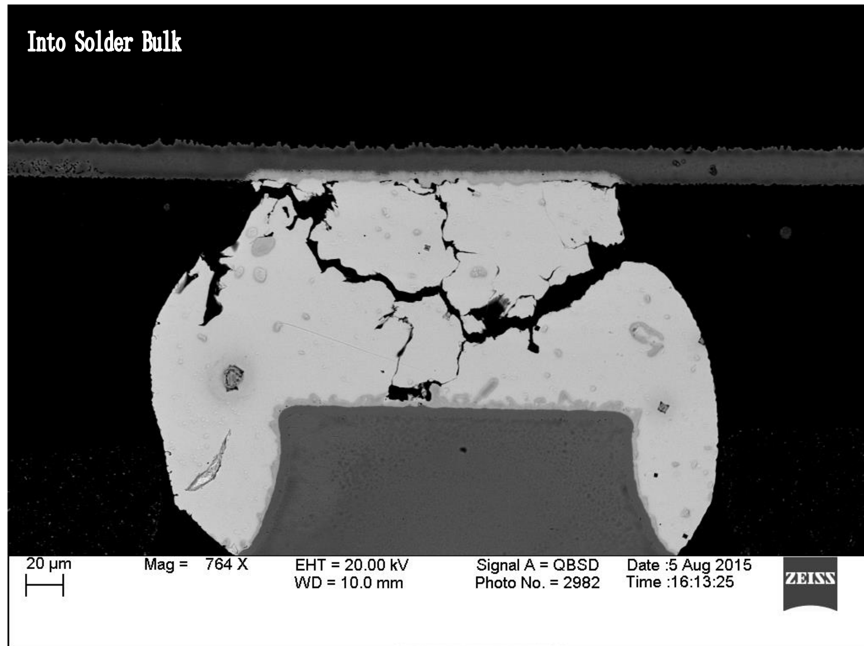

(b)

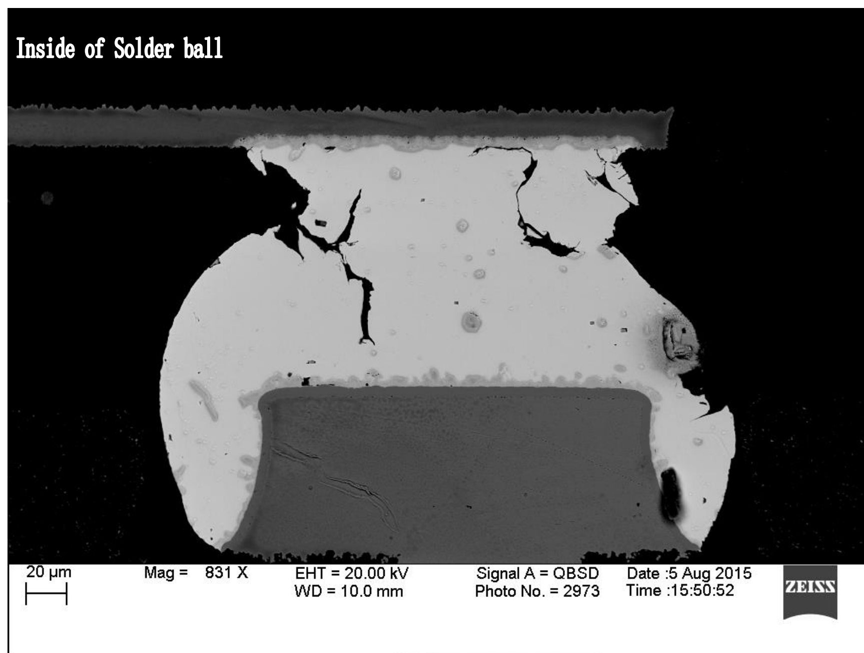

(c)

Figure 67. SEM Images of 10mm Package SAC105 Solder Interconnections after 1 Year Aging at 125°C: (a) Crack at Package Side and Goes Along with IMC Boundary, ENEPIG Finished, (b) Crack Goes into The Solder Ball, ENIG Finished, (c) Crack Generates from The Inside of Solder Ball, ENIG Finished.

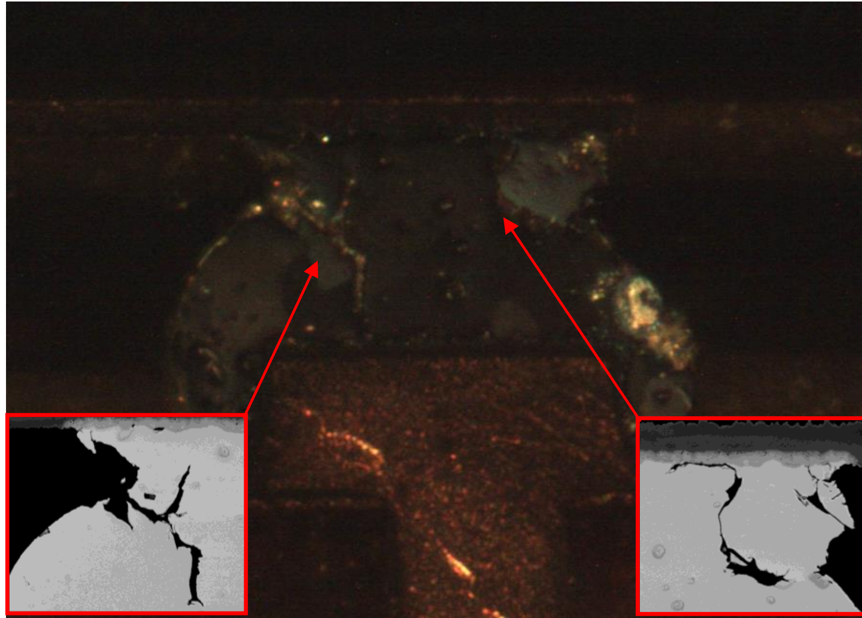

Figure 68. Cross-polarized Image of Figure 5.10(c).

As Figure 68 shows, the reason that crack generated from the inside of solder ball appears to be the grain structure recrystallization. It is clear that the fatigue failure comes up and propagated at grain boundaries. [84]

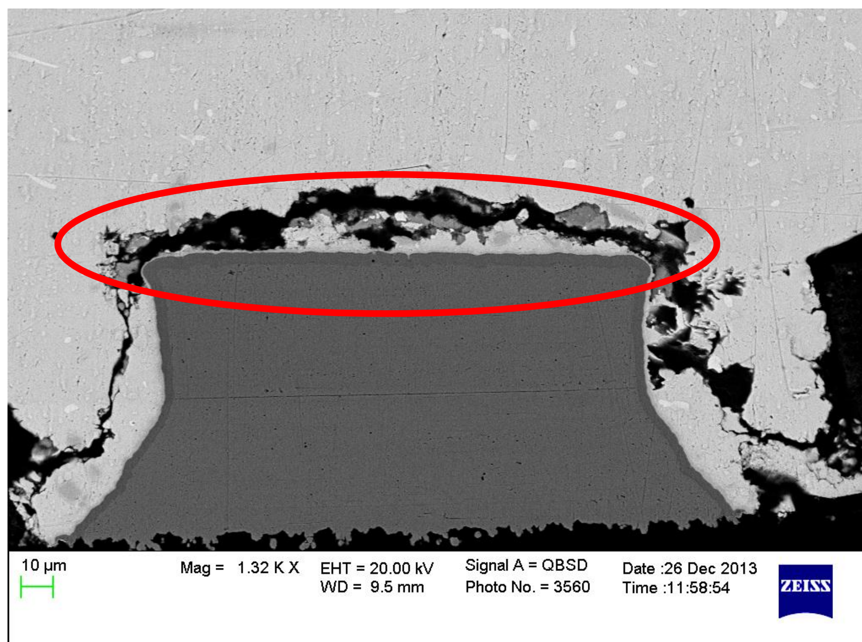

(a)

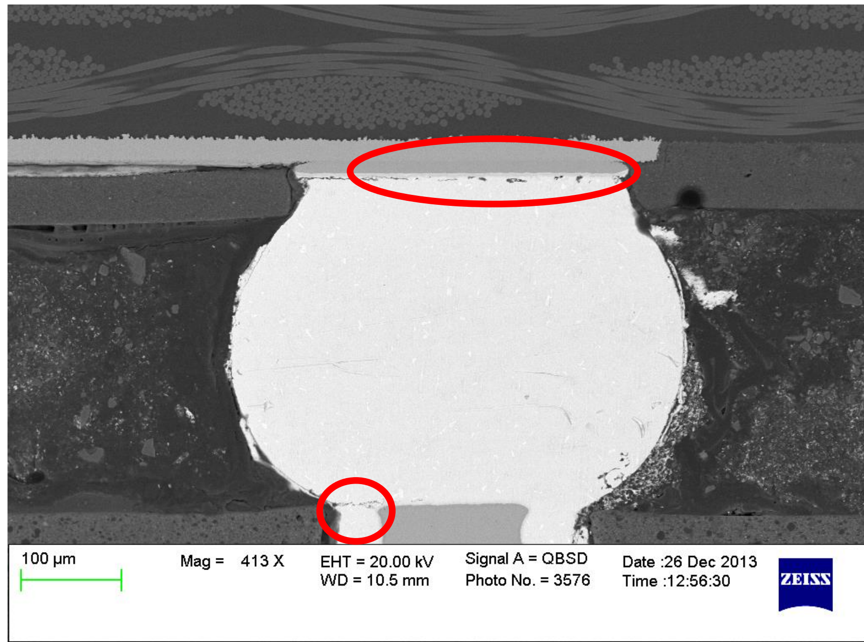

(b)

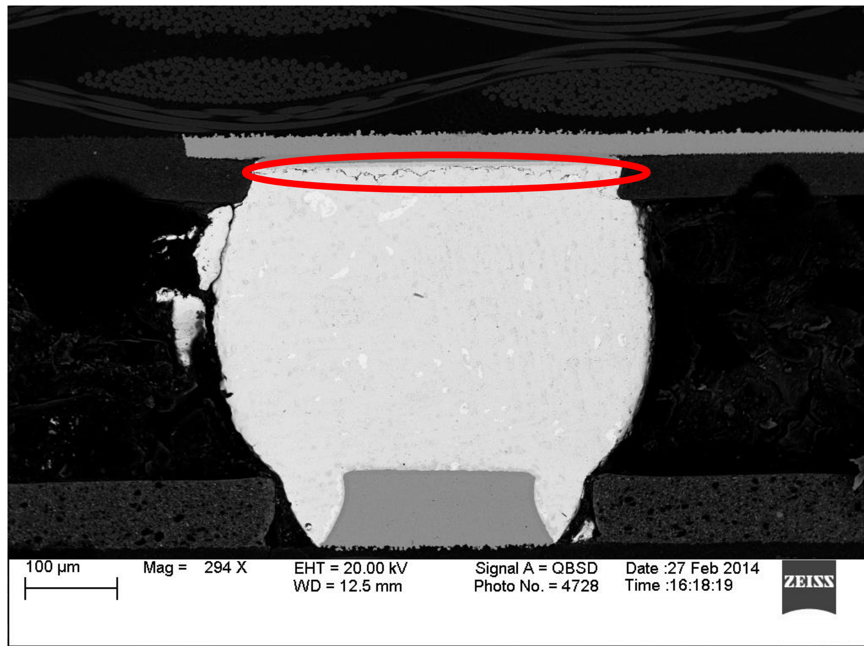

(c)

Figure 69. SEM images of 15mm package SAC305 solder interconnections after 1 year thermal aging at 125°C: (a) Crack at package side, ENIG finished, (b) Crack at both sides, ImAg finished, (c) Crack at board side, ENEPIG finished.

Figure 69 shows three typical failure modes for the 15mm package size, 0.8mm pitch BGA after thermal aging and cycling for SAC305 on ENIG, ENEPIG and ImAg surface finishes, respectively. The cracks may appear at package side only, board side only or even both sides.

5.3 Crack Propagation

The shear stress created from the CTE mismatches at the both package and board-side solder/finish interface cause plastic deformation, which generates cracks which propagate along those areas of the solder joint. [85]

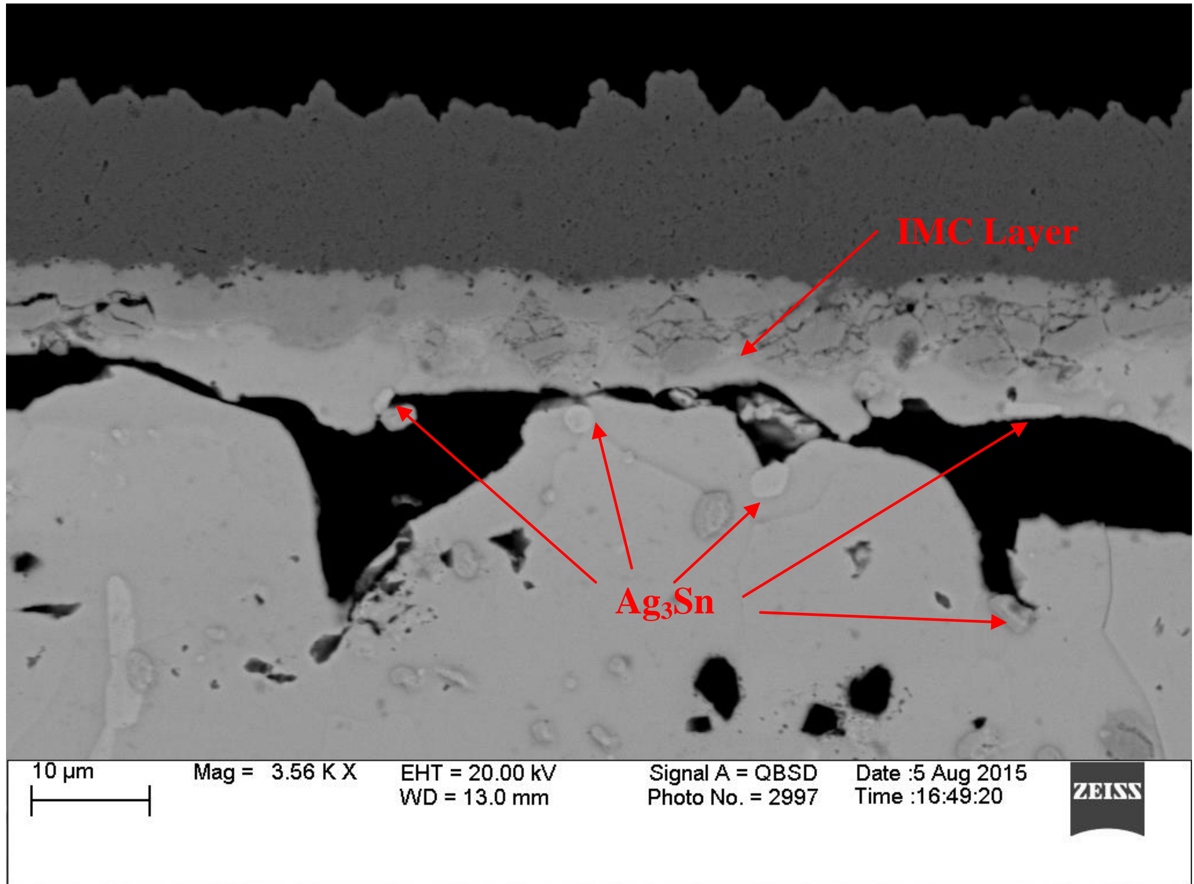

(a)

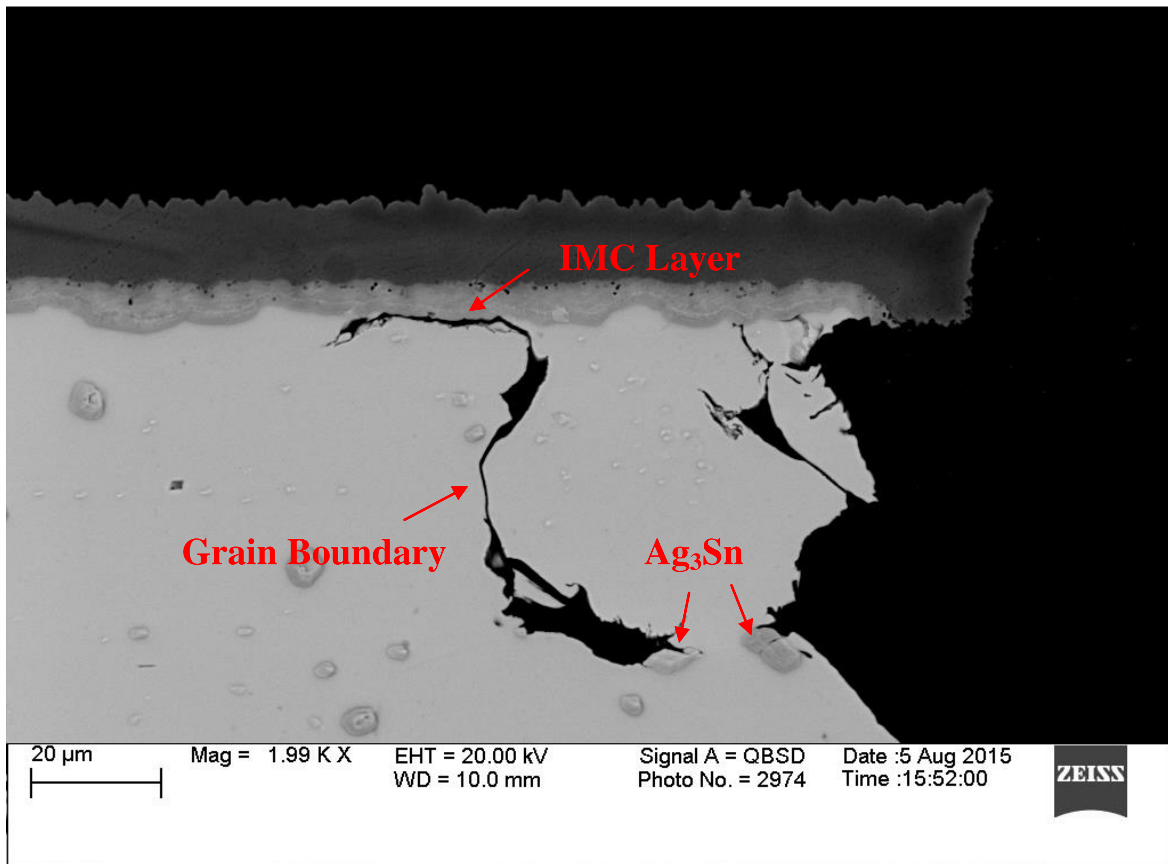

(b)

Figure 70. SEM Images of 10mm Package SAC105 Solder Interconnections after 6 Months aging at 125°C: (a) Crack Goes Along with IMC Boundary and Blocked by Ag_3Sn Particle, ENEPIG Finished, (b) Crack Propagation is subject to IMC Layer Boundary, Grain Boundary and Ag_3Sn Particles. ENIG Finished.

Finer pitch packages typically have less structural stability than larger pitch packages. Figure 70 shows the cross-polarized and SEM images of two 10mm SAC105 solder balls, those cracks which might be affected by grain boundaries. This is due to the formation of a continuous network of high-angle (grain) boundaries by local recrystallization increased grain structure movement along the interfacial region, thus, enhanced cracks to nucleate in and propagate through the recrystallized solder interconnections. [86]

Figure 70 also shows another two factors: 1) package side IMC boundaries; 2) larger IMC precipitates in the solder bulk as Ag_3Sn.

Chapter 6

6.1 Conclusion

1) According to the reliability performance of 19mm, 15mm, 10mm, and 5mm BGA package subjected to 24 months 125°C aging we could easily find the Weibull characteristic lifetime is dramatically reduced during isothermal aging at 125°C for SAC105/305 on a variety of package sizes.
2) Different Package Size BGA components have different reliability performances. For perimeter ball alignments, the 19mm and 15mm BGAs always have higher characteristic lifetimes than the 10mm, which shows that packages with large solder balls have higher reliability. On the other hand, the 5mm BGA has the highest characteristic life, indicating that packages with full array ball alignments perform better than perimeter ball alignments under high temperature aging + thermal cycling conditions.
3) For the SAC solder immersion with Ag, a first layer Cu_6Sn_5 (η-phase) intermetallic is formed at the board/solder joint interface. Then, a second layer of Cu_3Sn (ε-phase) is formed at the IMC layer/board interface during aging which reduces the mechanical behavior of the solder joint.
4) For ENIG/ENEPIG finishes, as figure 9 shows, in the interfacial reaction between the Ni layer and SAC 105 /SAC 305, ternary IMCs consisting of Cu, Ni and Sn are observed. The IMC layer is of Cu-Sn type with a small proportion of nickel: $(Ni,Cu)_6Sn_5$ and $(Ni,Cu)_3Sn_4$. [14] The nickel layer in ENIG/ENEPIG systems acts as a diffusion barrier which inhibits Cu dissolution into the solder to ensure better

reliability. Phosphorus is also present, due to the process deposition of the nickel layer. In our test, all components are finished with ENIG on package side.

5) For 10mm BGA package with ENIG or ENEPIG finished, the ranking of lifetime performance with thermal aging and cycling is that: SAC 305 > SAC 105>SnPb in all cases; For 15mm BGA package with ENIG or ENEPIG finished, the ranking of lifetime performance with thermal aging and cycling is that: SAC 305 > SAC 105>SnPb in most cases, except ENIG no aging group.

6) The Weibull characteristic lifetime is dramatically reduced during isothermal aging at 125°C for SAC105/305 on a variety of board finishes. Generally, the rank of the characteristic lifetimes for both SAC105/305 with different surface finishes follows the order: ENIG>ENEPIG>ImAg.

7) In particular, SAC105 undergoes a considerable lifetime reduction during aging and illustrates the risk in using SAC105 solder balls in applications where thermal fatigue failure is a concern. In all cases, SAC305 solder alloy using ImAg, ENIG, or ENEPIG has a longer lifetime than SAC105, both with/without thermal aging.

8) Failure analysis showed the IMC is thicker at corner side solder balls compared to center balls in most cases. The continuous growth of Cu-Sn IMC (SAC/ImAg systems) and Cu-Ni-Sn IMC (SAC/ENIG/ENEPIG systems) on board side solder joints finally result in fatigue failures. Under the help of imbedded Ag3Sn particles which form in the solder during aging, higher Ag content solder balls (SAC305) perform better than SAC105. For 15mm package size SAC105 BGA finished with ImAg, ENIG and ENEPIG, cracks initially start from the corner of the interconnection and then proceed along the interface IMC. For 10mm package size

SAC105 BGA finished with ENIG and ENEPIG, cracks most likely start from the corner of the package side and then proceed along the interface IMC and often into the solder bulk. Three factors are considered: Package side IMC boundaries, Ag3Sn particles and Grain boundaries.

6.2 Limitation and Uncertainty

1) SMT process: As figure 44(b) shows, SMT board manufacturing problems may generate early failure during thermal aging and cycling.
2) Wiring process: There are thousands of component needed to be wired. That may cause additional room temperature aging during the wiring process.
3) Aging and cycling process: Ovens are relatively old. Sometimes, they would stop working.
4) Components limitation: Components are provided by customer. It is hard to do Pitch/Package ratio comparison with thermal aging and cycling.
5) Further test is needed for Full array vs. Perimeter alignment comparison with same pitch and package size to find out the effect of alignment.
6) IMC measurement deviation: the accuracy of IMC layer thickness measurement is uncertain.
7) Cross section sample: The solder joint crack may be happened when cutting and polishing sample.

6.3 Publications

1) Long-term Aging Effects on Reliability Performance of Lead-Free Solder Joints, Z Hai, J Zhang, C Shen, J. L Evans, M. J Bozack, Proc. Surface Mount Technology International Conference, 362-370

2) Reliability Degradation of SAC105 and SAC305 BGA Packages under Long-Term, High Temperature Aging, Z Hai, J Zhang, C Shen, J. L Evans, M. J Bozack, Journal of SMTA

3) The Effect of Isothermal Aging on The Reliability of Sn-Ag-Cu Solder Joints Using Various Surface Finishes, Z Hai, J Zhang, C Shen, J. L Evans, M. J Bozack, SMTA International 2014

4) Reliability Performance of Lead-Free Solder Joints under Harsh Environments, Z Hai, J Zhang, C Shen, J. L Evans, M. J Bozack, IPC-ESTC 2014

5) Long Term Aging Effects on the Reliability of Lead Free Solder Joints In Ball Grid Array Packages With Various Pitch Sizes and Ball Alignments, Cong Zhao, Chaobo Shen, Zhou Hai, Jiawei Zhang, M.J. Bozack, and J. L. Evans, SMTA International 2015

6) Reliability Performance of Lead-Free SAC Solder Joints on ENIG and ENEPIG Subject to Long-Term Isothermal Aging, Z Hai, J Zhang, C Shen, E.K. Snipes, M.J Bozack, J.L.Evans, Journal of Mechatronics, 100-108

7) Effects on Reliability of Lead-Free Solder Joints under Harsh Environment, Z Hai, J Zhang, C Shen, C Zhao, JL Evans, MJ Bozack, International Symposium on Microelectronics 2014 (1), 000471-000476

8) Reliability Analysis of Aging Effect on Joint Microstructures in Sn-Ag-Cu Solder Joints in Thermal Cycling, C Shen, Z Hai, C Zhao, J Zhang, MJ Bozack, JC Suhling, JL Evans, ASME 2015 InterPACK 2015

9) Sn-Ag-Cu Solder Joints Interconnection Reliability of BGA Package during Thermal Aging and Cycling, C Shen, C Zhao, Z Hai, J Zhang, MJ Bozack, JC Suhling, JL Evans, International Symposium on Microelectronics 2015 (1), 000135-000140

10) Reliability Study and Failure Analysis for Surface Finishes on Sn-Ag-Cu Solder Joints during Thermal Cycling, C Shen, Z Hai, C Zhao, J Zhang, MJ Bozack, JC Suhling, JL Evans, Journal of Mechatronics, Accepted

Chapter 7

Future Work

Since there were limited numbers of test samples, there are a lot of variations for this test. Further research is needed to demonstrate the effect of ball alignment with same die size, package size and pitch size. Ball alignment test is suggested for 15mm and 5mm with same die/package ratio and the ball alignment test for 5mm with different die size in the next step.

According to the finding that bottom side IMC growth rates are lower than the top side, Ni layer thickness maybe a concern. Different Ni layer thickness tests are needed in the future to evaluate this issue.

And under the limitation of component options, it is unfortunate that the characteristic life time comparison with different die/package ratio test could not be performed. Data analysis is needed on current and future data in order to discover the characteristic lifetime variations of different surface finish like OSP and ENIG.

Because this kind of thermal test takes more than 1 year to complete, finite element analysis would be used to construct to model of the solder joint and correlated with test results to better predict the solder joint life. Detailed stress strain analysis can be achieved from the model to build up the joint thermal fatigue theory regarding long-term aging effect. Microstructure analysis would be kept on to discover the root cause of different of failure mode.

A polarized microscope is needed to deeply and clearly study morphology changes such as grain structure evolving and types of IMC growth at various geometric locations in order to understand the creep effect on joint reliability reduction.

Auburn is currently engaged in a multi-million dollar Solder Doping (micro-alloying) study to find a solution for the harsh environment electronics industry. This study is to evaluate the effect of long term isothermal aging and thermal cycling on the reliability of lead-free solder mixes with different solder doping, PC Board plating, and temperature aging for ball grid array (BGA), quad flat no lead packages (QFN) and 2512 Resistor from different environment of electronics.(Figure 71) The outcome data and further microstructure morphology study will be analyzed and compare with current project's results to construct a larger blueprint of lead-free solder joint reliability performance.

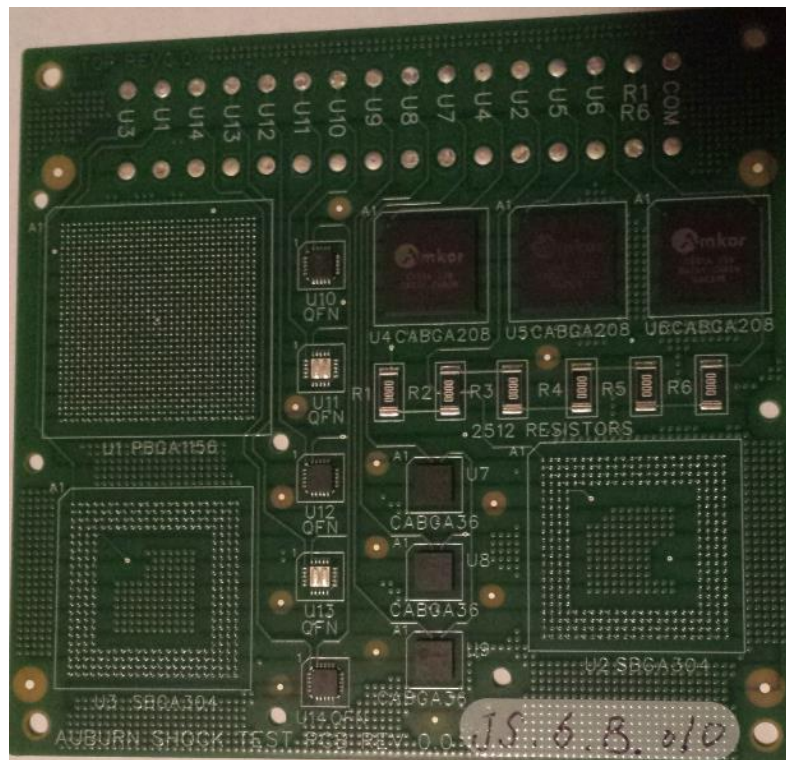

Figure 71. Test Board Design

The primary goal is to find a manufactureable solder paste that will mitigate the effects of aging on lead-free solder joints, and secondary goal would be to find a paste for solder doping that could be used for individual package reliability enhancement and a solder for solder-sphere replacement to enhance the solder joint reliability.

Twelve doped solder pastes supplied by eight high volume companies, as well as SAC105 and SAC305 lead-free solder balls together with three board platings of OSP, Immersion Silver and ENIG are being tested. Package sizes ranges from 15mm, 0.8mm pitch BGA to 6mm, 0.5mm pitch BGA, and QFN and 2512 Resistor were tested. (Table 20)

Table 20. Component Matrix

Item	Component	Pitch (mm)	I/O	Numbers per board	Note
3	15mm BGA	0.8	208	3	1-105,1-305,1-match
4	6mm BGA	0.8	36	3	1-105,1-305,1-match
5	5mm QFN	0.65	20	3	
6	2512 Resistor			6	

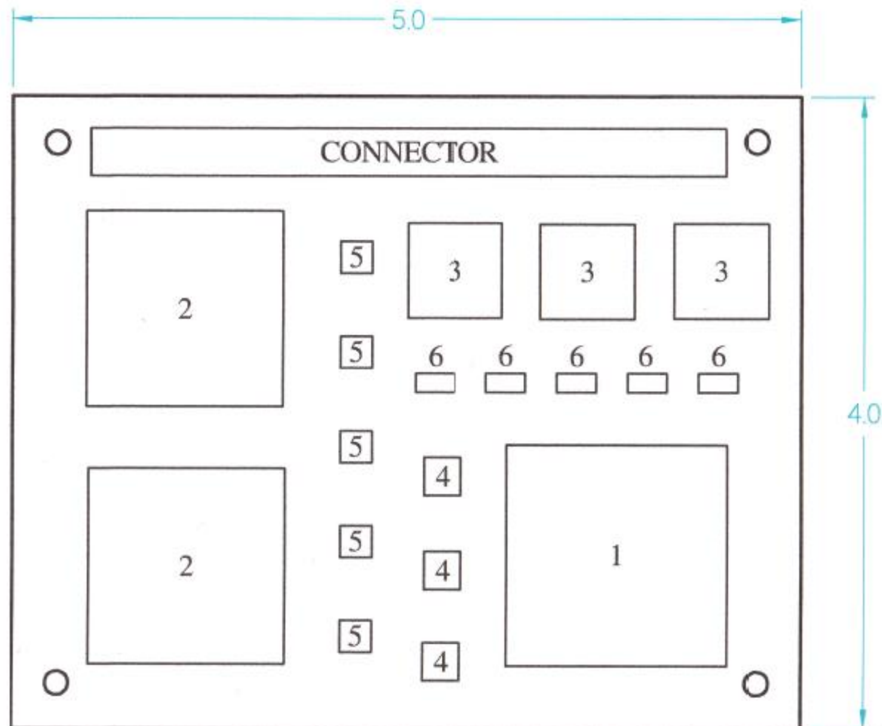

Figure 72. Componet Matrix

The isothermal temperature condition is 125℃ with aging time period of 12 months. A similar monitoring system and cycling profile should be used to keep data consistency.

Data analysis will be performed, and statistical Weibull distribution will be used here to show the characteristic life degradation for the different solder pastes under different conditions. Failure modes of solder joints as well as microstructure change will be investigated using Scanning Electron Microscope (SEM) to track different crack propagations across the solder bulk cross section, and also Intermetallic Compound (IMC) layers thickness will be measured. Energy-dispersive X-ray spectroscopy (EDX) will be employed also to analyze the chemical characterization of IMC layer for SAC/ImAg, SAC/OSP and SAC/ENIG systems.

Finally, computer simulations with finite element models will be built to compare with the test data. The ideal outcome for this project is to select the solder paste and board plating combination which provides the best reliability of each component category, and to further investigate how thermal aging effect influences the reliability to the lead free solder balls.

References

1. Ra y P. Prasad, "Surface Mount Technology Principles and Practice".
2. A. Syed and W. Kang, "Board level and Assembly and Reliability Considerations for QFN Packages", Amkor Technology, Inc.
3. K. Tsutsumi, M, Kohara, Y. Shinoya, T. Tada, K. Sakashita, H. Shibata and H. Nakata, "Composite-Type Pin Grid Array Package", IEEE transactions on components hybrids and manufacturing technology, Vol. CHMT-9, No. 4, 1986.
4. Inter, "Ball Grid Array (BGA) Packaging", 2000 Packaging Databook.
5. Land Grid Array (LGA) Socket and Package Technology" (PDF). Intel. Retrieved October 1, 2015.
6. Chapter 177 - Step-down μModule regulator produces 15A output from inputs down to 1.5V—no bias supply required: 1.5V to 5.5V input, 0.8V to 5V output from a 15mm × 15mm × 4.32mm LGA package, Analog Circuit Design, 2015, Pages 373-374, Alan Chern, Jason Sekanina
7. J. Fjelstad, "IC packaging - Nearing 50 years of evolution", Global SMT & Packaging, 2007
8. http://flipchips.com/tutorial/process/drop-in-lead-free-solder/
9. Qualitative electroless Ni/Au plating considerations for the solder mask on top of sequential build-up layers, Applied Surface Science, Volume 252, Issue 8, 15 February 2006, Pages 2717-2740, Sam Siau, Alfons Vervaet, Lieven Degrendele, Johan De Baets, Andre Van Calster
10. D.A. Benson, R. T. Mitchell, M. R. Tuck, D. R. Adkins, D. Shen, D. W. Palmer, "MicroMachined Heat Pipes in Silicon MCM Substrates", Microelectronics and Photonics Sandia National Laboratories.
11. Effect of surface finishes on electromigration reliability in eutectic Sn-58Bi solder joints, Microelectronic Engineering, Volume 120, 25 May 2014, Pages 77-84, Jae-Ha Kim, Young-Chul Lee, Sang-Min Lee, Seung-Boo Jung
12. Surface Finishes Utilized in the PCB Industry Presented by Dan Slocum, Jr. http://www.eeweb.com/blog/eeweb/pcb-surface-finishes-find-favor
13. SOLDER FAMILIES AND HOW THEYWORK, Low melting-temperature alloys are vital to successful

electronics assembly. Eric Bastow, Indium Corp. of America, Utica, New York

14. D.R. Frear, The mechanical behavior of interconnects materials for electronic packaging, JOM, 48 (1996), pp. 49–53
15. H. Mavoori, J. Chin, S. Vaynman, B. Moran, L. Keer, M. Fine, Creep, stress relaxation, and plastic deformation in Sn–Ag and Sn–Zn eutectic solders, J Electron Mater, 26 (1997), pp. 783–790
16. A review on thermal cycling and drop impact reliability of SAC solder joint in portable electronic products, Dhafer Abdulameer Shnawah, , Mohd Faizul Mohd Sabri, Irfan Anjum Badruddin, Microelectronics Reliability, Volume 52, Issue 1, January 2012, Pages 90–99
17. T. Miwa, K. Otsuka, Y. Shirai, T. Matsunaga and T. Tsuboi, "High Reliability and Low Cost Design in Plastic PGA Package with High Performance", Hitachi,Ltd.,Device Development Center SATASChipPAC, STATS ChipPAC Ltd. 2009.
18. https://www.eso-electronic.com/en/knowledge-base/manufacturing/article/how-does-smt-electronics-assembly-work/
19. D. Napp, "NCMS lead-free electronic interconnect program", Proceedings of Surface, Mount International, 1994, pp. 425-431.
20. Lead-free Solders in Microelectronics, Mulugeta Abtewa, Guna Selvadurayb, Materials Science and Engineering,Volume 27, Issues 5–6, 1 June 2000, Pages 95–141
21. Morphologies, orientation relationships and evolution of Cu6Sn5grains formed between molten Sn and Cu single crystals, H.F. Zou, H.J. Yang, Z.F. Zhang, Acta Materialia, Volume 56, Issue 11, June 2008, Pages 2649–2662
22. C. Srivalli, M.Z. Abdullah, Z. Samsudin, Effects of Fe2NiO4 nanoparticles addition into lead free Sn–3.0Ag–0.5Cu solder pastes on microstructure and mechanical properties after reflow soldering process, Mater. Des., 67 (2015), pp. 197–208
23. E.M.N. Ervina, S. Amares, T.C. Yap, A review: influence of nanoparticles reinforced on solder alloy, Soldering Surf. Mount Technol., 25 (4) (2013), pp. 229–241

24. L. Zhang, S.B. Xue, L.L. Gao, Z. Sheng, H. Ye, Z.X. Xiao, et al., Development of Sn–Zn lead-free solders bearing alloying elements, J. Mater. Sci. Mater. Electron., 21 (1) (2010), pp. 1–15
25. A.A. El-Daly, Y. Swilem, M.H. Makled, M.G. El-Shaarawy, A.M. Abdraboh, Thermal and mechanical properties of Sn–Zn–Bi lead-free solder alloys, J. Alloys Compd., 484 (1) (2009), pp. 134–142
26. J. Zhou, Y. Sun, F. Xue, Properties of low melting point Sn–Zn–Bi solders, J. Alloys Compd., 397 (2005), pp. 260–264
27. S. Chen, L. Zhang, J. Liu, Y. Gao, Q. Zhai, A reliability study of nanoparticles reinforced composite lead-free solder, Mater. Trans., 51 (10) (2010), pp. 1720–1726
28. M.A. Matin, W.P. Vellinga, M.G.D. Geers. "Thermomechanical fatigue damage, evolution in SAC solder joints," Materials Science and Engineering A 445–446 (2007), pp. 73–85.
29. Isothermal and thermal cycling aging on IMC growth rate in lead-free and lead-based solder interface, L.H. Xu, J.H.L. Pang, K.H. Prakash, T.H. Low, IEEE Trans. Compon. Packag. Technol., 28 (2005), pp. 408–414
30. W.F. Hosford, Physical metallurgy, CRC Press, Taylor and Francis Group, Boca Raton, FL USA (2005)
31. A review on thermal cycling and drop impact reliability of SAC solder joint in portable electronic products, Dhafer Abdulameer Shnawah, , Mohd Faizul Mohd Sabri, Irfan Anjum Badruddin, Microelectronics Reliability, Volume 52, Issue 1, January 2012, Pages 90–99
32. Effects of intermetallic compounds on properties of Sn–Ag–Cu lead-free soldered joints, K.S. Kima, S.H. Huha, K. Suganumab, Journal of Alloys and Compounds, Volume 352, Issues 1–2, 24 March 2003, Pages 226–236
33. Evolution of Ag_3Sn intermetallic compounds during solidification of eutectic Sn–3.5Ag solder, Hwa-Teng Lee, , Yin-Fa Chen, Journal of Alloys and Compounds, Volume 509, Issue 5, 3 February 2011, Pages 2510–2517
34. Evolution of Ag_3Sn at Sn–3.0Ag–0.3Cu–0.05Cr/Cu joint interfaces during thermal aging, Fei

Lina, , Wenzhen Bia, Guokui Jua, Wurong Wanga, Xicheng Weia, b, , Journal of Alloys and Compounds, Volume 509, Issue 23, 9 June 2011, Pages 6666–6672

35. Tsai I, Tai L, Yen SF, Chuang TH, Lo R, Ku T, et al. Identification of mechanical properties of intermetallic compounds on lead-fee solder. In: Proc 55th IEEE-ECTC conf; 2005. p. 687–91.
36. D. Suh, D.W. Kim, P. Liu, H. Kim, J.A. Weninger, C.M. Kumar, et al.Effects of Ag content on fracture resistance of Sn–Ag–Cu lead-free solders under high strain rate conditions, Mater Sci Eng A, 46–461 (2007), pp. 595–603
37. Interfacial reactions between molten Sn–Bi–X solders and Cu substrates for liquid solder interconnects, J.F. Lia, , , S.H. Mannana, M.P. Clodea, D.C. Whalleyb, D.A. Huttb, Acta Materialia, Volume 54, Issue 11, June 2006, Pages 2907–2922
38. Fracture mechanics analysis of solder joint intermetallic compounds in shear test, M.O. Alama, , , , H. Lua, Chris Baileya, Y.C. Chanb, Computational Materials Science, Volume 45, Issue 2, April 2009, Pages 576–583
39. Polarity effect of electromigration on intermetallic compound formation in SnPb solder joints, Yu-Dong Lua, b, , , Xiao-Qi Heb, Yun-Fei Enb, Xin Wanga, Acta Materialia, Volume 57, Issue 8, May 2009, Pages 2560–2566
40. Evolution of interfacial morphology of Sn–8.5Zn–0.5Ag–0.1Al–xGa/Cu system during isothermal aging, Nai-Shuo Liu, Kwang-Lung Lin, Journal of Alloys and Compounds, Volume 456, Issues 1–2, 29 May 2008, Pages 466–473
41. Interface reaction between SnAgCu/SnAgCuCe solders and Cu substrate subjected to thermal cycling and isothermal aging, Liang Zhanga, b, Song Bai Xuea, , , Guang Zenga, Li Li Gaoa, Huan Yea, Journal of Alloys and Compounds, Volume 510, Issue 1, 5 January 2012, Pages 38–45
42. Kinetics of interfacial reaction in bimetallic Cu Sn thin films, K.N. Tu, R.D. Thompson, Acta Metallurgica, Volume 30, Issue 5, May 1982, Pages 947–952
43. Huang, M.L. , Zhao, J.F. , Zhang, Z.J. Role of diffusion anisotropy in β-Sn in microstructural

evolution of Sn-3.0Ag-0.5Cu flip chip bumps undergoing electromigration , (2015) Acta Materialia

44. X. Ma, Analysis of Mechanical and Metallurgical Factors Relative to the Failure of Microelectronic Surface Mount Solder Joint, Harbin Institute of Technology, Harbin (2000)
45. Zhang, L.a, Xue, S.-B.a , Gao, L.-L.a, Zeng, G.a, Sheng, Z.a, Chen, Y.b, Yu, S.-L, Effects of rare earths on properties and microstructures of lead-free solder alloys, Journal of Materials Science: Materials in Electronics, Volume 20, Issue 8, 2009, Pages 685-694
46. Hwa-Teng Lee, , Ming-Hung Chen, Influence of intermetallic compounds on the adhesive strength of solder joints, Materials Science and Engineering: A, Volume 333, Issues 1–2, August 2002, Pages 24–34
47. V.M.F. Marquesa , C. Johnstona, P.S. Granta, Microstructural evolution at Cu/Sn–Ag–Cu/Cu and Cu/Sn–Ag–Cu/Ni–Au ball grid array interfaces during thermal ageing, Journal of Alloys and Compounds, Volume 613, 15 November 2014, Pages 387–394
48. S. Manian Ramkumara, Reza Ghaffarianb, 1, , Arun Varanasia, Lead-free 0201 manufacturing, assembly and reliability test results, Microelectronics Reliability, Volume 46, Issues 2–4, February–April 2006, Pages 244–262
49. M. Berthoua, P. Retailleaua, H. Frémontb, A. Guédon-Graciab, Jéphos-Davennel, Microstructure evolution observation for SAC solder joint: Comparison between thermal cycling and thermal storage, Microelectronics Reliability, Volume 49, Issues 9–11, September–November 2009, Pages 1267–1272
50. WEIQUN PENG and MARCO ELISIO MARQUES. Effect of Thermal Aging on Drop Performance of Chip Scale Packages with SnAgCu Solder Joints on Cu Pads. Journal of ELECTRONIC MATERIALS, Vol. 36, No. 12, 2007
51. T.Y. Lee, W.J. Choi, K.N. Tu, and J.W. Jang: Mater. Res. 17, 291 (2002).
52. LUHUA XU, JOHN H.L. PANG, and FAXING CHE. Impact of Thermal Cycling on SnAg-Cu Solder

Joints and Board-Level Drop Reliability. Journal of ELECTRONIC MATERIALS, Vol. 37, No. 6, 2008

53. Harris PG, et al. Role of intermetallic compounds in leadfree soldering. Soldering and surface mount technology, No. 30. MCB Univ. Press Ltd; 1998. p. 38–52.

54. Luhua Xu, John H. L. Pang, Kithva H. Prakash, and T. H. Low, Isothermal and Thermal Cycling Aging on IMC Growth Rate in Lead-Free and Lead-Based Solder Interface. IEEE Transactions on Components and Packaging Technologies(TCPT), 2005. 28(3)

55. Hwa-Teng Lee , Yin-Fa Chen , Ting-Fu Hong, Ku-Ta Shih. Effect of Cooling Rate on Ag3Sn Formation in Sn-Ag Based Lead-Free Solder. 2009 11th Electronics Packaging Technology Conference. 978-1-4244-5100-5/09/2009 IEEE

56. Sang-Su Ha1, Jongwoo Park and Seung-Boo Jung, Effect of Pd Addition in ENIG Surface Finish on Drop Reliability of Sn-Ag-Cu Solder Joint, Materials Transactions, Vol. 52, No. 8 (2011) pp. 1553 to 1559

57. Sandeep Menon, Adam Pearl,, Michael Osterman,, and Michael Pecht, Effect of ENEPIG Surface Finish on the Vibration Reliability of Solder Interconnects, Center for Advanced Life Cycle Engineering, University of Maryland,College Park, MD, 20742

58. M.N. Islam, Y.C. Chan, A. Sharif, M.O. Alam. Comparative study of the dissolution kinetics of electrolytic Ni and electroless Ni–P by the molten Sn3.5Ag0.5Cu solder alloy. Microelectronics Reliability 43 (2003) 2031–2037

59. Zhi-Quan Liu, Pan-Ju Shang, Feifei Tan, and Douxing Li, “Microstructural Study on Kirkendall Void Formation in Sn-Containing/Cu Solder Joints During Solid-State Aging”, Microsc. Microanal. 19, S5, 105–108, 2013

60. T.T. Mattila, V. Vuorinen, J.K. Kivilahti, “Impact of printed wiring board coatings on the reliability of lead-free chip-scale package interconnections”, J Mater Res, 19 (2004), pp. 3214–3223

61. Syed A, Scanlan J, Cha S, Kang W, Sohn E, Kim T, et al. “Impact of package design and materials on reliability for temperature cycling, bend, and drop loading conditions”. In: Proc 58th IEEE-

ECTC conf; 2008. p. 1453–61.

62. A.U. Telang, T.R. Bieler, A. Zamiri, F. Pourboghrat, “Incremental recrystallization/grain growth driven by elastic strain energy release in a thermomechanically fatigued lead-free solder joint”, Acta Mater, 55 (2007), pp. 2265–2277
63. J. A. Davis, M. J. Bozack, and J. L. Evans. “Effect of (Au, Ni)Sn4 Evolution on Sn-37Pb/ENIG Solder Joint Reliability Under Isothermal and Temperature-Cycled Conditions”. IEEE TRANSACTIONS ON COMPONENTS AND PACKAGING TECHNOLOGIES, VOL. 30, NO. 1, MARCH 2007
64. D.R. Frear, J.W. Jang, J.K. Lin, and C. Zhang. “Pb-Free Solders for Flip-Chip Interconnects” 122
65. T.T. MATTILA1 and J.K. KIVILAHTI. “Reliability of Lead-Free Interconnections under Consecutive Thermal and Mechanical Loadings”. Journal of ELECTRONIC MATERIALS, Vol. 35, No. 2, 2006
66. J. Zhang, Z. Hai, S. Thirugnanasambandam, J.L. Evans, M. J. Bozack, “Correlation of Aging Effects on Creep Rate and Reliability in Lead Free Solder Joints”, Journal of Surface Mount Technology, (2012), Vol. 25 (3), pp. 19-28 Orlando, FL.
67. J. Zhang, Z. Hai, S. Thirugnanasambandam, J. L. Evans, M. J. Bozack, Y. Zhang, J. C. Suhling, ”Thermal Aging Effects on the Thermal Cycling Reliability of Lead-Free Fine Pitch Packages,” Components, Packaging and Manufacturing Technology, IEEE Transactions,vol. 3, pp. 1348 – 1357, 2013.
68. J. Zhang, Z. Hai, S. Thirugnanasambandam, J. L. Evans, M. J. Bozack, Y. Zhang, J. C. Suhling, "Aging Effects on Creep Behaviors of Lead-Free Solder Joints and Reliability of Fine-Pitch Packages," proc. Surface Mount Technology International Conference, 2012.
69. J. Zhang, Z. Hai, S. Thirugnanasambandam, J.L. Evans, M. J. Bozack, "Isothermal Aging Effects on the Harsh Environment Performance of Lead-Free Solder," proc. 45th International Symposium on Microelectronics, pp. 000801-000808.
70. J. Zhang, Z. Hai, S. Thirugnanasambandam, J. L. Evans, M. J. Bozack, Y. Zhang, J. C. Suhling, "Aging Effects on Creep Behaviors of Lead-Free Solder Joints and Reliability of Fine-Pitch Packages,"

proc. Surface Mount Technology International Conference, 2012.

71. Z. Hai, J. Zhang, C. Shen, J. L. Evans, M. J. Bozack, “Long-term Aging Effects on Reliability Performance of Lead-Free Solder Joints,” Proc. Surface Mount Technology International Conference, 2013, pp. 362-370, Dallas, TX.
72. José María Servín Olivares and Cynthia Gómez Aceves. TOF SIMS Analysis for SnxOy, Determination on Lead-Free HASL PCBs, SMT Magazine, October 2013 28-44.
73. Y. D. Jeon, S. Nieland, A. Ostmann, H. Reichl and K. W. Paik, Studies on the interfacial reactions between electroless Ni UBM and 95.5Sn-4.0Ag-0.5Cu alloy, J. Electron. Mater. 32 (2003) 548–557.
74. C. E. Ho, R. Y. Tsai, Y. L. Lin and C. R. Kao, Effects of the Gold Thickness of the Surface Finish on the Interfacial Reactions in Flip Chip Solder Joints, J. Electron. Mater. 31 (2002) 584–590
75. Randy Schueller, CONSIDERATIONS FOR SELECTING A PRINTED CIRCUIT BOARD SURFACE FINISH, DfR Solutions, Minneapolis, MN, USA
76. Sang-Su Ha, Jongwoo Park and Seung-Boo Jung, Effect of Pd Addition in ENIG Surface Finish on Drop Reliability of Sn-Ag-Cu Solder Joint, Materials Transactions, Vol. 52, No. 8 (2011) pp. 1553 to 1559
77. Z Hai, J Zhang, C Shen, J. L Evans, M. J Bozack, Long-term Aging Effects on Reliability Performance of Lead-Free Solder Joints, Proc. Surface Mount Technology International Conference, 362-370
78. Z Hai, J Zhang, C Shen, J. L Evans, M. J Bozack, Reliability Degradation of SAC105 and SAC305 BGA Packages under Long-Term, High Temperature Aging, Journal of SMTA
79. Z Hai, J Zhang, C Shen, J. L Evans, M. J Bozack, The Effect of Isothermal Aging on The Reliability of Sn-Ag-Cu Solder Joints Using Various Surface Finishes, SMTA International 2014
80. Z Hai, J Zhang, C Shen, J. L Evans, M. J Bozack, Reliability Performance of Lead-Free Solder Joints under Harsh Environments, IPC-ESTC 2014

81. Cong Zhao, Chaobo Shen, Zhou Hai, Jiawei Zhang, M.J. Bozack, and J. L. Evans, Long Term Aging Effects on the Reliability of Lead Free Solder Joints In Ball Grid Array Packages With Various Pitch Sizes and Ball Alignments, SMTA International 2015

82. Z Hai, J Zhang, C Shen, E.K. Snipes, M.J Bozack, J.L.Evans, Reliability Performance of Lead-Free SAC Solder Joints on ENIG and ENEPIG Subject to Long-Term Isothermal Aging, Journal of Mechatronics, 100-108

83. Z. Hai, J. Zhang, C. Shen, C. Zhao, J. L Evans, M. J Bozack, Effects on Reliability of Lead-Free Solder Joints under Harsh Environment, International Symposium on Microelectronics 2014 (1), 000471-000476

84. C Shen, Z Hai, C Zhao, J Zhang, M. J Bozack, J. C Suhling, J. L Evans, Reliability Analysis of Aging Effect on Joint Microstructures in Sn-Ag-Cu Solder Joints in Thermal Cycling, ASME 2015 InterPACK 2015

85. C Shen, C Zhao, Z Hai, J Zhang, M. J Bozack, J. C Suhling, J. L Evans, Sn-Ag-Cu Solder Joints Interconnection Reliability of BGA Package during Thermal Aging and Cycling, International Symposium on Microelectronics 2015 (1), 000135-000140

86. C Shen, Z Hai, C Zhao, J Zhang, M. J Bozack, J. C Suhling, J. L Evans, Reliability Study and Failure Analysis for Surface Finishes on Sn-Ag-Cu Solder Joints during Thermal Cycling, Journal of Mechatronics, Accepted